

REGULATORY LIGHT CHAINS OF MYOSIN

BY

ANDREW JOHN BENNETT, B.Sc. (Leicester)

A thesis submitted in fulfilment of the requirements  
for the degree of Doctor of Philosophy at the  
University of Leicester.

Department of Biochemistry,  
School of Biological Sciences,  
Adrian Building,  
University of Leicester,  
University Road,  
Leicester, LE1 7RH

October, 1985.

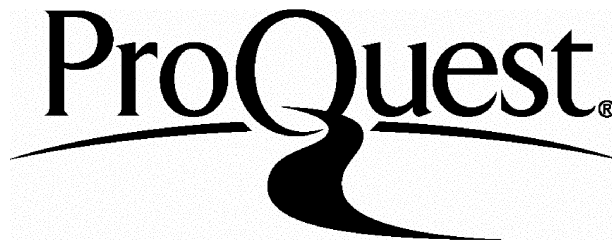
ProQuest Number: U367155

All rights reserved

INFORMATION TO ALL USERS

The quality of this reproduction is dependent upon the quality of the copy submitted.

In the unlikely event that the author did not send a complete manuscript and there are missing pages, these will be noted. Also, if material had to be removed, a note will indicate the deletion.



ProQuest U367155

Published by ProQuest LLC(2015). Copyright of the Dissertation is held by the Author.

All rights reserved.

This work is protected against unauthorized copying under Title 17, United States Code.  
Microform Edition © ProQuest LLC.

ProQuest LLC  
789 East Eisenhower Parkway  
P.O. Box 1346  
Ann Arbor, MI 48106-1346



PREFACE

The work presented in this thesis was performed in the department of Biochemistry at the University of Leicester, between October 1982 and October 1985. I am particularly indebted to my supervisor Dr C R Bagshaw, for his expert guidance, discussions and encouragement during the course of this work.

I would also like to thank Dr C Wells for advice, especially at the beginning of my research and later on for discussion of the work. The help of Miss K E Warriner and Mr N Patel in the general running of the laboratory was also greatly appreciated.

I wish to thank Professor M C R Symons FRS for the use of the epr equipment, Professor R A Chapman for the loan of rapid-reaction equipment, Dr A J Rowe for assistance in the use of ultracentrifuges and electron microscopes and Dr R R Harris for the use of the marine tanks. I thank Dr N C Millar and Dr A Cornish-Bowden, who kindly supplied versions of their computer programs, which greatly aided analysis of the data.

I acknowledge the Science and Engineering Research Council for the studentship I received.

ABBREVIATIONS AND CONVENTIONS

A	Actin
ADP	Adenosine 5' diphosphate
ATP	Adenosine 5' triphosphate
ATPase	Adenosine 5' triphosphatase
BAPTA	Bis-(0-aminophenoxy)ethane N,N,N',N'-tetra acetic acid
DTT	Dithiothreitol
DTNB	5,5'-Dithiobis-(2-nitrobenzoic acid)
EDTA	Ethylenediamine tetracetic acid
EGTA	Ethylene glycol-bis-( $\beta$ -aminoethyl ether) N,N,N',N'-tetra acetic acid
EPPS	[N-[2-Hydroxyethyl]-piperazine-N'-3-propane sulphonic acid
EPR	Electron paramagnetic resonance
ESR	Electron spin resonance
FPLC	Fast protein liquid chromatography
HMM	Heavy meromyosin
IANBD	4-(N-(iodoacetoxy)ethyl-N-methyl)amino-7-nitrobenz -2-oxa-1,3-diazole
M	Myosin
MOPS	3-[N-Morpholino]propane sulphonic acid
Pi	Inorganic phosphate
PPi	Inorganic pyrophosphate
PMSF	Phenylmethyl sulphonyl fluoride
RD	Regulatory domain
SI	Subfragment 1
SDS	Sodium dodecyl sulphate (Lauryl sulphate)
TEMED	N,N,N',N'-Tetramethylethylenediamine

TES	2-[2-Hydroxy-1,1-bis(hydroxymethyl)ethyl]amino-ethanesulphonic acid
TPCK	N-Tosyl-L-phenylalanine-chloromethyl ketone
Tris	2-Amino-2-(hydroxymethyl)-1,3-propanediol.

For the  $i$ th step of a reaction,  $k_{+i}$  is the forward rate constant,  $k_{-i}$  is the reverse rate constant and  $K_i (=k_{+i}/k_{-i})$ , the equilibrium constant. A \* indicates a conformationally different species to the unmarked species with the same symbol (eg. L and L\* would be conformationally different forms of the same RLC).

ABSTRACT

Scallop myosin is unusual in that the regulatory light chains (RLC) can be reversibly dissociated on removal of divalent metal ions. In this thesis the mechanism of the RLC dissociation was studied using several approaches. The dissociation of divalent metal ions from the non-specific divalent metal ion binding site of the scallop RLC was followed, either by a pH indicator method, or by a  $Mn^{2+}$  displacement method. The binding and release of the RLC itself, from the heavy chain/essential light chain complex was followed using the fluorophore 8-anilino-1-naphthalene sulphonate, which was found to be specific for the RLC binding site. The evaluation of the mechanism was greatly aided by the serendipitous discovery, that *Mercenaria* RLC bound to the scallop heavy chain/essential light chain complex in the absence of divalent metal ions. This allowed RLC exchange experiments to be performed which suggested the nature of the proposed mechanism.

The dissociation of the RLC from the scallop heavy chain/essential light chain complex, is largely explained by a refractory state mechanism. In this mechanism, the heavy chain/essential light chain complex is envisaged to exist in two forms, a nascent state which occurs immediately after RLC dissociation and a refractory state which is favoured on a long term basis. The formation of this refractory state, is the driving force for the net dissociation of the RLC from scallop myosin and subfragments.

Differences in the degree of RLC dissociation (HMM cf  $S1^{+RD}$ ) on addition of EDTA are explained by a change in the equilibrium constant for the refractory state transition. The mechanism is discussed with reference to existing structural information on RLC denuded myosin.

CONTENTS

PREFACE	i
ABBREVIATIONS AND CONVENTIONS	ii
ABSTRACT	iv
CONTENTS	1
CHAPTER 1: INTRODUCTION	4
The structure of striated muscle	5
The thick filament	7
The thin filament	11
Mg-ATPase and $\text{Ca}^{2+}$ regulation	14
Myosin light chains	21
CHAPTER 2: MATERIALS AND METHODS	32
Protein Purification and Preparation	32
General Methods	50
Experimental Methods and Principles	55
CHAPTER 3: DISSOCIATION OF DIVALENT METAL IONS FROM THE NON-SPECIFIC SITE OF MYOSIN	67
Dissociation of $\text{Ca}^{2+}$ from EGTA	68
Dissociation of $\text{Ca}^{2+}$ from myosin subfragments	73

Dissociation of $Mg^{2+}$ from myosin subfragments	75
CHAPTER 4: 8-ANILINO-1-NAPHTHALENE SULPHONATE, A FLUORESCENT PROBE FOR THE REGULATORY LIGHT CHAIN BINDING SITE OF SCALLOP MYOSIN	80
ANS binding to scallop myosin	82
ANS binding and its effect on the RLC equilibrium	83
The location of the ANS binding site	85
Desensitization of scallop HMM	88
The kinetics of the RLC interaction	90
CHAPTER 5: THE BINDING OF <i>MERCENARIA</i> RLC IN SCALLOP MYOSIN AND SUBFRAGMENTS	95
Binding of <i>Mercenaria</i> RLC as followed by ANS displacement.	96
Binding of fluorescently labelled <i>Mercenaria</i> RLC.	100
CHAPTER 6: LIGHT CHAIN INTERACTIONS AND $Ca^{2+}$ - SPECIFIC EFFECTS	102
Essential light chain interactions	103
Calcium specific effects on ANS fluorescence	106
CHAPTER 7: DISCUSSIONS	108
The mechanism of the RLC interaction	108

Effects of Ca<sup>2+</sup> 117

The effect of RLC interaction on structure 120

Appendix 1: Publications

Bibliography

## CHAPTER 1

### INTRODUCTION

Muscles have evolved in a wide diversity of ways, depending on the function they are required to fulfil. The differences are observable on the macroscopic, microscopic and molecular levels. On the microscopic level, the muscles can be clearly divided into two types. Under the light microscope, they appear either striped due to the alignment of their myofilaments, ie striated muscle, or unstriped with no visible structure at this resolution, ie smooth muscles. Striated muscle is typified by vertebrate muscles concerned with skeletal movement, these muscles can contract rapidly and are normally under voluntary control. However, these are not the only examples, and many others exist such as the striated adductor muscles of molluscs and insect flight muscle. As well as the normal cross-striated muscles, obliquely striated muscles occur. These are typically found in nematodes and annelids; the striations form an angle (approximately  $10^\circ$ ) to the fibre axis, the angle changing on contraction. Smooth muscles contract and constrict slower than striated muscles and are generally under involuntary control. They are typified by the muscles surrounding internal organs, but are also found in invertebrates, eg. molluscs, where they form the catch muscle which maintains the shell in the closed position for long periods of time. Cardiac muscles are a special case, in that they undergo regular, self-sustained contractions like smooth muscle, but show definite striations like skeletal muscles.

The striated muscles of vertebrates and invertebrates appear similar even under the electron microscope (Millman and Bennett, 1976). However, the constitution of the muscle cells can vary. Vertebrate muscle cells contain many myofibrils and are multinucleate, whereas those of scallops eg *Pecten maximus*, *Placopecten magellanicus* are uninucleate and contain only a single myofibril.

At the molecular level, all the muscles contain myosin and actin, which are arranged to allow contraction. The most striking differences occur in the way in which the muscles are regulated. Two major sites of regulation have been identified. In each case  $Ca^{2+}$  is involved to trigger contraction, however, this control may be mediated via the myosin or actin or in some cases jointly by both. This thesis is concerned with the control mediated via the myosin molecule. It considers the regulatory proteins and their interactions in the cross-striated adductor muscle from *Pecten maximus*. A muscle which is regulated by  $Ca^{2+}$ , which acts directly on the myosin molecule.

#### The structure of striated muscle

A muscle is comprised of many muscle fibres linked together by collagenous connective tissue. Each muscle fibre consists of one or more myofibrils, depending on the source of the muscle. The myofibrils are organised in repeating units called sarcomeres as shown in fig 1-1. These can be seen in micrographs of myofibrils, as the alternating light

(Isotropic, I) and dark (Anisotropic, A) bands, which give the muscle its typical striated appearance. In the myofibrils, thick and thin filaments overlap to produce this effect.

The thick filaments in the A-bands are composed mainly of myosin and are mechanically linked at their centre by a structure called the M-band in vertebrate muscle. No equivalent of the M-band has been observed in molluscan muscles, which could possibly account for the added disorder observed in these muscles. In the centre of the I band, a dark line is observed, known as the Z disk, which links the actin filaments. The sarcomere is defined as the repeating unit between one Z disk and the next.

On contraction of isolated myofibrils, the sarcomere is observed to shorten, showing that this is the unit where active shortening of the muscle occurs. During this contraction, the A bands remain at a constant length while the length of the I band changes. (Huxley and Niedergerke, 1954). The I band shortens in unison with the H-zone as first revealed by the phase-contrast microscopy of Huxley and Hanson (1954). Together with electron microscopy, which demonstrated the basis of the striations, these findings led to the proposal of the sliding filament model of muscle contraction. Contraction was proposed to occur by sliding of the interdigitating thick and thin filaments. The length of the sarcomere will thus depend on the extent of overlap of the filaments, rather than on their actual length. This model is generally accepted and is supported by evidence

from X-ray diffraction experiments (Haselgrove, 1975). These experiments show little change in axial periodicity within the X-ray pattern at a wide variety of sarcomere lengths. Also, the form of the X-ray pattern, on stimulation of active muscle, does not depend on the sarcomere length prior to stimulation, but only the length at which it is recorded.

Muscle contraction occurs due to interaction of myosin, within the thick filament, with actin in the thin filament. In striated muscles, the thick filaments form a hexagonal array surrounded by thin filaments. In vertebrate muscle 6 thin filaments surround each thick filament, whereas, in scallop striated muscle, approximately 12 thin filaments have been shown to surround each thick filament (Millman and Bennett, 1976). The tension that a muscle can produce is a function of the overlap of the thick and thin filaments and therefore the sarcomere length (fig 1-2). Increasing the overlap increases the tension, until a point where the filaments interfere with each other and tension again falls. (Gordon et al. 1966). If the muscle is passively stretched until there is no overlap, then no tension can be produced. These results suggest that the force is probably generated evenly throughout the A band and hence, the tension produced is linearly related to the amount of overlap, as was observed.

#### The thick filament

The most abundant protein in most muscles and the functional component of the thick filament is the protein, myosin.

The myosin molecule contains both actin binding sites and the sites for ATP hydrolysis. In some cases, the thick filament is referred to as a myosin filament, however this is not strictly correct because certain molluscan muscles may contain more paramyosin than myosin. The thick filaments of vertebrates are approximately 1.6  $\mu\text{m}$  long and 15 nm in diameter, whereas, molluscan thick filaments containing paramyosin are generally longer and wider. In these thick filaments the myosin binds to a central core of paramyosin (Szent-Györgyi et al., 1971). *Pecten maximus* thick filaments are 1.76  $\mu\text{m}$  long and 20 nm in diameter, but in muscles with higher paramyosin:myosin ratios may be 25-100  $\mu\text{m}$  long and 20-100 nm in diameter.

All muscle myosins have similar gross structural and physical properties, with a molecular weight between 450,000 and 500,000. The molecule is a highly assymmetric, hexamer (fig 1-3) composed of a pair of high molecular weight heavy chains (mw 200,000) and two pairs of low molecular weight light chains (mw 17-25,000). There are two classes of light chains, regulatory light chains which have a control function and essential light chains, whose exact function is unknown. The heavy chains are organised to give a two chain coiled-coil  $\alpha$ -helical tail, with two globular heads at one end of the molecule. Electron microscopy has revealed the tail to be approximately 140 nm long and 2 nm in diameter, while the heads are between 12 and 20 nm long and up to 7 nm in diameter. Elliott and Offer (1978), using rotary shadowed preparations, showed the heads appear pear shaped,

being larger at the tip than at the junction with the rod. They also observed flexibility of the heads around the head-tail junction and also at a well defined location within the tail. These results confirmed the existence of a hinge along the myosin tail and between the myosin head and tail.

The myosin molecule has been studied by proteolytic cleavage to look at the function of the various parts. It is particularly susceptible to cleavage at two locations which fit with the flexible hinge regions noted above. The subfragments produced have the advantage of being soluble at low ionic strength, unlike myosin. Heavy meromyosin (HMM) produced by cleavage along the myosin tail, retains ATPase activity and is regulated by  $\text{Ca}^{2+}$ . Subfragment 1 (S1), which is produced by cleavage between the head and tail, yields a globular molecule which contains the ATPase activity but is no longer regulated by  $\text{Ca}^{2+}$ . Both subfragments produced contain light chains, showing that they are bound to the head region of the myosin molecule. The head region also contains the ATPase site and the actin binding site of the myosin molecule (Margossian and Lowey, 1973). In scallop myosin, the head region (S1) can be further digested by trypsin, to yield a regulatory fragment, which contains the light chains (Szentkiralyi, 1984).

Recently, Winkelmann et al. (1985), have successfully crystallised subfragment 1 from chicken pectoralis muscle. By study of the crystals using X-ray diffraction techniques and electron microscopy, the molecule was shown to be

approximately  $160\text{\AA}$  long, with a maximum thickness of  $60\text{\AA}$  and showed marked curvature down the long axis. The molecule was broad at the tip, narrowing towards the 'neck' which joins the subfragment 1 to the myosin rod. The exact termination point of the molecule at this end was difficult to define, hence the length measurement is probably an underestimate.

Analysis of proteolytic rod sections reveal that every 3rd or 4th residue is hydrophobic, while between them are clusters of charged residues (McLachlan and Karn, 1982). In each  $\alpha$ -helix the hydrophobic residues form a continuous face which is responsible for binding to the other heavy chain. The clusters of charged residues are on the outside of the coiled-coil so formed and may therefore be responsible for the self-aggregation of the myosin molecule to form the thick filament.

Projections from the thick filament have been shown to be the myosin heads. Aggregates formed from LMM or rod which lack the myosin head do not have such projections. The projections or cross-bridges occur at regular intervals and give rise to a characteristic X-ray diffraction pattern. In vertebrate striated skeletal myosin, a meridional reflection is observed at 14.3 nm and a layer line at 42.9 nm, which arise from a helical arrangement of the cross-bridges (Huxley and Brown, 1967). This cannot be interpreted unambiguously, but it indicates that the cross-bridges are arranged on  $n$ -helical strands with a pitch of  $n \times 42.9$  nm and an axial

repeat of 14.3 nm. Evidence favours  $n=3$  for vertebrate skeletal muscles (Squire, 1974) which is supported by the fact that the filaments tend to fray into 3 subfilaments, suggesting a 3-fold symmetry in the packing of the backbone. (Maw and Rowe, 1980). In invertebrate systems, the axial repeat is similar to in vertebrate systems. The exact rotational symmetry varies from species to species and appears to depend on the size of the thick filament. (Wray et al. 1975). This work favoured a six or sevenfold rotational symmetry in *Placopecten* thick filaments with some splaying of the cross-bridges. In *Limulus* a three or fourfold symmetry was predicted. Other work by Millman and Bennett (1976) favoured a six stranded helix for the thick filament of the cross-striated adductors of *Pecten maximus* and *Placopecten magellanicus*. However, Vibert and Craig (1983), predicted a 7-fold rotational symmetry for scallop, based on image reconstruction of negatively stained electron micrographs. Hence, the exact symmetries are not clear and further work is required to clarify the exact structural organisation of the thick filaments from different invertebrates.

#### The thin filament

The major component of the thin filament is the protein, actin. This protein can occur either in a monomeric G-form or, when polymerised in a filamentous F-form as found in the thin filament. Actin monomers have a molecular weight of approximately 42,000 and are assymmetric.

Polymerisation of the G-actin monomer, gives rise to filaments which are polar. Actin not only occurs in muscle cells but is found in many non-muscle cells, being one of the most ubiquitous proteins.

Early experiments showed that the I-filaments contained, in addition to actin, a large amount of the protein tropomyosin. The ratio of the proteins was fairly constant in all the thin filaments studied. This strongly suggested the thin filament consisted of fixed proportions of the two molecules. Selby and Bear (1956) suggested two models for the basic structure of the thin filament, either a planar or helix net arrangement of the actin filaments. At this time it was impossible to distinguish between the two possibilities, with the evidence available. This problem was resolved by Hanson and Lowy (1963), who provided a direct visual demonstration of the basic structure of the thin filament, by electron microscopy. The actin filaments appeared as two intertwining helical strands of globular repeating units. Cross-over points occur between the strands every  $360\text{-}385\overset{\circ}{\text{Å}}$  and probably contain just over 13 globular subunits between them, organised in six helical turns. These observations fit well with the helix net model previously proposed. X-ray diffraction studies (Such et al., 1981) have shown that actin monomers consist of a large and small domain with overall dimensions of  $67 \times 40 \times 37\overset{\circ}{\text{Å}}$ . The structure resembles a  $\beta$ -pleated sheet surrounded by  $\alpha$ -helices, in each domain.

Tropomyosin, the other major protein component of the thin filament, is a rod-like, two chain  $\alpha$ -helical coiled-coil molecule approximately 40 nm long, with a diameter of 2 nm. The structure of the tropomyosin, together with the periodicity observed in actin filaments, gave rise to the idea that the tropomyosin molecule might lie along the long pitched 'groove' of the actin helix. Hanson and Lowy (1964) therefore proposed that the tropomyosin molecule was responsible for the repeats in the actin filament. They also suggested some other molecule might be involved to give the obvious density stripes seen at the cross-over points in electron micrographs. This is now known to be the case and the additional protein is troponin. Initially troponin was isolated in a complex with tropomyosin and later shown to be a globular protein with  $\text{Ca}^{2+}$  binding properties (Ebashi and Kodama, 1966). Troponin is therefore the third component of most thin filaments and is bound at the ends of the tropomyosin molecules, which lie in the actin 'grooves' (fig 1-4). In 1971, Greaser and Gergely showed that troponin was composed of three distinct subunits. These are now known as troponin C, which binds  $\text{Ca}^{2+}$ , troponin I, which acts to inhibit actomyosin interactions and troponin T which holds the complex to the actin. The ratio of these subunits was shown to be T:I:C of 1:1:1 and the troponin:tropomyosin:actin ratio equal to 1:1:7 (Potter, 1974). However more recently the ratio of the troponin components has been questioned, both in invertebrates (Lehmann et al., 1976) and in vertebrates (Sperling et al., 1979) and a T:I:C ratio of 1:2:1 has been suggested.

In molluscan muscle systems it was originally thought that troponin did not occur (Kendrick-Jones et al., 1970), however troponin I and C have now been identified though often in trace amounts (Lehman, 1981). No troponin T has been identified in any molluscan muscle and it is not known if a functional troponin complex exists, even in those molluscan muscles with greater amounts of the I and C subunits present.

### Mg-ATPase and Ca<sup>2+</sup> Regulation

Interaction between myosin and actin, with hydrolysis of ATP, drives muscle contraction. The myosin Mg-ATPase is activated by filamentous F-actin, but not by monomeric G-actin. Regulation of the actin-activated Mg-ATPase is mediated via Ca<sup>2+</sup>-binding proteins and ultimately by the level of Ca<sup>2+</sup> within the muscle cell. The overall ATPase mechanism can be divided into elementary steps. Rates and equilibria for these steps have been determined by several steady state and pre-steady state techniques. The rate of ATP cleavage is faster than the rate limiting step of the pathway. Evidence for the rate of cleavage comes from pre-steady state work, which revealed rapid formation of enzyme bound phosphate, a phenomenon known as the early phosphate burst (Lymn and Taylor, 1970). In the presence of low actin concentrations, ATP hydrolysis occurs after actomyosin dissociation (Lymn and Taylor, 1971). This observation gave rise to the classical Lymn-Taylor scheme, in which hydrolysis of ATP occurs in unattached myosin. In this scheme the rate limiting step was product release, which followed reattachment of the myosin to actin (fig 1-5a).

This kinetic scheme was related to contraction, as shown in the model in fig 1-5b. It was proposed that hydrolysis of ATP would change the conformation of the myosin molecule, producing a new angle of attachment of the myosin head to actin. Release of the products was envisaged as the power stroke, with myosin returning to its initial configuration. The power stroke was therefore the driving force, which caused sliding of the filaments and hence produced contraction in a muscle.

One prediction of this model was that the majority of ATP hydrolysis by myosin, would occur only when the myosin was not attached to actin. Stein et al. (1979) have produced evidence that at high actin concentrations this is not the case. ATP hydrolysis was observed to occur in the attached and unattached states. If this is the case how does contraction occur? Hydrolysis of ATP, if it occurred without detachment of myosin from actin, would mean the Lymn-Taylor scheme would not work. This type of hydrolysis is likely to be important for isometric contraction of muscle systems.

In order to overcome the problems associated with the Lymn-Taylor scheme, Stein et al. (1979) suggested an alternative scheme, in which myosin can bind to actin in more than one conformation, with different affinities. These conformations could then reflect the 45° and 90° states proposed by Lymn and Taylor. However, if no detachment occurs, why is the power stroke not reversed?

Eisenberg and Greene (1980), overcame this problem by proposing that because of constraints within the muscle, reversal of the power-stroke cannot readily occur on rebinding of ATP. A strained 90° state was therefore invoked, which rapidly detaches and rebinds to give a normal 90° state, before doing significant negative work (fig 1-6). In such a way the initial conformation is regained, ready for the next cycle of contraction. The assumption that the detachment and reattachment are rapid is based on evidence that myosin-ATP associates and dissociates from actin very rapidly in solution (Lyman and Taylor, 1971; Stein *et al.*, 1979). The rate limiting step in the model of Eisenberg and Greene is shown as a conformational change of the acto-myosin-ADP.Pi state. However this is not definite and it is not clear whether such a change, rather than hydrolysis of ATP or release of product, forms the rate limiting step.

It is likely that the basic ATPase mechanism is similar in all myosins, but in molluscan myosins there is an additional feature which involves Ca<sup>2+</sup> sensitivity of the ATP hydrolysis. When the Mg-ATPase of scallop myosin in the presence of actin is studied under steady-state conditions, the rate of hydrolysis of ATP increases three to four fold on addition of Ca<sup>2+</sup> to actoHMM and from ten to twenty fold with actomyosin. These values are a lot less than required to explain activation of ATP hydrolysis in stimulated muscles. Recently, Wells and Bagshaw (1984) used a turbidometric assay to study the actin-activated Mg-ATPase of scallop HMM. This showed a biphasic recovery of turbidity as ATP was hydrolysed in the absence of Ca<sup>2+</sup>. They explained this result in terms

of a heterogenous HMM population, comprising 20-30% unregulated molecules and 70-80% regulated molecules. When all the ATP is hydrolysed, the unregulated fraction rebinds to actin, while the regulated population undergoes a slow single turnover of ATP ( $k_{\text{obs}} = 1.8 \times 10^{-3} \text{s}^{-1}$ ). When this value is compared to that in the presence of  $\text{Ca}^{2+}$  ( $k_{\text{obs}} = 1.2 \text{s}^{-1}$  per head), a calcium activation of 650 fold is obtained, which approaches the value expected *in vivo*.

In addition to the  $\text{Ca}^{2+}$  activation of the actin-activated Mg-ATPase some  $\text{Ca}^{2+}$  activation of the Mg-ATPase of myosin alone is observed (Ashiba et al., 1980). This property has been studied in the scallop (*Pecten maximus*) by fluorescence methods (Wells et al., 1985a) and by the use of a limited turnover approach (Wells and Bagshaw, 1985). The nucleotide induced enhancement of tryptophan fluorescence was studied in myosin subfragments. Typically a two to three fold activation of the ATPase in the presence of  $\text{Ca}^{2+}$  was observed, as measured by the duration of the fluorescence enhancement, on addition of ATP to HMM. However, in this type of analysis with a large excess of ATP, the ATPase will be dominated by the unregulated population and a limited turnover approach is preferable. By use of an actin-chase experiment, the turbidity profile on addition of actin to HMM, previously incubated with ATP, were monitored. This showed that HMM alone, in the absence of  $\text{Ca}^{2+}$ , forms a long lived intermediate with ATP. The rate of ATP hydrolysis, in the absence of  $\text{Ca}^{2+}$ , was comparable to in the previous actoHMM turbidity experiments. The ATPase was activated about 100 fold by  $\text{Ca}^{2+}$ , in the absence of actin. Actin amplifies this  $\text{Ca}^{2+}$

sensitivity by enhancing this  $\text{Ca}^{2+}$  activation to give the 650 fold previously obtained. Single turnover experiments using  $[\gamma\text{-}^{32}\text{P}]$  ATP were then performed, to further study this activation. The results indicated that the phosphate release step was slow in the absence of  $\text{Ca}^{2+}$  and was likely to be a rate limiting step. Furthermore, the results of the actin chase experiment indicated ADP release was also affected by  $\text{Ca}^{2+}$ , the release being slower in the absence of  $\text{Ca}^{2+}$ .

As well as the nucleotide induced fluorescence enhancement, binding of  $\text{Ca}^{2+}$  ions to scallop myosin causes a fluorescence enhancement. (Wells et al., 1985b) This binding was too fast to measure by manual mixing methods and was rapidly reversed on addition of EGTA to chelate the  $\text{Ca}^{2+}$ . The fluorescence enhancements induced by the ATP and  $\text{Ca}^{2+}$  were shown to be associated with two separate tryptophan containing domains, as indicated by the responses of different subfragments. The  $\text{Ca}^{2+}$  effect was located in the "neck" region of the myosin, unlike the nucleotide effect which was in the remainder of the head region of the molecule.

How is the effect of  $\text{Ca}^{2+}$  mediated? In muscle systems,  $\text{Ca}^{2+}$  regulation can be broadly subdivided into actin-linked (thin filament) regulation and myosin-linked (thick filament) regulation. Some muscles appear to have only thin filament control eg. vertebrate striated muscle, and others only thick filament control, eg Molluscan striated adductor muscle. However, most invertebrate muscles possess both kinds of regulation (Lehman and Szent-Györgyi, 1975).

The Mg-ATPase of myofibrils from vertebrate skeletal muscle is  $\text{Ca}^{2+}$  sensitive, however, on purification of the myosin and actin this property is lost. The  $\text{Ca}^{2+}$  sensitivity is conferred on the myofibrils by the proteins, troponin and tropomyosin, acting on the thin filament. In the absence of calcium, it is thought that the troponin and tropomyosin block the interaction of myosin with the actin filament. On addition of  $\text{Ca}^{2+}$ , the  $\text{Ca}^{2+}$  binds to the troponin and causes a movement of tropomyosin towards the centre of the actin 'groove' (Huxley, 1973), hence unblocking the interaction. This is the basis of the steric-blocking mechanism for acto-myosin interaction, in thin filament regulation. More recent work (Taylor and Ames, 1981), has considerably refined this model, but the basic idea of the steric-blocking of myosin attachment by tropomyosin in the relaxed state, is still retained.

Thick filament regulation was first discovered in molluscan muscle (Kendrick-Jones et al., 1970). They discovered that thin filaments from *Mercenaria* or *Aquipecton* were incapable of bestowing calcium sensitivity on preparations of rabbit myosin. Calcium specific sites were found to be present in molluscan myosin preparations, but not in rabbit myosin preparations. Two types of thick filament regulation are now known to occur, one is a phosphorylation mechanism, the other is a direct  $\text{Ca}^{2+}$  effect. The thick filament control of Mg-ATPase activity by phosphorylation, was first discovered in platelets (Adelstein and Conti, 1975). Since then, it has been found in many non-muscle and vertebrate

smooth muscle cells, as well as in a few invertebrate muscles. The myosin becomes activated by phosphorylation at a single serine residue, located on the regulatory light chain. (Jakes et al., 1976). This process is controlled by calcium, via a calcium-calmodulin complex which activates a myosin light-chain kinase. The kinase specifically phosphorylates the myosin, this phosphorylation being reversible by specific phosphatases. Stoichiometric amounts of MgATP have been shown to cause disassembly of some myosin filaments to give myosin monomers. Phosphorylation of the regulatory light chain causes reassembly of the myosin into filaments (Suzuki et al., 1978). Phosphorylation was shown to have an effect on the conformation of the myosin monomer in solution; however, Trybus and Lowey (1984), have shown this effect to be very salt dependant. The salt alone can cause a change in conformation, the effect of phosphorylation only being observed over a narrow range of salt concentrations.

In molluscan adductor muscles thick filament regulation does not operate via a phosphorylatory pathway. No phosphorylation of the RLC by light chain kinases occurs, under conditions in which other myosins are phosphorylated (Jakes et al., 1976). In these muscles the regulation is mediated by a direct binding of the  $\text{Ca}^{2+}$  to the myosin molecules, which requires the presence of the regulatory light chain.

### Myosin Light Chains

The light chains of myosin can be divided into two classes on the basis of their chemical structure, electrophoretic mobilities and the methods required to dissociate them from the myosin molecule. Regulatory light chains (RLC), so named because of their involvement in the  $\text{Ca}^{2+}$  regulation of the Mg-ATPase of molluscan systems, form one class. The other class are the essential light chains (ELC), which are more difficult to remove without irreversible loss of the ATPase activity. Removal of these light chains has however recently been achieved in vertebrate skeletal myosin, without loss of the ATPase (Wagner and Giniger, 1981). Both classes of light chains are common to all myosins, however, not all the RLC studied have a proven regulatory function in the myosin molecule.

Regulatory light chains are released from scallop adductor myosin by treatment with EDTA. The temperature of the EDTA treatment affects the amount of RLC dissociation. At  $0^{\circ}\text{C}$ , about half the RLC are released while at higher temperature ( $25-35^{\circ}\text{C}$ ), all the RLC are released (Chantler and Szent-Györgyi, 1980). On removal of either one or both of the RLC subunits from the molecule, the ATPase is permanently activated and  $\text{Ca}^{2+}$  regulation is lost. Readdition of the RLC, to stoichiometric amounts, reduces the ATPase activity in the absence of  $\text{Ca}^{2+}$ , restoring the requirement for  $\text{Ca}^{2+}$  to activate the molecule. (Szent-Györgyi et al., 1973; Kendrick-Jones et al., 1976).

The rebinding of the RLC to the denuded myosin was proposed to occur in a negatively co-operative manner (Chantler and Szent-Györgyi, 1980). More recent studies (Chantler, 1985) have shown that the co-operative effects of RLC interaction are temperature dependent. At temperatures of less than 17°C, Chantler confirms that there is co-operativity between the myosin heads, with respect to RLC rebinding in the presence of divalent cations and RLC dissociation in the absence of divalent cations. This co-operativity is apparently lost at higher temperatures, the RLC dissociating in a random manner in the absence of divalent cations.

One possible explanation of the RLC interaction was given by Kendrick-Jones and Jakes (1976), it was proposed that on dissociation of the RLC from myosin, the heads of the molecule would clump together and trap the second RLC. Subsequently, this model was modified by Bagshaw (1980), who suggested the RLC binding was a dynamic equilibrium. In this model, the exposed RLC binding site on one head was proposed to associate with the opposite face of the second head, so perturbing the equilibrium constant for light chain binding to the first head. Evidence in support of head-head interaction was provided by Wells and Bagshaw (1983). They showed using saturation transfer EPR spectroscopy, that on removal of the RLC from double-headed scallop preparations, the motion of the heads was restricted. This supports the idea of intramolecular aggregation, however, the exact structural basis for the observed co-operativity remains unclear.

As regulatory light chains of scallop myosin can be reversibly dissociated by treatment with EDTA, hybrid myosins can be produced to study the role of different RLC. (Kendrick-Jones et al., 1976; Sellers et al., 1980). Scallop myofibrils from which all the RLC have been removed will form hybrids containing only one type of foreign RLC, up to a final stoichiometry of two moles RLC per mole of myosin. Using such an approach the foreign RLC tested could be divided into two major classes; those that produced a functional myosin with respect to  $\text{Ca}^{2+}$  regulation and those which did not. The classes which were functional could be further subdivided by the calcium concentration required to activate the ATPase. Light chains from molluscs eg. *Mercenaria*, *Spisula* and some other invertebrates eg. *Urechis*, which require calcium binding for myosin activation, behaved like native scallop RLC. They restored the  $\text{Ca}^{2+}$  sensitivity of the actin-activated Mg-ATPase and also restored the high-affinity calcium binding sites. RLC from *Limulus*, cricket, chicken gizzard and platelet myosin also restored the  $\text{Ca}^{2+}$  sensitivity of the actin-activated Mg-ATPase, but had a far lower affinity for calcium binding and hence, higher calcium concentrations were required for ATPase activation. Hybrids produced with vertebrate striated (chicken, rabbit), bovine cardiac and lobster claw RLC were insensitive to the calcium concentration and no calcium specific binding sites were restored. In these hybrids, the ATPase is not depressed in the absence of calcium ions. The results reflect the source of the regulatory light chains and the role they have in their native myosins.

Both the ELC and RLC are single polypeptide chains with a molecular weight of between 17,000 and 25,000. Physical characterisation studies on the light chains were performed by Stafford and Szent-Györgyi (1978). They concluded that the light chains could generally be described by an ellipsoidal model, with a long axis of  $100 \pm 20 \text{Å}$ . The internal structure of the isolated light chains was found to be very stable, being almost unaffected by pH, ionic strength and temperature. This indirectly suggests that much of this structure is probably retained when the RLC is bound to the myosin molecule.

The light chains were initially proposed to be located at or near the 'neck' region, where the myosin head joins to the tail, on the basis of digestion studies (Bagshaw, 1977). Further evidence in support of this location has come from the electron microscopy studies of Flicker et al., (1983). Light chain specific antibodies, raised either to the RLC or ELC, were shown to bind preferentially to the narrow 'neck' region of the myosin molecule near the junction with the tail, for both classes of light chain. Other evidence for the location of the RLC comes from the desensitization of the myosin molecule. In this case the loss of mass appears to be in the 'neck' region of the molecule. The RLC and ELC are known to be in close proximity to each other. Regulatory light chains protect the thiol group of the ELC from reaction with iodoacetate, under conditions in which heavy chain thiol groups are labelled. If the RLC are removed, then the reactivity of the ELC thiol group is greatly increased, however, it can not be specifically labelled

(Hardwicke et al., 1982). Cross-linking studies have also been performed on the two light chains using photochemical cross-linking reagents. Wallimann et al., (1982), showed that the RLC will cross-link with the ELC and concluded that they cannot be more than 6 to 8Å<sup>o</sup> apart on the myosin head. The light chains were observed to overlap for at least half their length. Further studies (Hardwicke et al., 1983) looked at the relative positions of the ELC and RLC under conditions which cause relaxation, contraction or rigor. The results indicated that the light chains can move, but that this movement was restricted to the N-terminal region of the RLC. No change was observed in the relative positions of the C-terminal regions. Cross-linking of the N-termini of the RLC and ELC to each other results in a molecule with a high ATPase in the absence of Ca<sup>2+</sup>, while cross-linking of the C-termini has no effect. This suggests movement of the N-terminus of either the ELC or RLC is required for regulation to occur. Both the light chains have been isolated attached to a 14000 molecular weight peptide fragment of the heavy chain (Szentkirályi, 1984) which probably represents the C-terminal end of the subfragment-1 region of myosin (Bennett et al., 1984). Hence the interaction between ELC and RLC is not surprising.

Probably more surprising is the result of Hardwicke and Szent-Györgyi (1985) which showed that the RLC from different heads of myosin can be cross-linked together. The results indicate a separation of less than 9Å<sup>o</sup> between the N-termini of the two RLC, but a larger distance between the C-termini.

The distance between the N-termini of the RLC is not affected by changes in condition from rigor to rest. Therefore, the movement observed between the RLC and ELC is probably a result of motion of the ELC, on the myosin head.

Based on the amino-acid sequence data and the crystal structure of carp parvalbumin, Kretsinger (1980) identified a homologous family of  $\text{Ca}^{2+}$  binding proteins. This family included myosin light chains (ELC and RLC), calmodulin, troponin C and parvalbumins. None of these proteins are enzymes, but calmodulin, troponin C and light chains can all act to modify other enzymes in the presence of calcium. From the X-ray structure of parvalbumin, Kretsinger (1980) showed the existence of three domains or E-F hand structures (Fig 1-7). An E-F hand refers to the conformation of the peptide chain about a bound Ca (II) ion, which has been likened to the shape of a right hand. It comprises an  $\alpha$ -helix E, a  $\text{Ca}^{2+}$  binding loop and an  $\alpha$ -helix F, corresponding to the extended forefinger, clenched middle finger and extended thumb respectively. The domain is characterised by having hydrophobic residues on the inner face of the two  $\alpha$ -helices and oxygen-containing residues at the appropriate positions in the  $\text{Ca}^{2+}$  binding loop that provide the co-ordinating ligands.

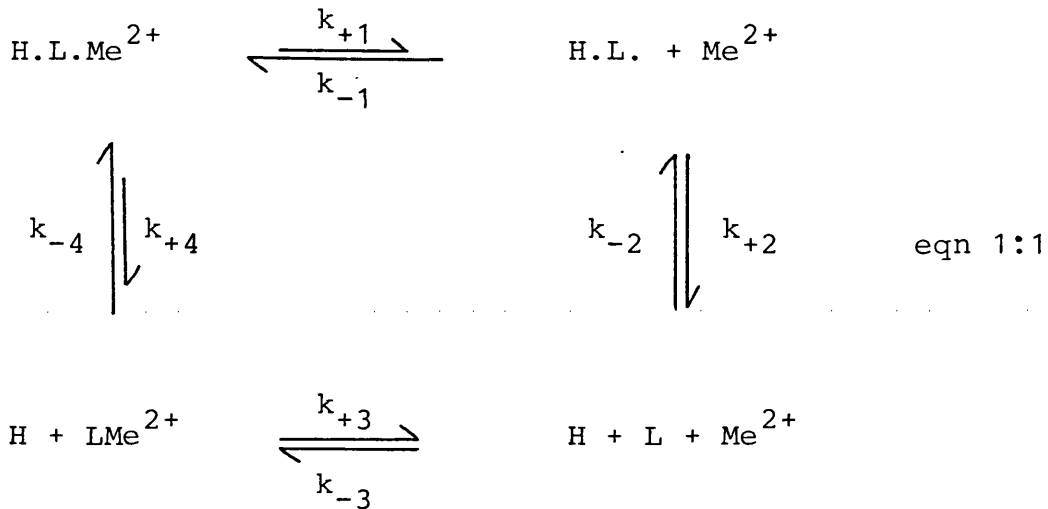
Myosin RLC contain homologous sequences corresponding to four E-F hands, as shown in Table 1-1. However, the structural implications are complicated because of non-conservative substitutions and deletions. Domain 1 is complete and



is therefore predicted to bind  $\text{Ca}^{2+}$ . The other 3 domains suffer from extensive deletions or non-conservative substitutions which are likely to alter the conformation of the E-F hand (Kendrick-Jones and Jakes, 1976). The study of  $\text{Ca}^{2+}$  binding sites of the RLC is complicated by the fact that they are influenced by the presence of the heavy chain. This situation was clarified by electron paramagnetic resonance studies using the paramagnetic Mn(II) ion (Bagshaw, 1977; Bagshaw and Kendrick-Jones, 1979). It was concluded from these studies that all species of myosin regulatory light chains contain one high-affinity, non-specific divalent metal ion binding site. In addition molluscan myosins contain two  $\text{Ca}^{2+}$  specific sites, but these sites are not necessarily located on the RLC. Bagshaw and Reed (1977) suggested that the non-specific site was not competent to act as a control for the early events of contraction, because of the slow exchange of  $\text{Ca}^{2+}$  and  $\text{Mg}^{2+}$  at this site.

Based on this evidence it was proposed that domain 1 of the RLC accounts for the high-affinity, non-specific divalent metal ion binding site and that the calcium-specific molluscan site probably involves ligand groups from the heavy chain and/or the essential light chain. This has been confirmed by the work of Chantler and Szent-Györgyi (1980), which showed that low-affinity  $\text{Ca}^{2+}$  binding sites remain on the myosin in myofibrils denuded of RLC. Readdition of the RLC restores the high-affinity  $\text{Ca}^{2+}$  binding sites lost on their removal from the myosin.

In scallop myosin, the non-specific site is involved in the association of the RLC with the heavy chain/ELC complex. This site must be occupied by either  $\text{Ca}^{2+}$  or  $\text{Mg}^{2+}$  for the RLC to remain associated (Bagshaw and Kendrick-Jones, 1979). The aim of this thesis was to study the mechanism of the RLC chain interaction with the myosin molecule. A minimal scheme for the dissociation of the RLC is given in eqn.1:1.



where H = myosin heavy chain/essential light chain complex,  
 L = regulatory light chain and  
 $\text{Me}^{2+}$  = divalent metal ion

This scheme is not a complete description of the mechanism and other factors must be considered. It does not take into account the fact that there are likely to be multiple interactions of the RLC with the heavy chain and essential light chain (Bagshaw and Kendrick-Jones, 1980; Hardwicke et al., 1983) and RLC dissociation is therefore likely to occur in more than one kinetically-distinct step. The degree of dissociation also depends on the molecular species being

studied. Regulatory light chains will dissociate readily from two-headed myosin, HMM or myofibrils, whereas in  $S1^{+RD}$  dissociation is limited (Stafford et al., 1979). In addition to the non-specific sites,  $Ca^{2+}$ -specific sites are present in myosin, which regulate ATPase activity (Szent-Györgyi et al., 1973). These sites complicate the evaluation of RLC dissociation, especially when calcium is present. However eqn 1:1 does define the overall thermodynamic relationships between the heavy chain/essential light chain complex and the regulatory light chain, and supplies a basis for further characterisation of the kinetic mechanism. The experimental approach to light chain dissociation can be conveniently divided into two sections, (i) metal ion dissociation, (ii) light chain detachment.

In rabbit skeletal myosin, dissociation of divalent metal ions from the non-specific site of the RLC is accompanied by an increase in protein fluorescence (Werber et al., 1972). Bagshaw and Reed (1977) used this fluorescence change to study the dissociation of  $Ca^{2+}$  and  $Mg^{2+}$  from the high-affinity, non-specific divalent metal ion binding site, by stopped-flow methods. Dissociation was found to occur with rate constants of  $0.46s^{-1}$  and  $0.057s^{-1}$  for  $Ca^{2+}$  and  $Mg^{2+}$  respectively. In scallop myosins, an analogous fluorescence change was not observed, so alternative methods for determining the rate of dissociation of these metal ions were required. Two methods have been employed, the first involves the use of pH indicators to follow proton fluxes, the second the use of the paramagnetic Mn(II) ion, which binds to the non-

specific site.

Dissociation of the RLC has been studied mainly using the fluorophore 8-anilino-1-naphthalene sulphonate (ANS), but also by labelling of light chain sulphhydryl groups with fluorescent probes. Previously, ANS, has proved a useful probe to study protein interactions. When free in aqueous solution, ANS has a very low quantum yield ( $Q = 0.004$ ). In non-aqueous solutions or when the ANS is bound to a macromolecule the intensity of the fluorophore emission is increased (typically  $Q = 0.2$  to  $0.7$ ). ANS has been used in several systems as a fluorescent, conformational probe to look at the effect of modulators and interactions. (eg glutamate dehydrogenase, Dodd and Radda, 1969; Apomyoglobin and Apohaemoglobin, Stryer, 1965). Cheung and Morales (1969), showed that ANS bound to rabbit skeletal myosin. On binding of the ANS to the protein, its fluorescence was enhanced and blue shifted. The quantum yield was estimated to be 0.48 and extensive energy transfer was observed between protein tryptophan residues and bound ANS. Preliminary work (Bagshaw et al., 1982), had indicated that ANS bound to scallop myosin and appeared to be a probe for the RLC binding site. The work presented in this thesis, extends this observation and relates the results to the interaction of the RLC with the heavy chain/essential light chain complex.

The results obtained are discussed with respect to the function of the RLC in the myosin molecule. What is the likely nature of the intramolecular association on the removal

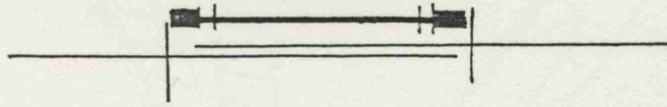
of the RLC? Is it likely to be a head-head interaction or some other change? How does the degree of RLC association in *in vitro* assays affect  $\text{Ca}^{2+}$  sensitivity of the ATPase activity obtained and can this be improved by changing storage conditions?

Fig 1-2

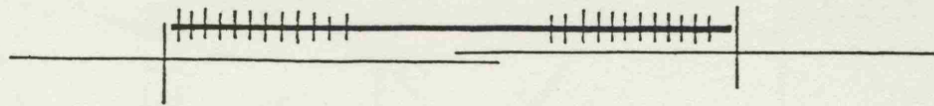
The dependence of active tension generation on sarcomere length in a frog muscle fibre

The passive elasticity of a relaxed muscle increases rapidly above a sarcomere length of 2.5  $\mu\text{m}$  and this has been subtracted from the total tension of the stimulated muscle. The positions indicated correspond to sarcomere lengths of (a) 1.05  $\mu\text{m}$ , (b) 1.65  $\mu\text{m}$  (c) 2.2  $\mu\text{m}$  and (d) 3.65  $\mu\text{m}$  (Based on Gordon et al., 1966)

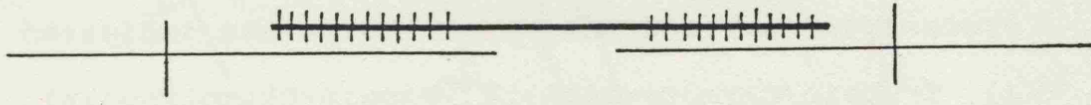
a)



b)



c)



d)

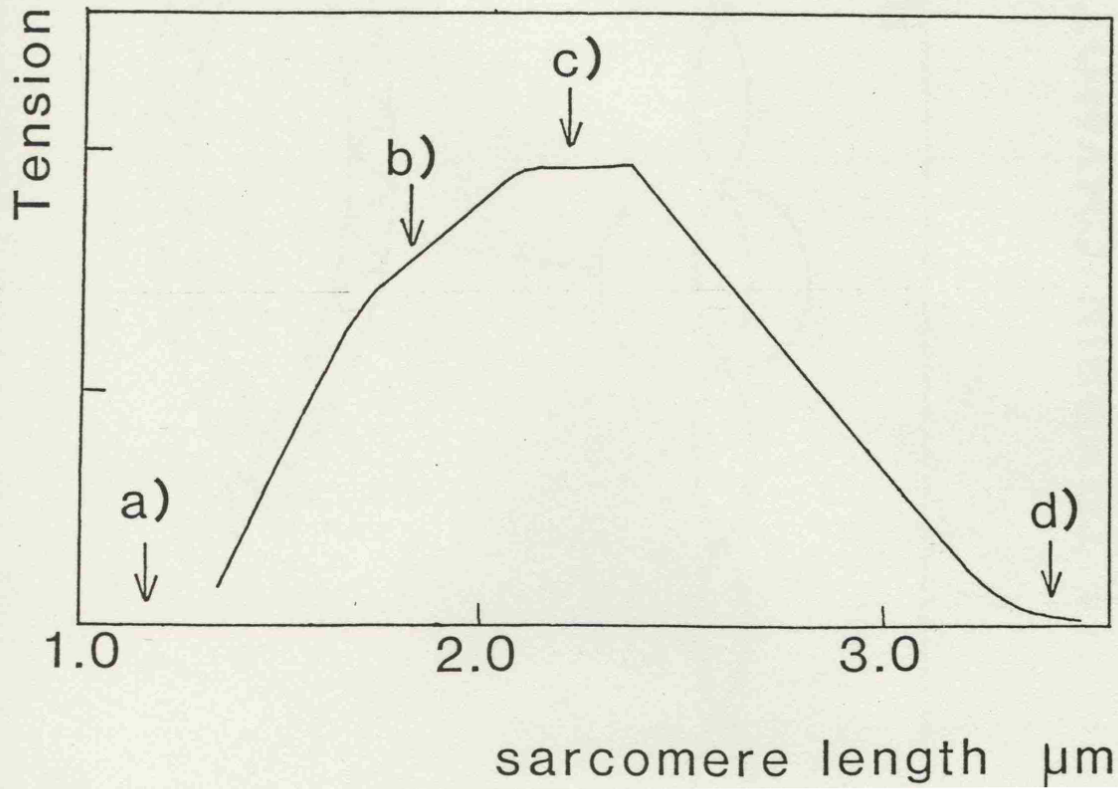
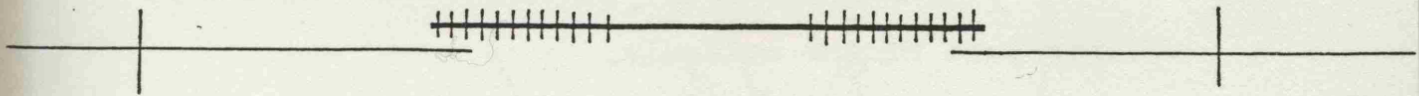
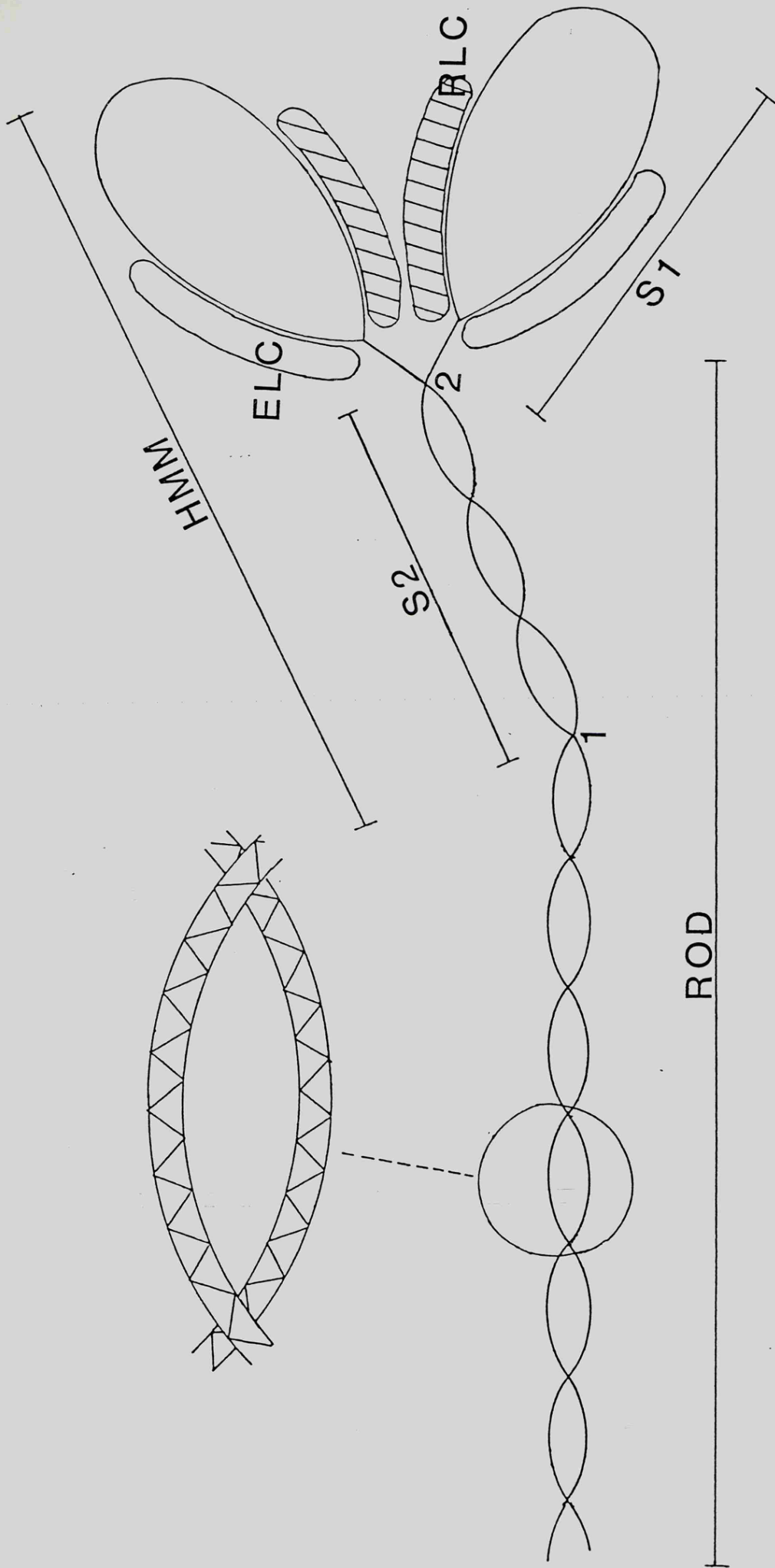


Fig 1-3

Schematic diagram of the myosin molecule

Proteolytic enzymes attack at the points indicated (1, Trypsin/Chymotrypsin; 2, Papain/Chymotrypsin), to release the subfragments indicated. The enlarged section of the rod indicates the coiled-coil nature of this part of the molecule.



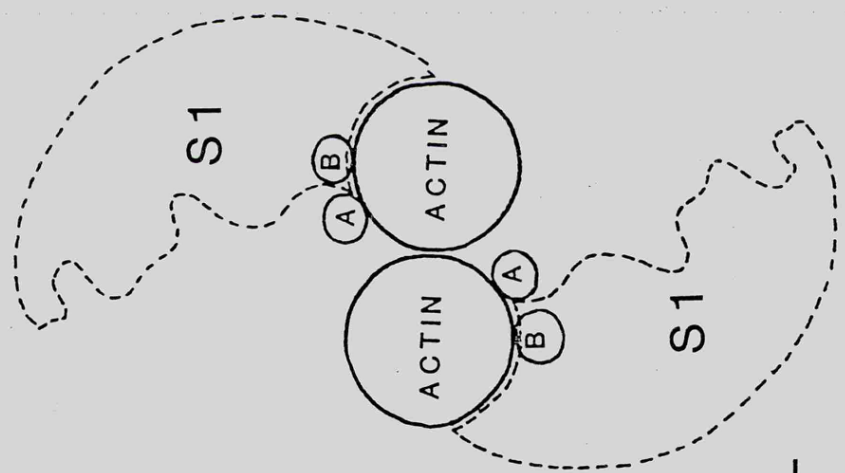
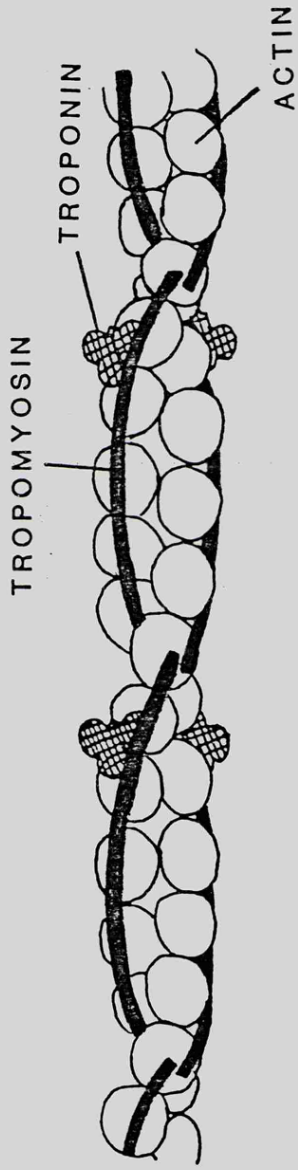
1. TRYPSIN/CHYMOTRYPSIN

2. PAPAIN /CHYMOTRYPSIN

Fig 1-4

The organisation of actin, tropomyosin and troponin  
in the thin filament

The cross-section of the filament indicates the relative positions of the tropomyosin, suggested to occur for thin filament regulation, in the steric-blocking mechanism.



TROPOMYOSIN:

A-ACTIVE POSITION

B-BLOCKED POSITION

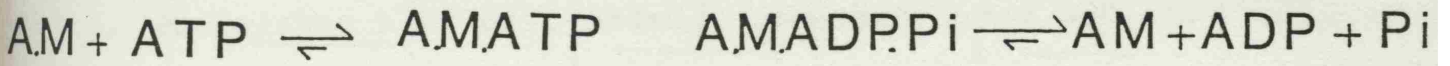
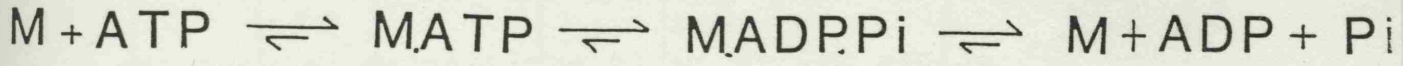
STERIC BLOCKING MODEL

Fig 1-5

Hydrolysis of ATP by myosin and actomyosin

- (a) The kinetic model of Lymn and Taylor, in which ATP dissociates the actomyosin prior to its hydrolysis.
  
- (b) Correlation of the cross-bridge cycle with chemical states according to the Lymn-Taylor (1971) model.

a)



b)

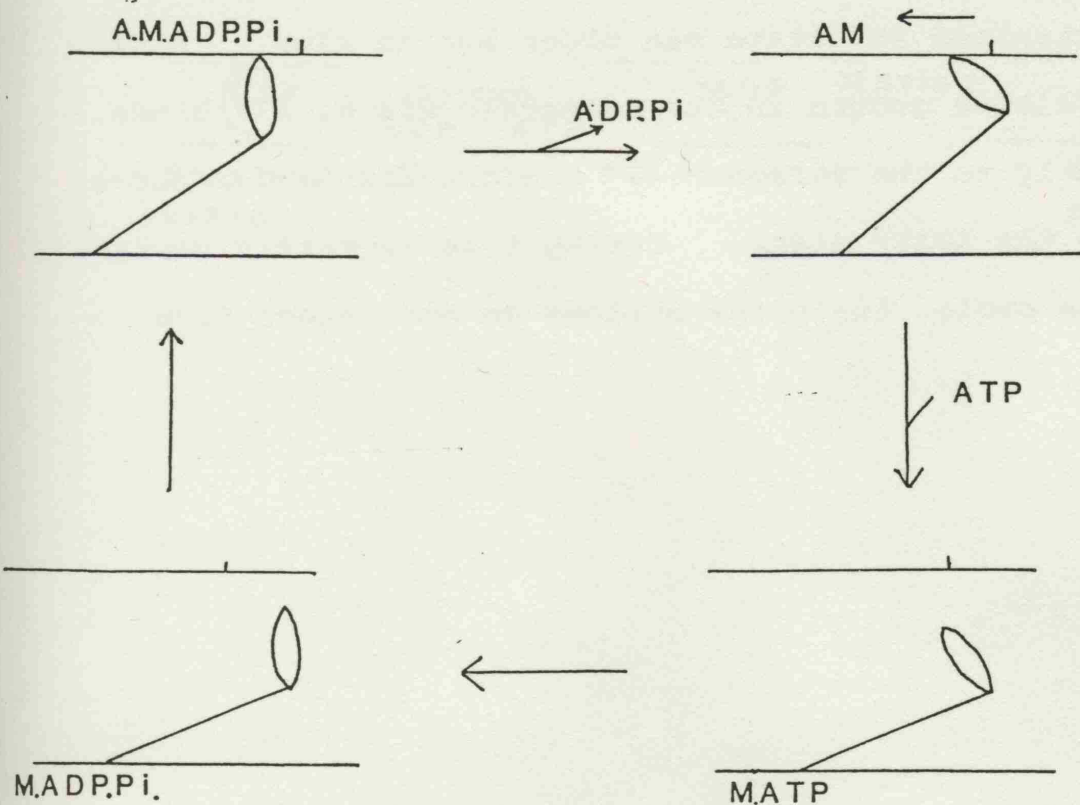


Fig 1-6

Cross-bridge model of Eisenberg and Greene (1980)

The 90° states are in rapid equilibrium between the actin free and actin bound states. The symbol  $\leftrightarrow$  indicates a transition with no activation energy or defined rate constant. Rather, it is a continuous conformational change as the filaments slide past each other. This is stage 2 of the transition from the unstrained 90° conformation to the unstrained 45° conformation. Stage 1 is represented by the Pi release step in this model. Isometric contraction, where there is no motion of the filaments, is the result of strain in the 45° cross-bridge state not being relieved. The model assumes ADP release from the strained 45° state can occur but is slow. After ADP release occurs in the isometric state, ATP binds directly to the strained 45° conformation and returns it to the AMATP state. During this isometric cross-bridge cycle, the cross-bridges do not detach from actin.

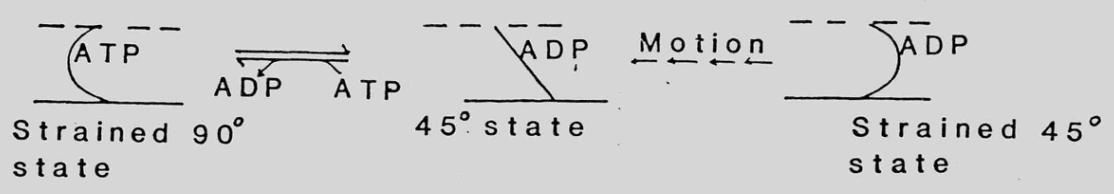
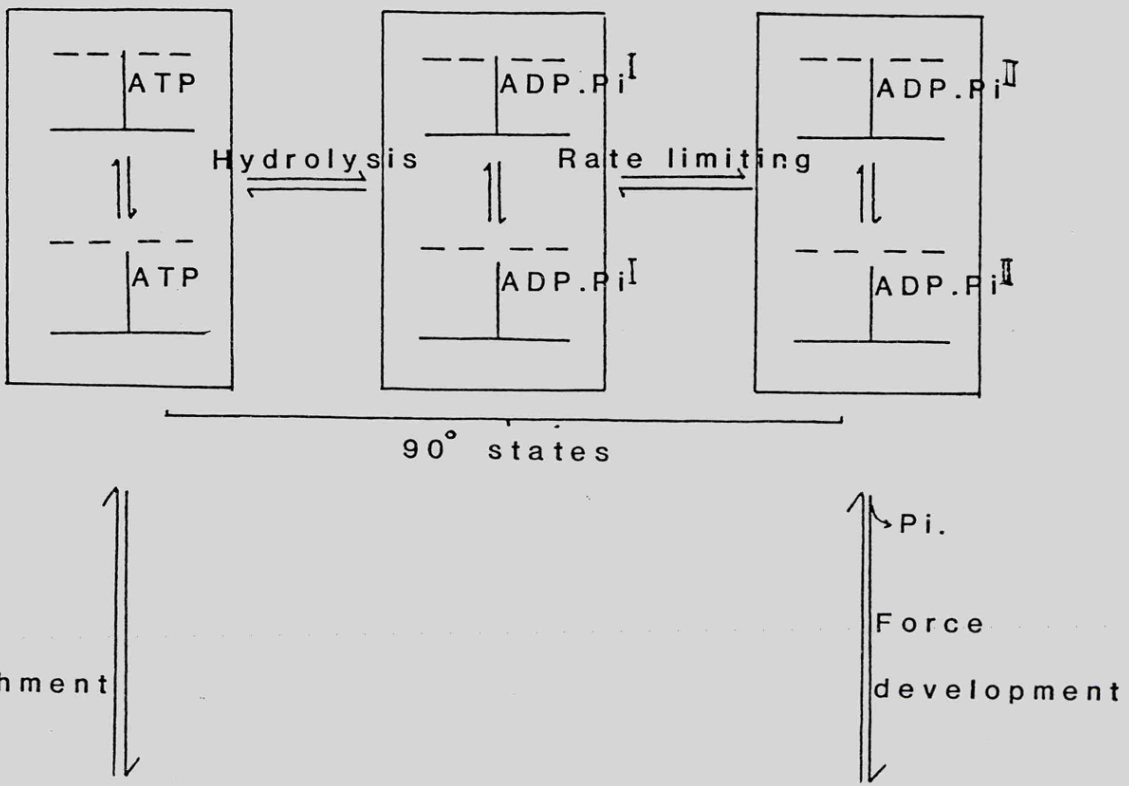
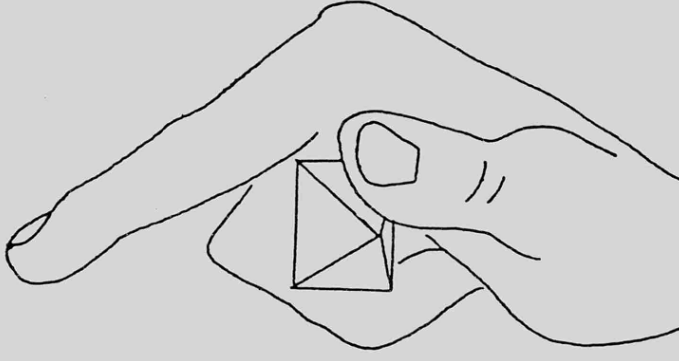
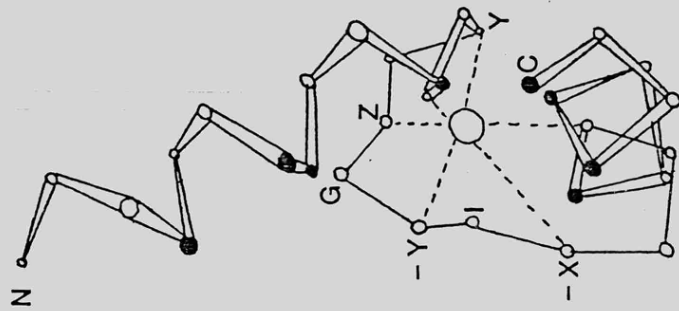


Fig 1-7

The EF-hand domain (Kretsinger, 1980)

The sequence of the domain is indicated below the diagram, where  $\bar{h}$  represents the amino-acids which contribute hydrophobic side chains to the core of the protein. The vertices of the octohedron, which represents the oxygen ligands about the  $\text{Ca}^{2+}$  ion, are indicated by X, Y and Z. The highly conserved Gly (G) and Ile (I) are labelled.



h . . . h h . . . h X . Y . Z . G - Y I - X . . - Z h . . . h h . . . h

## CHAPTER 2

### MATERIALS AND METHODS

#### PROTEIN PURIFICATION AND PREPARATION

##### STORAGE OF SCALLOP MUSCLE

Live scallops (*Pecten maximus*), obtained from the Marine Biological Station, Millport, were dissected so as to leave the striated adductor muscle in the shell at an extended length. The shells containing the muscles were rinsed in water, then placed in cold glycerination solution (40 mM NaCl, 5 mM sodium phosphate, 1 mM MgCl<sub>2</sub>, 0.1 mM EGTA, 50% (v/v) glycerol, 3 mM sodium azide, pH 7.0) and soaked overnight at 4°C. The muscles were removed from the shells and each muscle cut into 50-60 strips. The muscle strips were then soaked in glycerination solution for a further 48 hours, at 4°C, with two changes of the buffer and stored at -20°C in the same solution.

##### SCALLOP MYOFIBRIL PREPARATION

Scallop myofibrils were prepared essentially according to the method of Lehman and Szent-Györgyi (1975). In a typical preparation glycerinated muscle strips, equivalent to approximately one and a half scallop adductor muscles, were used. The glycerination solution was drained from the muscle strips and the strips blended (3 x 5 seconds, Braun Multiquick) in 1 litre of cold magnesium wash buffer (40 mM NaCl,

1.0 mM  $MgCl_2$ , 0.1 mM EGTA, 5 mM sodium phosphate, pH 7.0) at 4°C. The resulting suspension was then filtered through fine nylon net, to remove any unblended material. The filtrate was centrifuged for 10 minutes at 4°C (Sorvall RC5B, GSA rotor,  $RCF_{av} = 17310g$ ) to sediment the myofibrils. The myofibril pellet was resuspended to give a fine suspension in 1 litre of magnesium wash buffer and recentrifuged. The supernatant was discarded and the step repeated. If the final myofibril pellet was to be stored, 0.5 M sodium azide was added to give a final concentration of 3 mM sodium azide, at the last step. The myofibrils were then stored at 4°C. A yield of approximately 3 grams of myofibrils was obtained.

#### SCALLOP MYOSIN PREPARATION

Scallop myosin was prepared, from myofibrils, by an ammonium sulphate fractionation procedure (Chantler and Szent-Györgyi, 1978; Focant and Huriaux, 1976). The myofibrils were resuspended, on ice, in cold 40 mM NaCl, 5 mM sodium phosphate, pH 7.0, to give a fine suspension of 15-20 mg/ml. Cold 3 M NaCl and 0.1 M EGTA were then added, to give final concentrations of 0.6 M and 1 mM respectively. The suspension was left, at 4°C for 10 minutes, before addition of 0.1 M ATP to a final concentration of 5 mM. After incubation for a further 10 minutes, actomyosin was obtained by centrifugation at 4°C, for 10 minutes. (Sorvall RC5B, GSA rotor,  $RCF_{av} = 17310g$ ). The actomyosin supernatant was made 20 mM with respect to  $MgCl_2$ , and a further 5 mM with respect to ATP. Saturated ammonium sulphate, at 4°C, was added to give a

final 40% saturation and the actin precipitate removed by centrifugation (as above). Myosin was precipitated from the supernatant by further addition of cold saturated ammonium sulphate, to give a final 65% saturation. The suspension was centrifuged (as above) and the myosin pellets collected.

The myosin pellets were resuspended in magnesium wash buffer and dialysed in two litres of the same, for twelve hours, with one change of buffer. The myosin precipitating on dialysis, was centrifuged (as above), the pellets resuspended in one litre of magnesium wash buffer, recentrifuged, and the step repeated. If the myosin was to be stored, 3 mM sodium azide was added in the final wash. Typically a yield of 600 mg of myosin was obtained, from 3 grams of myofibrillar protein.

#### SCALLOP HEAVY MEROMYOSIN PREPARATION

Scallop heavy meromyosin (HMM) was made by tryptic digestion of myosin, using a modification of the procedure of Wells and Bagshaw (1983). Myosin was dissolved in 0.6 M NaCl, 10 mM sodium phosphate, 1 mM MgCl<sub>2</sub>, 1 mM CaCl<sub>2</sub>, 0.1 mM EGTA, pH 7.0, to give a solution of approximately 10 mg/ml. Solutions of 1 mg/ml TPCK-treated trypsin (Sigma, Poole) and 2 mg/ml soybean trypsin inhibitor (Sigma, Poole) were prepared in distilled water. The myosin solution was digested for 3 minutes at 20°C, with the trypsin, at a ratio of 1:1000 w/w trypsin;myosin. Digestion was stopped by addition of 5 mg trypsin inhibitor/mg trypsin. The digested preparation was then dialysed against 20 mM NaCl, 5 mM sodium phosphate,

1 mM MgCl<sub>2</sub>, 0.1 mM EGTA, pH 7.0, for 4 hours at 4°C, with two changes of buffer. Undigested myosin and light meromyosin (LMM) which precipitated, were removed by centrifugation for 10 mins at 4°C. (Sorvall RC5B, SS34, RCF<sub>av</sub> = 31,180g). Ammonium sulphate was then added to the supernatant to give 65% saturation. This precipitated the heavy meromyosin, which was collected by centrifugation (as above), resuspended in the required buffer and dialysed for 12 hours, at 4°C. Any precipitate forming on dialysis was removed by centrifugation.

#### SCALLOP SUBFRAGMENT 1 PREPARATION

Scallop subfragment 1 was prepared from myosin essentially as described for rabbit skeletal subfragment 1. (Bagshaw and Reed, 1976). Two forms of subfragment 1 (S1) were prepared, depending on the conditions of digestion. (Margossian *et al.*, 1975; Stafford *et al.*, 1979). Subfragment 1 containing the regulatory light chain was obtained by papain digestion in the presence of 1 mM MgCl<sub>2</sub> and 1 mM CaCl<sub>2</sub>. Such preparations are denoted S1<sup>+RD</sup> to distinguish them from S1<sup>-RD</sup>, produced in the presence of EDTA, which lacks the regulatory domain.

Freshly prepared myosin was resuspended to give a fine suspension in 0.12 M NaCl, 20 mM sodium phosphate pH 7.0 (containing either 2 mM EDTA or divalent metal ions) of between 10 and 20 mg/ml. Activated papain solution (132 µl papain (Sigma P3125), 300 µl 0.1 M dithiothreitol (DTT), 500 µl 3.0 M KCl, 2.065 ml water) was prepared, and the myosin suspension digested at 20°C, for 7 minutes, with 0.1 volume

of papain solution. The digestion was stopped by addition of iodoacetate (50 mM in 0.5 M sodium phosphate pH 7.0) to a final concentration of 0.05 mM, and further incubation at 20°C for 3 minutes. The digested myosin was diluted with cold 1 mM MgCl<sub>2</sub>, 1 mM CaCl<sub>2</sub> buffer to give a final concentration of 0.04 M NaCl. Any precipitate of undigested myosin or rod, was removed by centrifugation for 10 minutes, at 4°C (Sorvall RC5B, SS34, RCF<sub>av</sub> = 31180g). Ammonium sulphate was added to the supernatant to give 65% saturation and precipitate the subfragment 1. The resulting solution was centrifuged (as above) and the pellets resuspended and dialysed against the required buffer for 12 hours, at 4°C. Any precipitate forming during dialysis, was removed by centrifugation (as above).

#### SCALLOP REGULATORY FRAGMENT PREPARATION

The regulatory fragment was prepared by tryptic digestion of Scallop S1<sup>+RD</sup> (Szentkiralyi, 1984). Subfragment 1 (15 mg/ml) in 40 mM NaCl, 20 mM EPPS, 1 mM MgCl<sub>2</sub>, 1 mM CaCl<sub>2</sub> at pH 8.0 was digested with TPCK - treated trypsin at a ratio of 1:250 w/w trypsin:S1, for 20 minutes at 20°C. The reaction was stopped by addition of 5:1 w/w soybean trypsin inhibitor : trypsin.

A DEAE-cellulose (Whatman DE52) column 35 x 1.7 cm was pre-equilibrated at 4°C with 40 mM NaCl, 20 mM EPPS, 1 mM MgCl<sub>2</sub>, 1 mM CaCl<sub>2</sub>, pH 8.0. The digest was loaded, and eluted using a gradient comprising 0.04M to 1 M - NaCl, 20 mM EPPS, 1 mM MgCl<sub>2</sub>, 1 mM CaCl<sub>2</sub> at pH 8.0. The absorbance was monitored

at 280 nm (figure 2-1) using an LKB 2138 Uvicord analyser and an LKB 2065 chopper bar recorder. Fractions were collected on a LKB 2070 fraction collector. The fractions containing the fragment were identified by SDS gel electrophoresis, pooled and dialysed for 12 hours at 4°C in the required buffer. The fragment was stored at -20°C.

#### SCALLOP REGULATORY LIGHT CHAIN PREPARATION

Scallop regulatory light chains (RLC) were prepared by a modification of the procedure of Kendrick-Jones et al., (1976). Scallop myofibrils (2 mg/ml) in 40 mM NaCl, 5 mM sodium phosphate buffer pH 7.0 were incubated at 25°C with continuous stirring. EDTA was then added to a final concentration of 10 mM, incubation being continued for a further 15 minutes. The suspension was centrifuged for 10 minutes at 20°C (Sorvall RC5B, GSA,  $RCF_{av} = 17310g$ ). Isoelectric precipitation of the RLC in the supernatant was performed at pH 4.5 by addition of 1 M HCl, while monitoring the pH on a pH meter. The RLC precipitate was collected by centrifugation (as above). The precipitate was resuspended in cold magnesium wash buffer and dialysed in the same buffer for 12 hours at 4°C. After dialysis, the remaining precipitate was removed by centrifugation for 10 minutes at 4°C. (Sorvall RC5B, SS34,  $RCF_{av} = 31180g$ ). 0.1 M sodium acetate pH 4.5 buffer was prepared and the RLC was isoelectric precipitated, by dialysis at 4°C, followed by centrifugation (as above). The precipitate was resuspended in 50 mM NaCl, 25 mM Tris-HCl, 0.5 mM MgCl<sub>2</sub>, pH 8.0 and dialysed for 12 hrs, in the same buffer. Urea was added to the dialysed RLC, to give a final concentration of 2M, ready for column

purification.

A DEAE-cellulose column (Whatman DE52, 1.5 x 30 cm) was preequilibrated with 50 mM NaCl, 25 mM Tris-HCl, 2 M Urea, 0.5 mM MgCl<sub>2</sub>, pH 8.0. The absorbance of the eluting buffer was monitored at 280 nm, using an LKB 2138 Uvicord analyser and an LKB 2065 chopper bar recorder. Fractions were collected using an LKB 2070 Utrarac II fraction collector. The RLC sample was loaded, and eluted using a gradient comprising 0.05 M to 0.25 M NaCl, 25 mM Tris-HCl, 2 M Urea, 0.5 mM MgCl<sub>2</sub>, pH 8.0. A typical absorbance trace is shown in figure 2-2. Fractions corresponding to the peaks on the absorbance trace were measured on a Pye Unicam SP8-100 UV/Vis spectrophotometer, the RLC peak being identified by the characteristic tyrosine/phenylalanine spectrum of the RLC.

The fractions containing the RLC were pooled and dialysed against 0.1 M sodium acetate pH 4.5 buffer for 12 hours, to remove urea and isoelectric precipitate the regulatory light chains. The RLC were collected by centrifugation (as above), resuspended in a minimum volume of the required buffer and dialysed for 12 hours. Regulatory light chains were stored at -20°C.

#### SCALLOP ESSENTIAL LIGHT CHAIN PREPARATION

Scallop essential light chains (ELC) were prepared by a modification of the guanidine-HCl procedure of

Kendrick-Jones et al. (1976).

Myosin was resuspended in cold 5M guanidine-HCl, 50 mM Tris-HCl, 0.3M KCl, 3 mM EDTA, 5 mM DTT, pH8.0, to give approximately 6 mg/ml, and stirred gently at 4°C for 12 hours. One volume of cold distilled water was then added, followed by 4 volumes of cold 95% ethanol and the mixture left for 15 minutes. The white precipitate produced was centrifuged for 10 minutes at 4°C. (Sorvall RC5B, GSA,  $RCF_{AV} = 17310g$ ). Ethanol was evaporated from the supernatant, in a rotary evaporator (Büchl rotavapor 'R') at 38°C. The remaining solution was dialysed against 2 litres 50 mM NaCl, 25 mM Tris-HCl, 0.5 mM MgCl<sub>2</sub>, 0.5 mM DTT pH 8.0, at 4°C, for 12 hours with one change of buffer.

A DEAE-cellulose column (Whatman DE52, 30 x 1.5 cm) was pre-equilibrated with 50 mM NaCl, 2 M urea, 25 mM Tris-HCl, 0.5 mM MgCl<sub>2</sub>, 0.5 mM DTT pH 8.0. The dialysed ELC, were centrifuged for 10 min at 4°C (Sorvall RC5B, SS34,  $RCF_{AV} = 31180g$ ) to remove any precipitate. Urea was added to the supernatant, to give a final concentration of 2M. The sample was loaded onto the column and eluted using a gradient comprising 0.05 M to 0.25 M NaCl, 25 mM Tris-HCl, 0.5 mM MgCl<sub>2</sub>, 0.5 mM DTT, 2M urea at pH 8.0. The absorbance of the eluate was monitored at 280 nm. A typical trace is shown in fig 2+3. The fractions containing ELC were identified by urea-polyacrylamide gel electrophoresis (fig 2-4) pooled and ammonium sulphate added to give 70% saturation.

The ELC were collected by centrifugation (as above) and dialysed in the required buffer for 12 hours at 4°C. The ELC were stored at -20°C.

#### CLAM MUSCLE PREPARATION

Clams (*Mercenaria mercenaria*) were obtained from Sea Salter Shellfish Company, Whitstable, Kent. The shellfish were dissected, the pink adductor muscle was separated from the white muscle, and soaked in cold glycerination solution (40 mM NaCl, 5 mM sodium phosphate, 1 mM MgCl<sub>2</sub>, 0.1 mM EGTA, 50% v/v glycerol, 3 mM sodium azide, pH 7.0) overnight at 4°C. The solution was changed and the muscle stored at -20°C.

#### *Mercenaria* RLC PREPARATION

*Mercenaria* RLC were prepared by a modification of the procedure of Kendrick-Jones et al., 1976.

Previously dissected pink adductor muscle was diluted in magnesium wash buffer, blended (3 x 5 seconds, Braun Multiquick) and filtered through fine nylon net. The resultant suspension was centrifuged for 10 minutes at 4°C (Sorvall RC5B, GSA, RCF<sub>AV</sub> = 17310g). The myofibril pellets obtained were resuspended in magnesium wash buffer, centrifuged and the step repeated.

The myofibrils were resuspended in 40 mM NaCl, 5 mM sodium phosphate pH 7.0, to give a suspension of approximately 2 mg/ml. EDTA and DTNB were both added to a final concentration of 5 mM and the suspension incubated at 25°C for 10 minutes with continuous stirring. The suspension was centrifuged (as above) and ammonium sulphate added to give 40% saturation. The precipitate was removed by centrifugation (as above). Regulatory light chains in the supernatant were then precipitated by addition of ammonium sulphate to 75% saturation, and collected by centrifugation. The pellets were resuspended in 50 mM NaCl, 25 mM Tris-HCl, 0.5 mM MgCl<sub>2</sub>, 1 mM DTT, pH 8.0 and dialysed for 12 hours to remove the ammonium sulphate and DTNB.

The RLC were then purified on a DEAE-cellulose column (Whatman DE52, see scallop RLC preparation) or by FPLC (Pharmacia, Mono Q). Urea was added to the sample to give a final concentration of 2M. The sample was loaded onto the column and eluted by a gradient comprising 0.02 to 0.5 M NaCl, 25 mM Tris-HCl, 0.5 mM MgCl<sub>2</sub>, 2 M urea, 1 mM DTT, pH 7.5. Several peaks were present in the FPLC absorption trace (figure 2-5). The RLC peak was identified by urea-polyacrylamide gel electrophoresis. Fractions containing the RLC were pooled and dialysed against 0.1 M sodium acetate pH 4.5 buffer, to precipitate the RLC. The RLC was collected by centrifugation (Sorvall RC5B, SS34,  $R_{CF_{AV}} = 31180g$ , 10 minutes), resuspended in 40 mM NaCl, 10 mM EPPS, 0.1 mM MgCl<sub>2</sub>, 0.1 mM EGTA, pH 8.0 and dialysed for 12 hours. The RLC was stored at -20°C.

RABBIT SKELETAL MYOSIN PREPARATION

Rabbit skeletal myosin was prepared by a simplified method, based on that of Margossian and Lowey (1982). A white New Zealand rabbit (7-8 kg) was killed and bled. The back and white leg muscles were removed and placed in iced deionised water to chill the muscle. After cooling, the muscle was minced (Moulinex Charlotte 3), weighed and extracted with 3 volumes of Guba-Sraub buffer (0.3 M KCl, 0.15 M potassium phosphate pH 6.5) for 30 minutes with gentle stirring at 4°C (time from killing to extraction was approximately 30 minutes). Extraction was stopped by addition of 4 volumes of cold deionised water and the solution was filtered through 3 layers of fine nylon net. The filtrate was further diluted with cold deionised water to give a final ionic strength of approximately 0.04 M. (The extracted mince was retained for acetone powder preparation). After 4 hours at 4°C, the supernatant was siphoned off and the precipitate remaining was collected by centrifugation. (Sorvall RC5B, GSA, RCF<sub>AV</sub> = 17310g, 10 min). The precipitate was dispersed in 250 ml of 0.6 M KCl, 5 mM imidazole pH 7.0 and allowed to dissolve overnight. Cold deionised water (1.14 volumes) was added, slowly, with continuous stirring, to precipitate the actomyosin. This precipitate was removed by centrifugation (as above) and discarded. Myosin in the supernatant was precipitated by addition of 6 volumes of cold deionised water, and left for 15 minutes before being centrifuged (as above). The myosin precipitate was redissolved in 250 ml of 0.6 M KCl,

5 mM imidazole pH 7.0 and the dilution step repeated.

The final precipitate was dissolved in 150 ml cold 1.2 M KCl, 10 mM sodium phosphate, 2 mM MgCl<sub>2</sub>, 0.2 mM EDTA, 6 mM sodium azide, pH 7.0, mixed with an equal volume of glycerol and stored at -20°C.

#### ACETONE POWDER PREPARATION

The minced muscle pellet was stirred in 5 volumes of 0.4% w/v NaHCO<sub>3</sub>, 0.1 mM CaCl<sub>2</sub> for 30 minutes. The suspension was then passed through nylon net, the filtrate discarded and the pellet resuspended in 1 volume of 10 mM NaHCO<sub>3</sub>, 10 mM Na<sub>2</sub>CO<sub>3</sub>, 0.1 mM CaCl<sub>2</sub>. After 10 minutes, the resulting suspension was poured into 5 litres of deionised water at room temperature and immediately filtered through fine nylon net, at 4°C. As much water as possible was removed from the pellet, and the pellet resuspended in 1 litre of cold (4°C) acetone for 15 minutes. The acetone was then decanted and a further litre of cold acetone added. After a further 15 minutes, the residue was filtered and dried for storage at -20°C, until required for actin preparation.

#### RABBIT ACTIN PREPARATION

Approximately 4g of rabbit muscle acetone powder was suspended in 80 mls of buffer containing 0.5 mM ATP, 0.5 mM DTT, 0.2 mM CaCl<sub>2</sub>, 10 mM Tris-HCl pH 8.5. The suspension was

incubated on ice for 1 hours, before being filtered through fine nylon net. The filtrate, containing the crude G-actin, was collected and refiltered using filter paper (Whatman No. 1). After filtration the solution was centrifuged, (MSE 50, 43114-125 rotor, 1 hr,  $RCF_{AV} = 120000g$ ). The supernatant was collected and sodium phosphate,  $MgCl_2$  and  $KCl$  added to give 10 mM, 1 mM and 50 mM final concentrations respectively. This solution was then incubated for 1 hour at  $20^\circ C$ , prior to addition of solid  $KCl$  to give a final concentration of 0.85 M, followed by incubation for 15 hours at  $4^\circ C$ , to polymerise the actin. The F-actin was collected from the solution by centrifugation for 2.5 hours (as above). The actin pellet was resuspended in cold 2 mM Tris, 1 mM DTT, 100  $\mu M$  ATP, pH 8.0 and dialysed for 12 hours at  $4^\circ C$ , with one change of buffer. Clarification of the preparation was performed by centrifugation in a Sorvall RC5B (SS34, 10 min,  $4^\circ C$ ,  $RCF_{AV} = 31180g$ ). The clarified actin was polymerised by addition of  $NaCl$  and  $MgCl_2$  to give 0.1 M and 2 mM respectively. If the actin was to be stored, sodium azide was added to give a final concentration of 1 mM and the preparation kept at  $4^\circ C$ .

#### RABBIT-HEAVY MEROMYOSIN PREPARATION

Rabbit heavy meromyosin (HMM) was produced from myosin, by digestion with  $\alpha$ -chymotrypsin, essentially according to Weeds and Taylor (1975).

Rabbit myosin was dissolved in 0.6 M  $NaCl$ , 0.05 M potassium

phosphate, 1 mM MgCl<sub>2</sub>, 1 mM CaCl<sub>2</sub>, pH 7.0 buffer to give a 2% w/v myosin solution and allowed to dissolve. Stock solutions of 0.5 mg/ml  $\alpha$ -chymotrypsin (Sigma C4129) in deionised water and 0.1 M phenyl methane sulphonyl fluoride (PMSF, BDH Chemicals Ltd) in absolute ethanol were prepared. The 2% myosin solution was incubated at 20°C for 5 minutes and  $\alpha$ -chymotrypsin added to give a final concentration of 0.05 mg/ml. After digestion for 10 minutes, the reaction was stopped by addition of PMSF to give a final concentration of 0.3 mM. Prior to addition, the PMSF was diluted in buffer to prevent denaturation of the protein. The reaction was incubated for a further 5 minutes.

Light meromyosin (LMM) present in the digest was precipitated by dialysis at 4°C in 0.02 M NaCl, 0.01 M triethanolamine, 1 mM DTT, pH 7.0. The precipitate was removed by centrifugation for 10 minutes at 4°C (Sorvall RC5B, SS34, RCF<sub>AV</sub> = 31180g) and the HMM supernatant dialysed into the required buffer.

#### RABBIT SUBFRAGMENT 1 PREPARATION

Rabbit skeletal subfragment 1 (S1) was prepared either by papain digestion (Bagshaw and Reed, 1976, see scallop preparations) or by  $\alpha$ -chymotrypsin (Weeds and Taylor, 1975) which produces a preparation lacking any regulatory light chains.

Rabbit myosin, previously stored in glycerol at -20°C, was diluted with 16 volumes of cold deionised water, centrifuged

(Sorvall RC5B, GSA,  $RCF_{AV} = 17310g$ , 10 minutes, 4°C), and resuspended in cold 0.6 M NaCl, 1 mM EDTA, 20 mM sodium phosphate pH 7.0 buffer. The myosin was allowed to dissolve and dialysed for 12 hrs in 0.12 M NaCl, 20 mM sodium phosphate pH 7.0 at 4°C to produce myosin filaments. Stock solutions of 1 mg/ml  $\alpha$ -chymotrypsin in deionised water and 0.1 M PMSF in absolute ethanol were prepared. The myosin filaments were equilibrated at 20°C for 3 minutes, and  $\alpha$ -chymotrypsin added to give a final concentration of 0.05 mg/ml. After digestion for 10 minutes the reaction was stopped by addition of PMSF to 0.1 mM and incubation for a further 3 minutes. Two volumes of cold, deionised water was added to precipitate the myosin rod, which was removed by centrifugation (as above).

Ammonium sulphate was added to the supernatant to give 65% saturation and precipitate the chymotryptic S1 (CS1). The solution was centrifuged (Sorvall RC5B, SS34, 31180g, 10 minutes, 4°C) to pellet the CS1, the pellets were redissolved in 40 mM NaCl, 10 mM triethanolamine pH 7.1, and dialysed for 12 hours, to remove the ammonium sulphate. The CS1 was then dialysed in the required buffer for the experiment.

#### RABBIT SKELETAL DTNB-LIGHT CHAIN PREPARATION

Rabbit DTNB light chain was made from rabbit myosin by essentially the same procedure as that used for *Mercenaria* RLC. The RLC was purified on DEAE cellulose (Whatman DE52) as for scallop RLC.

DESENSITIZATION OF SCALLOP MYOSIN AND MYOFIBRILS

Scallop myosin or myofibrils were resuspended in 40 mM NaCl, 5 mM sodium phosphate pH 7.0 to give a fine suspension of 2-4 mg/ml. Desensitization was performed at either 0°C (to remove 50% of RLC) or 25°C (to remove all the RLC). The desensitization was initiated by addition of 0.1 M EDTA to give a final concentration of 10 mM, and the suspension incubated for 5 minutes, at the desired temperature. The desensitized preparation was precipitated by centrifugation at either 4°C or 20°C respectively for 10 minutes (Sorvall RC5B, GSA,  $RCF_{AV} = 17310g$ ). After centrifugation, the samples were resuspended in cold 40 mM NaCl, 10 mM Tris-HCl pH 8.0 to remove EDTA and phosphate and recentrifuged at 4°C (as above). The desensitized myosin or myofibril pellet was resuspended in the required buffer.

Estimation of the amount of desensitization was made by urea-polyacrylamide gel electrophoresis, (fig 2-6) stained with 0.2% w/v fast green. The gels were scanned using a Pye Unicam SP8-100 spectrophotometer in the densitometer mode (Table 2-1).

Table 2-1 Results of Gel scans from figure 2-6

Preparation	Ratio RLC/ELC	% RLC remaining
MYOSIN	0.6	100
0° DES. MYOSIN	0.27	45
25° DES. MYOSIN	0.11	18

LABELLING OF LIGHT CHAINS WITH 4-(N-(IODOACETOXY)ETHYL-  
N-METHYL AMINO-7-NITROBENZ-2-OXA-1,3 DIAZOLE

4-(N-(iodoacetoxy)ethyl-N-methyl amino-7-nitrobenz-2-oxa-1,3 diazole (IANBD) was dissolved in acetone to give a solution of 10 mg/ml. *Mercenaria* RLC or scallop ELC were then incubated with an equimolar amount of the label in the dark, at 4°C for 4 hours on a rocking platform (A600, DENLEY, ENGLAND). The buffer used during labelling was 40 mM NaCl, 20 mM EPPS, 100 µM MgCl<sub>2</sub>, 100 µM DTT at pH 8.0. Prior to addition of the IANBD, the label was diluted in reaction buffer, to prevent denaturation of the protein. After 4 hours the labelled preparation was centrifuged (Ependorf, Bench model, full speed, 3 minutes, 4°C) to remove any remaining insoluble label. The labelled light chains were dialysed for 16 hours in 40 mM NaCl, 20 mM EPPS, 100 µM MgCl<sub>2</sub>, 100 µM DTT, pH 8.0 with one change of buffer. Labelled light chains were stored at -20°C.

ESTIMATION OF PROTEIN CONCENTRATION

Protein concentrations were routinely measured in a Pye-Unicam SP8-100 UV/Vis spectrophotometer, using the absorbance at 280 nm ( $A_{280}$ ). Samples which were insoluble were solubilised by boiling in 1% sodium dodecyl sulphate prior to checking the absorbance. All measurements were made by scanning from 340 nm to 220 nm so that an estimation for the baseline could be obtained. Table 2-2 gives the values used for the  $A_{1\text{ cm.}280\text{ nm}}^{1\%}$  of the proteins. (Chantler and Szent-Györgyi, 1978; Bagshaw and Kendrick-Jones, 1979; Wells and Bagshaw 1983).

Table 2-2

Protein	$A_{1\text{ cm } 280\text{ nm}}^{1\%}$
Scallop myofibrils	7.2
" myosin	5.4
" HMM	6.5
" S1	7.9
" RLC	1.8
" ELC	5.5
Rabbit myosin	5.4
" HMM	6.5
" S1	7.9
" DTNB-LC	5.5
<i>Mercenaria</i> RLC	5.5

### CONCENTRATION OF PROTEINS

Proteins were concentrated when necessary, using a Minicon B15 Ultrafiltration cell or Centricon concentrator (Amicon Ltd). The Centricon concentrators were centrifuged at 4,000g in a MSE Chilspin at 4°C. Both methods were used to concentrate the proteins up to 30 mg/ml. All the soluble myosin subfragments could be concentrated in this way as long as their molecular weights were greater than the cut-off of the membranes.

### GENERAL METHODS

#### pH MEASUREMENTS

Unless otherwise stated, all pH measurements were made at 20°C. Buffers were checked either on a Radiometer (Copenhagen) PHM82 Standard pH meter with a Russell (Scotland) CMAWL Combination electrode or on a Petracourt PHM 4 portable pH meter with a Russell gel filled combination electrode.

#### DENSITOMETRY OF GELS

Mini polyacrylamide gels were scanned on a Pye Unicam SP8-100 UV/Vis spectrophotometer with a 790826 densitometer attachment. The gels were normally previously stained in 0.2% fast green. Scans were performed at 635 nm.

SDS POLYACRYLAMIDE GRADIENT GEL ELECTROPHORESIS

SDS polyacrylamide gel electrophoresis was performed, based on the method of Laemmli (1970). Gradients of 7.5 to 20% w/v acrylamide were produced by mixing two solutions, to produce a linear gradient.

Gel solutions	7.5%	20%	4.5% Stacking gel
1.5M Tris-HCl pH 8.8, 0.4% w/v SDS	2.25 ml	2.25 ml	-
0.5M Tris-HCl pH 6.8, 0.4% w/v SDS	-	-	2.45 ml
30% w/v acrylamide, 0.8% bisacrylamide	2.25 ml	6.0 ml	1.5 ml
Deionised water	4.475 ml	0.5 ml	6.0 ml
Glycerol	-	0.225 ml	-
TEMED	5 $\mu$ l	5 $\mu$ l	10 $\mu$ l
10% ammonium persulphate	20 $\mu$ l	20 $\mu$ l	40 $\mu$ l

The gel (size, 15 x 11 x 0.2 cm) was overlaid with isobutanol and allowed to set (typically 30 minutes). Excess isobutanol was then removed, and a 4.5% stacking gel added. A comb was placed in the stacking gel, to produce wells for loading the sample. Samples were prepared by mixing 60  $\mu$ l of protein solution (2-4 mg/ml) with 5  $\mu$ l of  $\beta$ -mercaptoethanol, and 35  $\mu$ l of sample buffer (0.18 M Tris-HCl, 5.7% w/v SDS, 29% v/v glycerol, 0.005% w/v bromothymol blue at pH 6.8). The samples were boiled for 2 minutes to ensure complete dissociation and typically 20  $\mu$ l of a 2 mg/ml solution was loaded onto

the gel. The running buffer used was 0.025 M tris base, 0.2 M glycine, 0.1% w/v sodium dodecyl sulphate. Gels were run for 4 hrs at 20 mA with water cooling, using a Chandos power pack, stained in 10% v/v acetic acid, 50% v/v methanol, 0.2% w/v Kenacid blue (BDH Chemicals Ltd) for 4 hrs and destained by diffusion, in 10% v/v acetic acid, 50% v/v methanol. The destained gels were stored in 10% v/v acetic acid. Gels showing examples of protein preparations are shown in figure 2-7.

#### MINI-GEL ELECTROPHORESIS

Mini SDS-polyacrylamide gels (13 x 6 x 0.4 cm) or urea-polyacrylamide gels were used for rapid separation of proteins. Gel mixtures were as follows:

Gel Solution	15% SDS polyacrylamide	10% urea-polyacrylamide
30% w/v acrylamide, 0.8% bisacrylamide	5.0 ml	2.77 ml
Separating buffer (3M Tris-HCl pH 8.8)	1.25 ml	1.04 ml
20% w/v SDS	50 µl	-
Urea	-	4g
TEMED	5 µl	5 µl
10% w/v ammonium persulphate	30 µl	30 µl
β-mercaptoethanol	-	1 µl
Deionised water	3.665 ml	1.3 ml

The gels were poured, overlaid with deionized water and allowed to set (normally 15 minutes). Samples were prepared by mixing equal volumes of protein solution (2-4 mg/ml) with either SDS sample buffer (2% w/v SDS, 2% v/v  $\beta$ -mercaptoethanol, 25% v/v glycerol, 20 mM sodium phosphate pH 7.0) and boiled, for SDS gels or with urea sample buffer (3g urea, 0.5 ml H<sub>2</sub>O, 0.5 ml separating buffer, 0.2  $\mu$ l  $\beta$ -mercaptoethanol) and warmed to 60°C, for urea gels. Bromothymol blue was added to the sample to act as a tracking dye. Electrophoresis was performed in 50 mM Tris-glycine pH 8.6 buffer, with 0.1% SDS for SDS gels, or without SDS for urea gels. The gels were run for 45 minutes at 20 mA, stained in 0.2% Kenacid blue (or fast green), 50% methanol, 10% acetic acid and destained by diffusion in 50% methanol, 10% acetic acid. The gels were stored in 10% acetic acid.

#### PYROPHOSPHATE POLYACRYLAMIDE GEL ELECTROPHORESIS

Pyrophosphate gels were run by a modification of the method of Hoh (1976). Pyrophosphate solubilizes the proteins without denaturation, therefore allowing separation according to their native molecular weight. Tubes were washed in 0.1 M HCl for 12 hours and dried, one end of each tube was then sealed with nescofilm. A 3.8% acrylamide gel mixture was prepared, and adjusted to pH 9.0, before addition of the ammonium persulphate. The gels were overlaid with deionised water and allowed to set. Samples were prepared to give a final protein

Gel solution	3.8% gel mixture
0.2M sodium pyrophosphate pH 9.0	10 ml
30% w/v acrylamide	6.5 ml
1.25% w/v Bis acrylamide	4.8 ml
Glycerol	5.0 ml
TEMED	112 $\mu$ l
Cysteine	18 mg
1 M MgCl <sub>2</sub>	50 $\mu$ l
Deionised water	23.45 ml
10% w/v ammonium persulphate	80 $\mu$ l
	-----
Total	50 ml
	-----

concentration of approximately 1 mg/ml, in 40 mM sodium pyrophosphate, 50% v/v glycerol, 1 mM MgCl<sub>2</sub>, 0.4 mg/ml cysteinewith bromothymol blue as a tracking dye. The gels were run at 4°C, in 40 mM sodium pyrophosphate, 10% v/v glycerol, 1 mM MgCl<sub>2</sub> at pH 9.0 for 24 hours at a constant current of 3 mA/gel. Buffer was continuously flowed between the upper and lower reservoirs by means of a peristaltic pump, both reservoirs were continuously stirred. After electrophoresis the gels were stained in 0.2% v/v Kenacid blue, 50% v/v methanol, 10% v/v acetic acid, destained in 50% v/v methanol, 10% v/v acetic acid and stored in 10% acetic acid. An example of such tube gels is shown in fig 2-8 for papain digestion of scallop myosin.

EXPERIMENTAL METHODS AND PRINCIPLES

STEADY-STATE ACTIN ACTIVATED Mg<sup>2+</sup>-ATPase MEASUREMENTS

Principle

When ATP is hydrolysed (eqn 2:1), protons are liberated into solution. The rate of production of H<sup>+</sup> may



be determined from the amount of NaOH required to maintain a constant pH, using an automatic burette. The stoichiometry of H<sup>+</sup> produced per ATP can be calculated from the pk's involved, and thus when ATP is hydrolysed at a given pH, the rate of ATP hydrolysis can be calculated. A correction factor of 1.5 per ATP is obtained at pH 7.5 and 1.15 at pH 8.0 (White, 1982).

Method

The actin activated Mg<sup>2+</sup>-ATPase of myofibrils, myosin and subfragments was followed by proton liberation using a Radiometer RTS 822 pH stat. 0.5-1.0 mg of protein was assayed at 25°C in an 8 ml reaction mixture, containing 20 mM NaCl, 1 mM MgCl<sub>2</sub>, 0.1 mM EGTA, 0.5 mM ATP at pH 7.5. Rabbit F-actin was added at a weight ratio of 1:3 for scallop myofibrils or myosin and approximately 1:1 for HMM or S1. The ATPase activities were first recorded in the absence

of  $\text{Ca}^{+2}$  (ie. 0.1 mM EGTA) and then in the presence of 0.2 mM  $\text{CaCl}_2$  ( $\sim 0.1$  mM free  $\text{Ca}^{2+}$ )

## SPECTROSCOPIC MEASUREMENTS

### (a) Stopped flow

#### Principle

Stopped-flow techniques can be used to study reactions which are too fast to measure by manual methods. In this technique, the solutions to be mixed are placed in two drive syringes. On rapidly pushing these syringes, the solutions pass into a mixing chamber and then into the observation cell. The solution previously in the observation cell passes into a collection syringe which pushes a microswitch to trigger the recording apparatus. The time taken for the solution to flow from the mixing chamber to the observation cell is referred to as the "dead-time" of the machine. This is typically between 1 and 3 ms and limits the speed at which the reaction can be monitored. Constant temperature is maintained by a circulating water bath. Changes in absorption/transmission or fluorescence in the observation cell are followed with time. In the case of absorption/transmission for small changes in transmission (<10%), the change in transmission is approximately proportional to the change in concentration. The machine actually measures

intensity (I) and hence directly measures the transmission (T) eqn 2:2.

$$T = I/I_0 \qquad \text{eqn 2:2}$$

Conversion to an absorbance value requires further electronic circuitry and may introduce additional undesirable noise. For small changes, the signal to noise ratio needs to be as large as possible, therefore for these changes transmission is preferred. For larger changes (>10%), absorption must be used because of the non-linearity <sup>of the</sup> transmission.

#### Method

Rapid changes in transmission were recorded using an Aminco-Morrow stopped-flow apparatus (1 cm optical pathlength) attached to a DW2 dual wavelength spectrophotometer. The signal was captured using a C.F.Palmer 8137 signal averager and displayed on a Tetronix RM 561A oscilloscope. A constant temperature of 20°C was maintained using a Churchill circulating water bath. Reactions, using bromophenol blue as a pH indicator, were monitored using the differential transmission at 618 nm and 420 nm. Those using phenol red were monitored at wavelengths of 560 nm and 430 nm.

Proteins to be used for rapid absorption stopped-

flow, using pH indicators, were dialysed to remove excess buffer. This was performed at 0°C, against the desired solution, using a Radiometer RTS 822 pH stat, to maintain the dialysate at a constant pH.

Fluorescence stopped-flow work was performed with a home-made stopped-flow accessory, mounted in a Baird-Atomic SFR 100 spectrofluorimeter, which allowed delivery of the reactants within 50 ms. The observation cell comprised a 2 mm internal diameter quartz tube, mounted in a 45 x 12 x 12 mm cell, so that it fitted the standard holder of the fluorimeter. The reactants were injected from two 5 ml syringes, via capillary tubing (T/Pe, Amicon-Wright) to a mixing jet built into the base of the observation cell. Fluorescence was monitored in the 90° mode as described in the fluorescence section.

(b) Electron spin resonance (esr)

Principle

$Mn^{2+}$  gives an esr signal, unlike  $Ca^{2+}$  and  $Mg^{2+}$ , due to the presence of unpaired electrons. Therefore esr can be used to follow exchange between  $Mn^{2+}$  and other metal ions. Unpaired electrons in a molecule can assume two orientations, either with or against an applied magnetic field. Electron spin resonance is the result of the interchange between these

orientations, with the absorption of electromagnetic energy by the electrons. This absorption of energy from the microwave radiation ( $\sim 10^{10}$  Hz) is normally measured as the first derivative of the absorption spectrum. This is the result of the modulation system employed in detection in esr spectrometers.

Manganese possesses five unpaired electrons in its 'd' orbitals and therefore five transitions are possible. In a crystal this would give rise to five peaks in the esr spectrum. However, in solution (ie  $\text{Mn}(\text{H}_2\text{O})_6^{2+}$ ) all the electrons are effectively equivalent and the five transitions are superimposed. However, since each electronic transition is coupled to the nuclear spins, six hyperfine coupling peaks are clearly observed in the  $\text{Mn}(\text{H}_2\text{O})_6^{2+}$  spectrum (fig 2-9a). If the  $\text{Mn}^{2+}$  is bound to a protein the electrons are no longer equivalent and the signal is quenched and broadened to give a "powder" spectrum as shown for scallop RLC in fig 2-9b. This change in the spectrum is the result of the manganese ion no longer being free to tumble and the presence of an asymmetric environment. Changes in the amplitude of the  $\text{Mn}^{2+}$  signal on binding allow this binding to be monitored.

#### Method

Esr measurements were obtained using a Varian E109 spectrometer at a microwave frequency of 9.1GHz.

The time course of  $Mn^{2+}$  binding was followed by recording the intensity of the second hyperfine peak ( $m_I = 3/2$ ) of the  $Mn(H_2O)_6^{2+}$  signal, at a field strength of 3059G. Rapid mixing of the protein and manganese solutions was achieved by injecting the reactants through a perspex dual-jet mixing chamber, from two 250  $\mu$ l glass syringes (Scientific Glass Engineering, Australia), into a 1 mm diameter quartz tube located in the spectrometer cavity. Injection of the first 2 x 125  $\mu$ l aliquots, allowed the spectrometer to be tuned at 50 mW. The second injection allowed the signal to be recorded within approximately one second of mixing. Nitrogen was flushed through the dewar, containing the quartz capillary, to maintain the temperature at a constant 20°C. At the end-point of each reaction the esr spectra were scanned, to check on the extent of bound and free  $Mn^{2+}$ .

(c) Fluorescence

Principle

In some molecules, the absorption of a photon is followed by emission of light of a longer wavelength (ie lower energy), this emission is referred to as fluorescence. When a molecule is excited, radiation is absorbed to promote an electron from one electronic energy level, the ground state, to another, the excited state. Within each of these states there are several

vibrational energy levels. If the molecule is initially in the ground state and the absorbed energy is greater than that required to reach the first excited state, the excess energy can be absorbed as vibrational energy. This vibrational energy is rapidly dissipated as heat and the molecule drops to the lowest vibrational level of the excited state. The excited state molecule can then return to the ground state, by either emitting fluorescence or by a non-radiative transition. Because of the loss of energy, the fluorescence will be of longer wavelength than the initially absorbed light. The ratio of the number of emitted to absorbed photons is defined as the quantum yield ( $Q$ ), which is a measure of the fluorescence efficiency. Molecules which have high vibrational levels, can dissipate the energy as heat, by non-radiative transitions between vibrational levels of the same energy, in the ground and excited state. This is the most common way for excitation energy to be lost. The amplitude and wavelength of the fluorescence emission are very sensitive to environmental factors. The effect of the environment is mainly to provide radiationless processes that compete with fluorescence to reduce  $Q$ , a phenomenon known as quenching. These processes are normally the result of collisions between molecules with exchange of energy, or long range energy transfer processes which act to dissipate the energy.

If a solution of a fluorophore contains molecules

of a second compound, which may be excited at the emitting wavelength of the first molecule, some of the emitted photons may excite the second molecule to produce an excited acceptor species. This can also occur by a non-radiative process called resonance energy transfer. As different electronic states have different electron distributions, there is a change in dipole during a transition between the two states. If two molecules can undergo transitions of equal energy but opposite sign, their transition dipoles may couple (dipolar coupling). The excited state energy of one molecule (the donor) can thus be transferred to the other (the acceptor), which may then itself fluoresce. The probability of this occurring depends on the overlap of the relevant absorption and emission spectra, the distance separating the molecules and their relative orientations. An example of this phenomenon, is the transfer between protein tryptophan residues and ANS (fig 2-10a). The emission spectrum of tryptophan overlaps the absorption spectrum of ANS (fig 2-10b) and if the distance and orientation are correct, resonance energy transfer will occur between the molecules.

In practice fluorescence may be monitored in two ways, the 90° mode, where emitted light is monitored at 90° to the incident light or in the front face mode, where emitted light is measured from the surface illuminated by the incident light. This second method

is particularly useful for looking at strongly absorbing solutions, or solutions which may cause a large degree of light scattering. Under experimental conditions, the observed signal from a solution, relative to the concentration of the fluorophore, generally decreases as the concentration increases. This decrease is called the 'inner filter' effect and is due to attenuation of the light. Attenuation of the exciting beam may occur in regions of solution in front of the point from which the fluorescence is collected by the detection system, or due to absorption of the emitted fluorescence within the solution. To reduce these effects, the fluorophore should be used at as low a concentration as possible.

#### Method

Fluorescence assays were performed using a Baird-Atomic SFR100 spectrofluorimeter, operating in the ratio mode. Measurements were normally performed in a 3 ml quartz fluorescence cell (1 cm optical path length), unless otherwise stated (see stopped-flow section). The temperature was maintained at 20°C, by a water cooled block attached to a Tempette TE8A circulator mounted on a Techne RB5 refrigerated water bath. ANS fluorescence emission was monitored at 460 nm (10 nm slit), by exciting the fluorophore either directly at 380 nm (5 nm slit) or via the protein tryptophan residues at 295 nm (5 nm slit). The ANS

was routinely used at 20  $\mu\text{M}$ , as a compromise between signal intensity and undesirable inner-filter effects. Fluorescence of IANBD-labelled scallop ELC or *Mercenaria* RLC was monitored at 530 nm (10 nm slit) by exciting at 470 nm (10 nm slit). The intrinsic tryptophan fluorescence was followed at 340 nm by exciting at 295 nm.

Changes in the fluorescence of solutions of scallop myofibrils were followed in the front-face mode. In myosin solubilised in 0.6 NaCl or myosin subfragments the fluorescence was monitored using the 90° mode.

(d) Determination of binding ratios

Principle

Binding ratios can be efficiently determined by a procedure first used by Hummel and Dreyer (1962). A gel column is pre-equilibrated with buffer containing the ligand at the desired concentration. A protein sample, in a minimal volume is then equilibrated with ligand at the same concentration. If the protein binds ligand, the solution will then be depleted of the ligand. When the sample is run on the column, the protein is separated from the ligand depleted solution, the protein moving ahead with the bound ligand. The elution profile will then exhibit a peak due to that bound to the protein, followed by

a trough due to the ligand depleted solution. In principle the area of the peak and trough will be the same. In practice, however, when spectrophotometric methods are used the measurement of the area of the trough is more reliable. This is because the scattering or absorption caused by the protein itself can interfere.

As the maximum separation of the peak and trough is required, a gel should be used which totally excludes the protein and a length:diameter ratio of at least 10 should be used for the column. The effluent from the column is passed into a flow cell, located in a spectrophotometer, so that a continuous elution profile is obtained. From the trace the area of the trough is determined and the amount of ligand bound calculated from equation 2:3.

$$\mu\text{moles bound} = \frac{\text{area of trough}}{ab(\epsilon_L \times 10^{-3})} \quad \text{eqn 2:3}$$

where a is the recorder pen displacement which corresponds to unit absorbance and b, is the chart movement corresponding to a 1 ml increment of column effluent.

#### Method

A 140 mm x 5 mm column was packed with Sephadex - G50 and equilibrated in the required buffer. The

buffer eluting from the column, was passed through a flow cell located in the sample holder of a Perkin-Elmer lambda 5 UV/Vis spectrophotometer. A constant flow rate was maintained using a peristaltic pump (Uniscil UMP3). For ANS, the absorbance of the eluting solution was monitored at 380 nm. The area of the troughs were measured using an Apple graphics tablet, attached to an Apple II+ microcomputer.

#### ANALYSIS OF DATA

Time courses, where appropriate, were analysed by a least squares fit to an exponential. For multiple-step schemes the time courses of the formation and decay of the various intermediates were computed by numerical integration. The values assigned to the rate constants were adjusted by trial and error to give an acceptable fit to the observed profile. The computer programs used are described by Millar (1984). Calculations of concentrations at equilibrium, in multicomponent systems, was achieved using the iterative procedure of Storer and Cornish - Bowden (1976). All computations were performed using an Apple II+ microcomputer.

Fig 2 -1      Purification of the regulatory fragment

The tryptic digest of S1<sup>+RD</sup>, was purified by ion exchange on a Whatman DE52 column (35 x 1.7 cm) at 4°C. The fragment was eluted by a 800 ml (total) NaCl gradient, comprising 0.04 to 1.0M NaCl, 20 mM EPPS, 1 mM MgCl<sub>2</sub>, 1 mM CaCl<sub>2</sub> at pH 8.0, running at a flow rate of 17 ml/hour. The regulatory fragment was found in fractions 33 to 37.

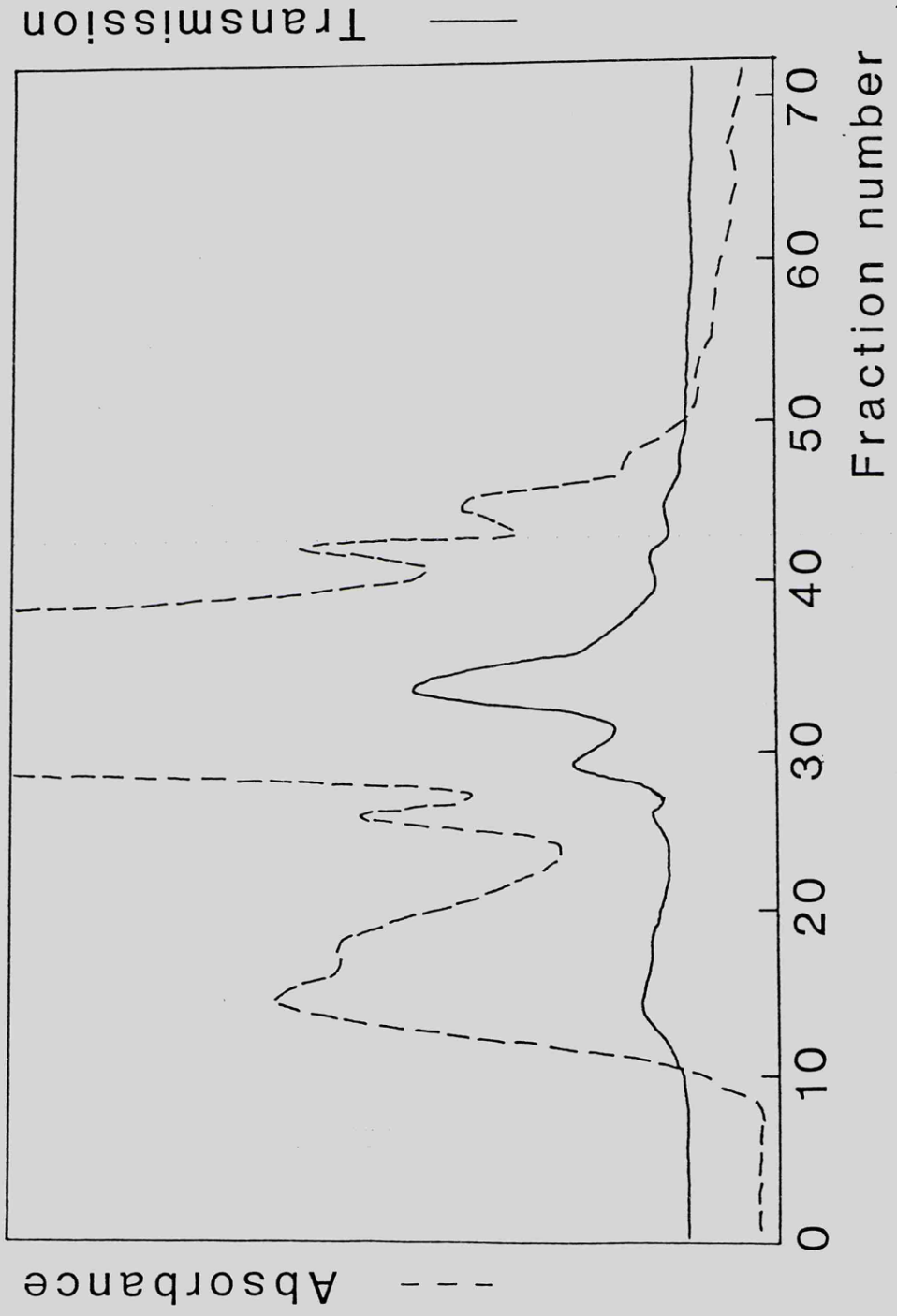


Fig 2-2      Scallop regulatory light chain purification

The scallop regulatory light chains were purified by ion-exchange on a Whatman DE-52 column (30 x 1.5 cm). The proteins were eluted by a 500 ml (total) NaCl gradient comprising 50-250 mM NaCl, 25 mM Tris-HCl, 0.5 mM MgCl<sub>2</sub>, 2 M urea at pH 8.0. The regulatory light chains eluted in fractions 25 to 28.

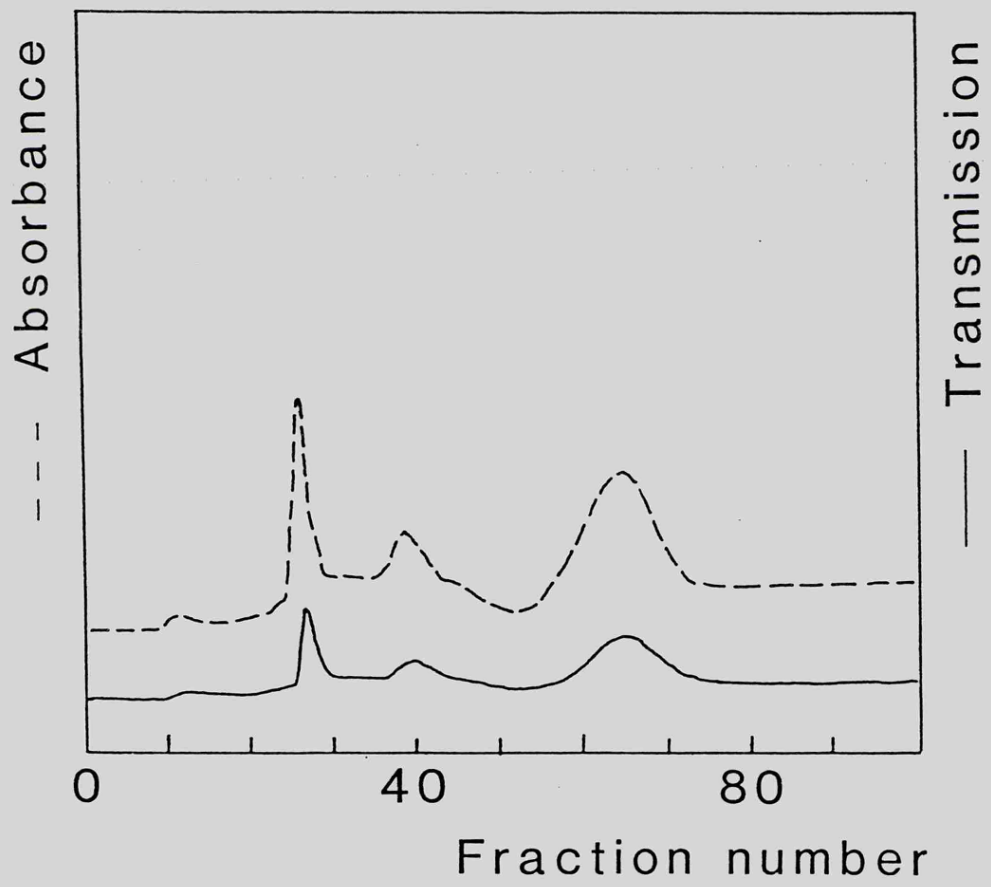


Fig 2-3 Scallop essential light chain purification

The essential light chains were purified by ion-exchange using a Whatman DE52 column (30 x 1.5 cm). The proteins were eluted by a 500 ml (total) NaCl gradient, comprising 50-250 mM NaCl, 25 mM Tris-HCl, 0.5 mM MgCl<sub>2</sub>, 2 M urea, 0.5 mM DTT pH 8.0. Essential light chains were identified in fractions 55 to 63.

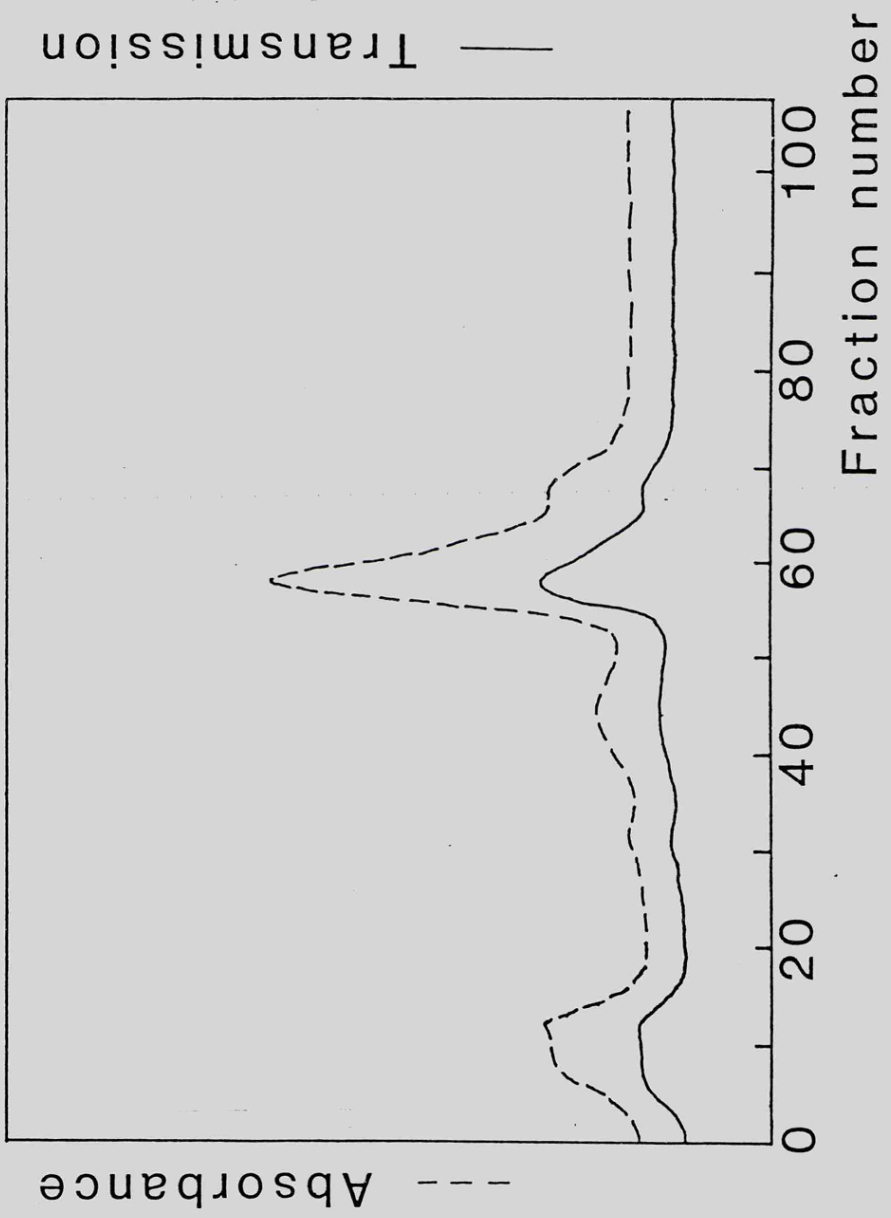


Fig 2-4     Mini urea-polyacrylamide gel to identify  
ELC fractions from ion-exchange column

Tracks (a) and (f), are myofibril markers run to show the relative position of the RLC, ELC and tropomyosin. The other tracks are the fractions eluted as shown in fig 2-3, with (b) fraction 55 (c) fraction 59 (d) fraction 61 and (e) fraction 63. Fraction 63 was observed to contain contaminant tropomyosin so was discarded.

a

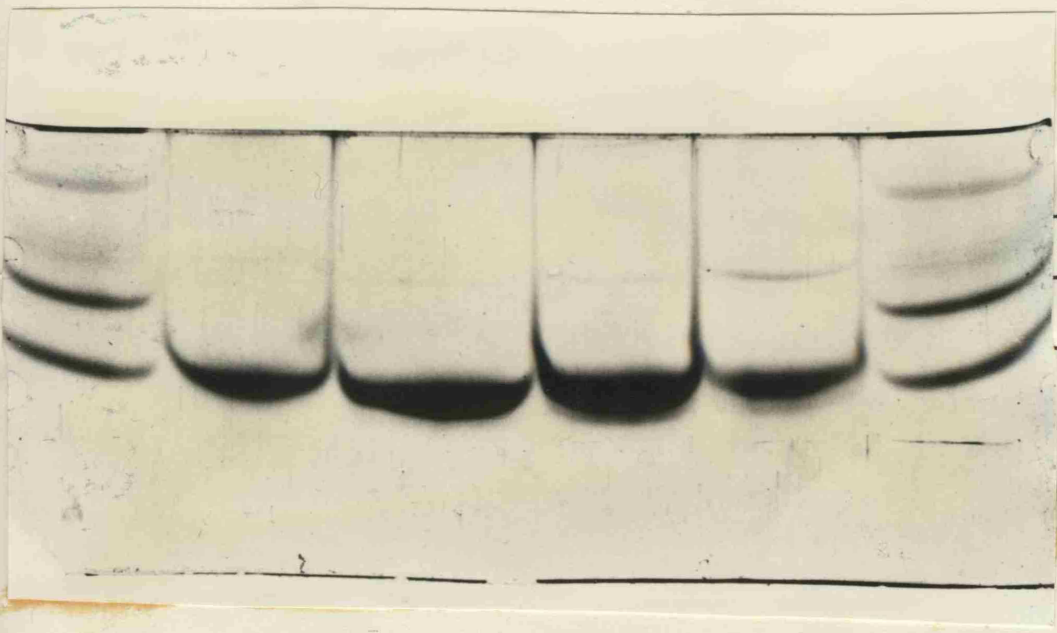
b

c

d

e

f



— TROPOMYOSIN  
— RLC  
— ELC

Fig 2-5    FPLC purification of *Mercenaria* RLC

The RLC were purified on a Pharmacia FPLC apparatus using a 1 ml Mono Q ion-exchange column. A 15 ml gradient comprising 0.02 M to 0.5 M NaCl, 25 mM Tris-HCl, 0.5 mM MgCl<sub>2</sub>, 2 M urea, 1 mM DTT at pH 7.5 was used to elute the protein. The flow rate was 1 ml/min. The RLC eluted at 0.2 M NaCl, as a sharp peak in fractions 11 and 12.

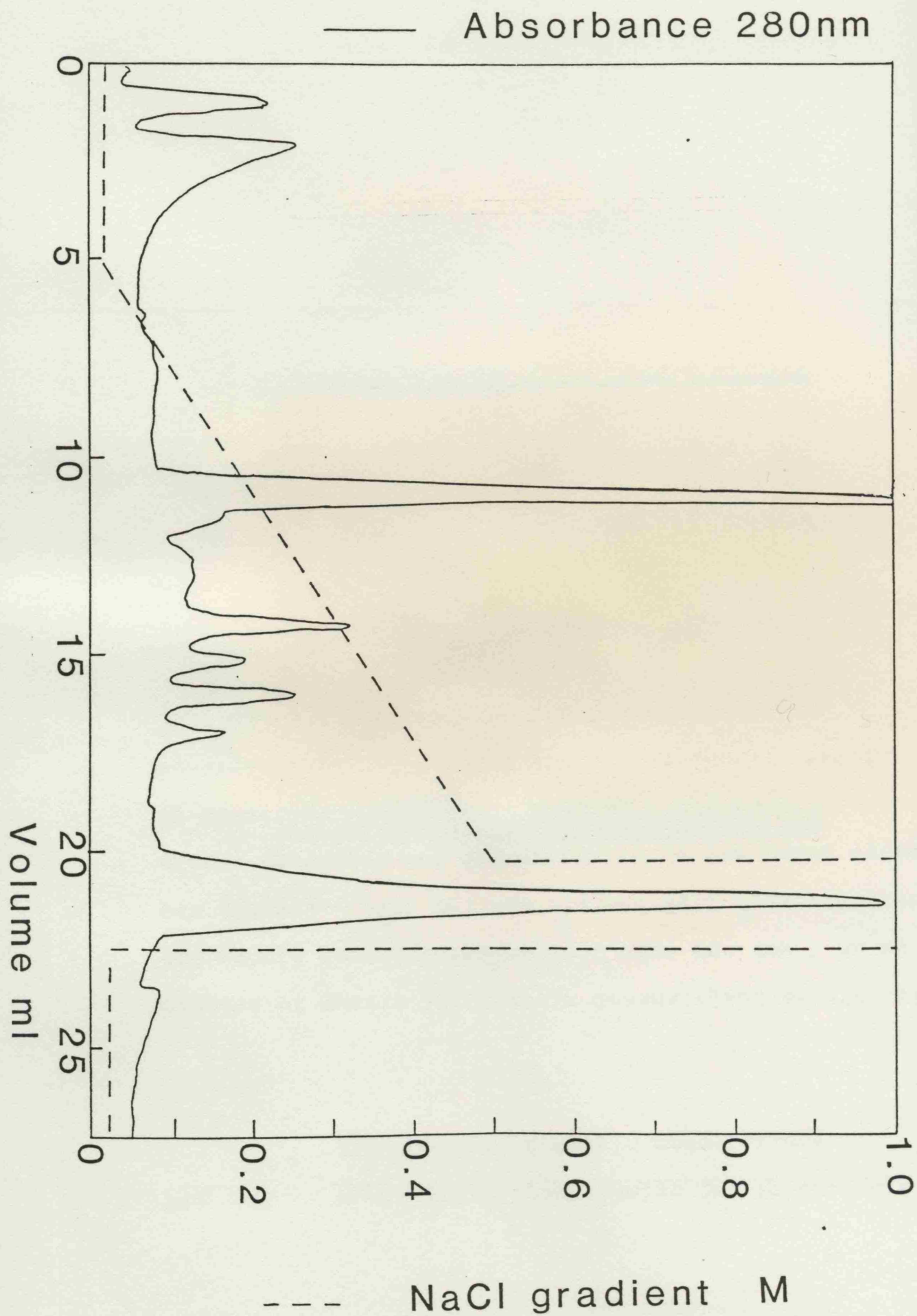


Fig 2-6

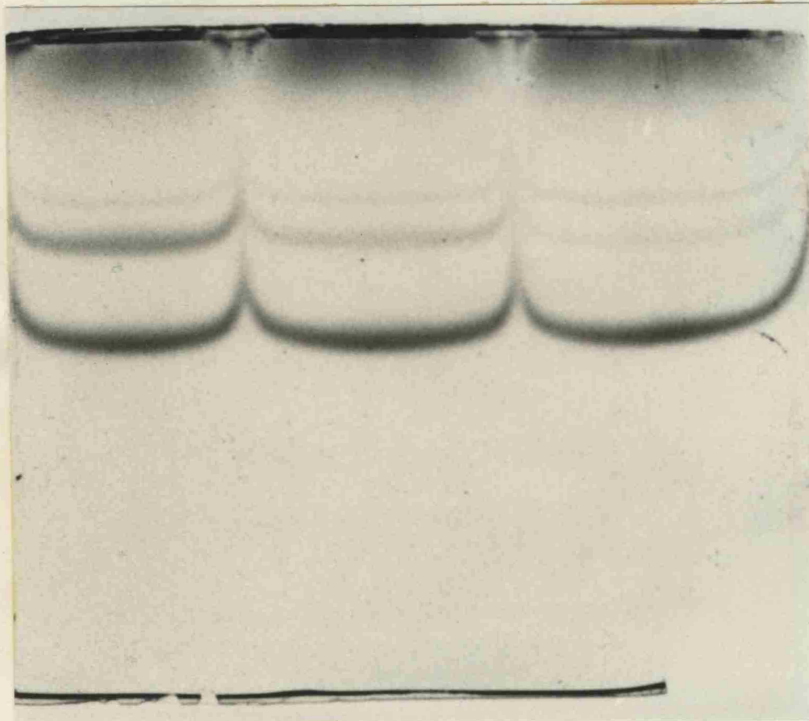
Mini urea-polyacrylamide gel to estimate  
RLC content of myosin preparations

Samples of myosin (a), myosin desensitised at 0°C (b) and myosin desensitised (c) at 25°C were run for 1 hr at 3mA per channel. The gel was stained with 0.2% w/v fast green, destained and the intensity of the bands estimated by densitometry. This revealed that the desensitised myosins contained 10% and 45% of the initial RLC for the 25°C and 0°C treated preparations respectively.

a

b

c



— TROPOMYOSIN  
— RLC  
— ELC

Fig 2-7    SDS Polyacrylamide gel electrophoresis of  
scallop myosin and its proteolytic subfragments

*Pecten maximus* myosin and its proteolytic fragments were electrophoresed on a SDS/7.5 - 20% (w/v) polyacrylamide gradient gel as follows:- (a) myosin; (b) HMM; (c)  $S1^{+RD}$ ; (d)  $S1^{-RD}$ ; (e) regulatory fragments.  $S1^{+RD}$  and the regulatory fragment contain a truncated form of the RLC (mRLC).  $S1^{-RD}$ , which lacks the regulatory domain, has no intact light-chain band and also has a slightly smaller heavy chain component than  $S1^{+RD}$ .



Fig 2-8      Pyrophosphate - polyacrylamide gel  
electrophoresis of a papain digest of  
scallop myosin

Papain digests of *Pecten maximus* myosin were run on pyrophosphate/3.8% (w/v) polyacrylamide gels for 24 hours at 3mA/gel. Digestion was performed with 0.03 units papain/mg myosin, in 0.6 M NaCl, 20 mM EPPS, 1 mM MgCl<sub>2</sub>, 100 μm EGTA, 200 μM CaCl<sub>2</sub> at pH 8.0 and 20°C. Samples were removed from the reaction mixture and digestion stopped by addition of iodoacetic acid. They were electrophoresed as follows:-

- (a) 80 min. (b) 40 min, (c) 20 min, (d) 10 min,  
(e) 5 min, (f) 2 min and (g) native myosin.

Disappearance of intact myosin and appearance of single headed myosin, S1<sup>+RD</sup> and rod was observed (cf. Stafford et al., 1979).

a

b

c

d

e

f

g



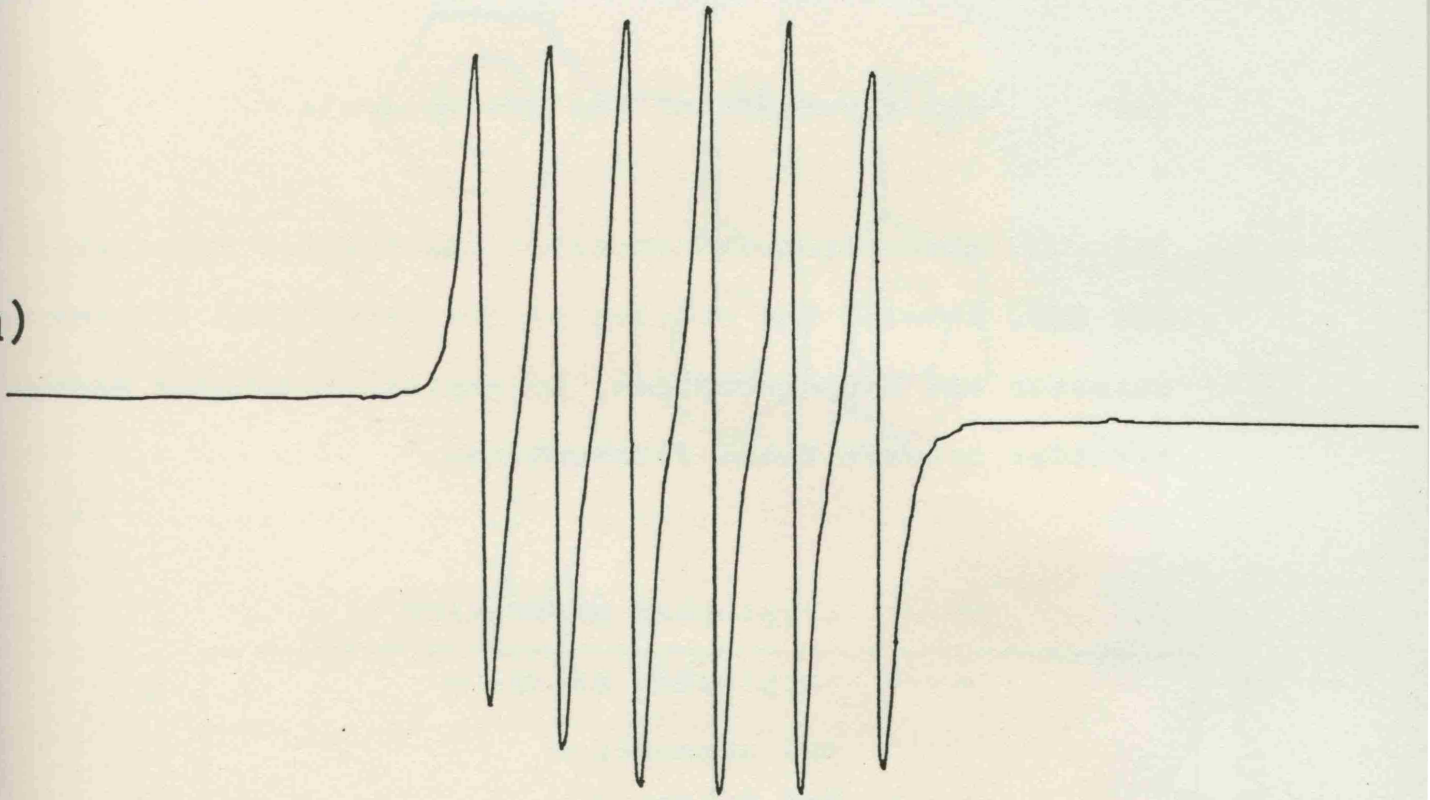
- myosin
- s.h. myosin
- Rod
- S1

Fig 2-9

Electron paramagnetic resonance spectra  
of Mn<sup>2+</sup>

Electron paramagnetic resonance spectra of (a) 100  $\mu\text{m}$   $\text{Mn}(\text{H}_2\text{O})_6^{2+}$  and (b)  $\text{Mn}^{2+}$  bound to scallop RLC were recorded in a Varian E109 spectrometer at 20°C. The microwave frequency was 9.26 GHz at a field strength of 3306G. Scans were performed over 8 minutes with a scan range of  $2 \times 10^3\text{G}$ .

a)



b)

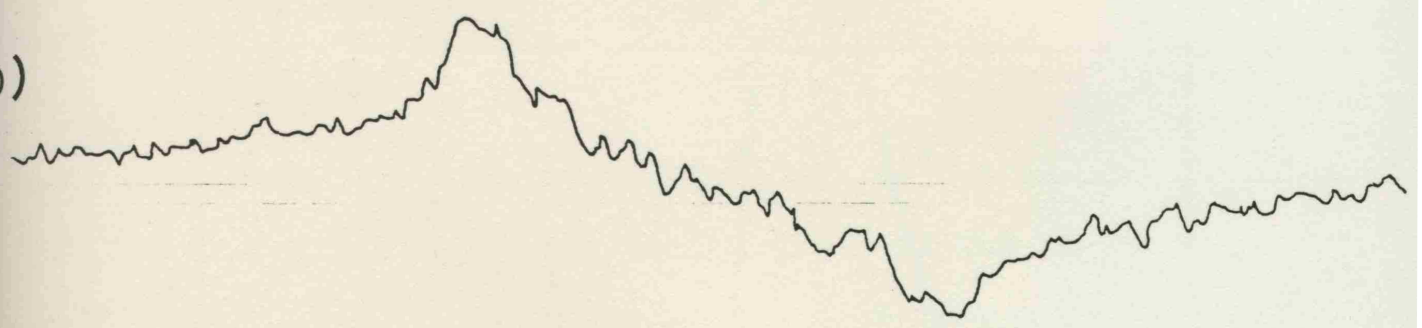


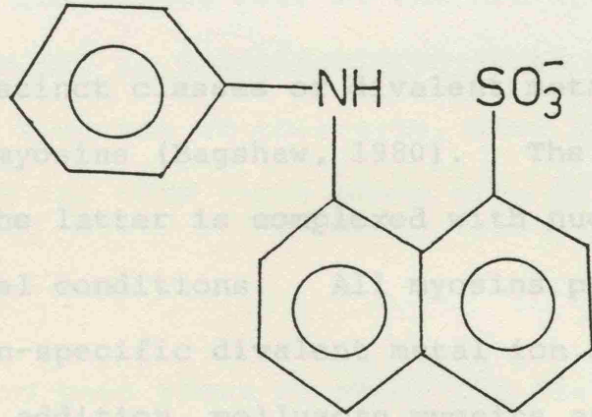
Fig 2-10      8-anilino-1-naphthalene sulphate, a  
a fluorescence probe

- (a)      the structure of the ANS molecule
- (b)      absorption and emission spectra for tryptophan and ANS, showing the overlap of the tryptophan fluorescence emission and ANS absorption, to explain resonance energy transfer between these fluorophores.

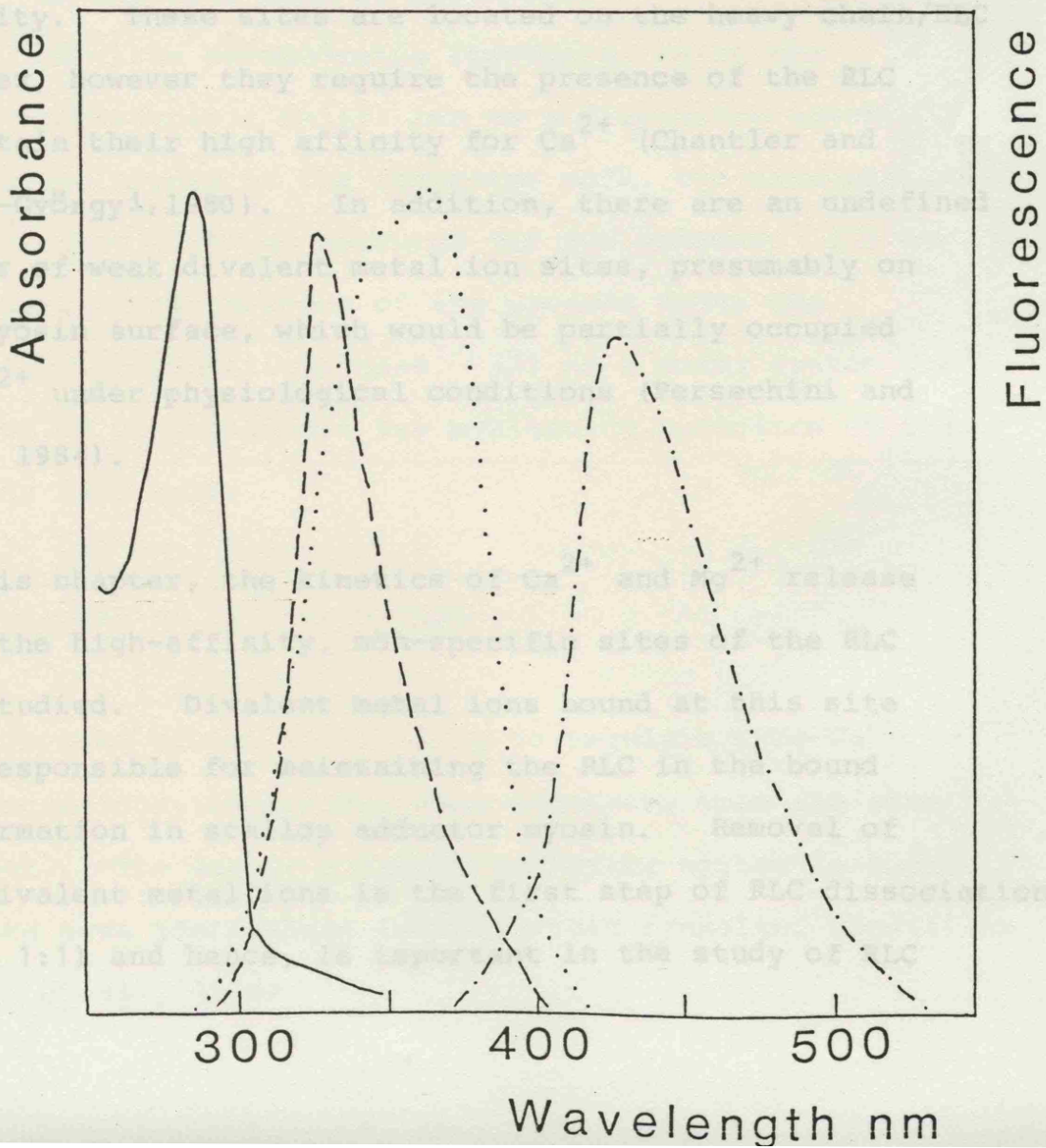
———— tryptophan absorption  
----- tryptophan emission  
..... ANS absorption  
-.-.- ANS emission

a)

DISSOCIATION OF DIVALENT METAL IONS FROM THE NON-SPECIFIC BINDING SITE OF MYOSIN



b)



CHAPTER 3

DISSOCIATION OF DIVALENT METAL IONS FROM THE NON-SPECIFIC  
BINDING SITE OF MYOSIN

There are four distinct classes of divalent metal ion binding sites present in myosins (Bagshaw, 1980). The ATPase site binds  $Mg^{2+}$  when the latter is complexed with nucleotide, under physiological conditions. All myosins possess two high-affinity, non-specific divalent metal ion sites located on their RLC. In addition, molluscan myosins and a few other myosins have two  $Ca^{2+}$  - specific sites, which are directly involved in myosin linked regulation of ATPase activity. These sites are located on the heavy chain/ELC complex, however they require the presence of the RLC to retain their high affinity for  $Ca^{2+}$  (Chantler and Szent-Györgyi, 1980). In addition, there are an undefined number of weak divalent metal ion sites, presumably on the myosin surface, which would be partially occupied by  $Mg^{2+}$  under physiological conditions (Persechini and Rowe, 1984).

In this chapter, the kinetics of  $Ca^{2+}$  and  $Mg^{2+}$  release from the high-affinity, non-specific sites of the RLC are studied. Divalent metal ions bound at this site are responsible for maintaining the RLC in the bound conformation in scallop adductor myosin. Removal of the divalent metal ions is the first step of RLC dissociation (eqn. 1:1) and hence, is important in the study of RLC

interactions. In rabbit myosin, dissociation of divalent metal ions from the non-specific site of the DTNB light chain (RLC) has already been studied (Bağshaw and Reed, 1977). Does the functional role of the non-specific site in maintaining the RLC in the associated state in scallop myosin affect the kinetics of this site, when compared to the kinetics of the DTNB light chain site in rabbit myosin?

Two approaches have been taken to study the dissociation of the divalent metal ions:

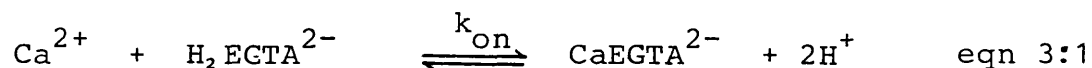
- (1) pH indicator measurements to follow changes in pH, as the ions bind to chelators,
- (2) electron paramagnetic resonance, using the paramagnetic Mn(II) ion as a displacing agent.

During the course of the indicator work, the dissociation of  $\text{Ca}^{2+}$  from EGTA was measured for two reasons. (1) to provide a direct measure of the process under the experimental conditions used. (2) as a model system for the use of pH indicators for monitoring reactions on the seconds time scale.

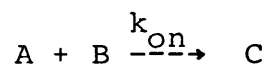
#### Dissociation of $\text{Ca}^{2+}$ from EGTA

EGTA is used almost universally to regulate free  $\text{Ca}^{2+}$  concentrations, especially when magnesium ions are also present. The use of a CaEGTA buffering system is known to have some limitations under certain transient conditions. (Smith et al., 1984).

At neutral pH the predominant EGTA species is  $\text{H}_2\text{EGTA}^{2-}$  and the overall reaction for  $\text{Ca}^{2+}$  binding to this species can be written as in eqn 3:1



The binding of  $\text{Ca}^{2+}$  to EGTA is therefore a second-order reaction. Such second-order kinetics are best analysed by converting them to pseudo-first-order, by using one of the reactants in excess over the other. Hence for a reaction



if  $[\text{B}]_0 \gg [\text{A}]_0$ , then  $[\text{B}]_0$  can be considered to remain almost constant during the reaction thus,

$$\frac{d[\text{C}]}{dt} = -\frac{d[\text{A}]}{dt} = k_{\text{on}} [\text{A}][\text{B}]_0 \quad \text{eqn 3:2}$$

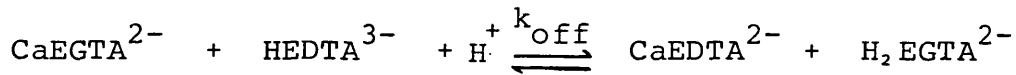
The disappearance of A and appearance of C, follow exponential first-order kinetics with a pseudo-first-order rate constant,  $k_{\text{obs}} = k_{\text{on}}[\text{B}]_0$ . Plotting values for  $k_{\text{obs}}$  against  $[\text{B}]_0$  yields the rate constant,  $k_{\text{on}}$ . Therefore following proton release with pH indicators in a stopped-flow apparatus, as  $\text{Ca}^{2+}$  is mixed with excess EGTA, yields traces such as those shown in fig 3-1. From these traces values of  $k_{\text{obs}}$  were calculated by a least squares fit to an exponential. The values of  $k_{\text{obs}}$  were then plotted against

the EGTA concentration (fig 3-2), to yield second-order rate constants ( $k_{on}$ ) of  $2.5 \times 10^6 \text{ M}^{-1} \text{ s}^{-1}$  and  $1.9 \times 10^7 \text{ M}^{-1} \text{ s}^{-1}$ , for the association of  $\text{Ca}^{2+}$  with EGTA at pH 7.0 and 8.0 respectively.

The determination of the  $k_{on}$  value at pH 8.0 is most prone to error, because its measurement is only just outside the dead-time of the apparatus. This also limits the range of EGTA concentrations that can be used, as the rate of  $\text{Ca}^{2+}$  binding increases with increasing chelator concentration. Hence, the psuedo-first order assumptions are marginal for the range of EGTA concentrations employed. However, the values obtained for the psuedo-first order rate constant ( $k_{obs}$ ) produce a linear relationship when plotted against the EGTA concentration, suggesting the assumptions made are still valid. The failure of the graphs for the second-order rate constant ( $k_{on}$ ) to pass through zero, is the result of trace amounts of contaminant  $\text{Ca}^{2+}$  in the buffers. This acts to slightly raise the effective  $\text{Ca}^{2+}$  concentration and lower the effective EGTA concentration in the solutions, which would produce the observed effect.

The dissociation of  $\text{Ca}^{2+}$  from EGTA can be measured, because the effective affinity of  $\text{Ca}^{2+}$  for EDTA is higher than for EGTA, under the experimental conditions. Therefore, mixing  $\text{CaEGTA}^{2-}$  with  $\text{HEDTA}^{3-}$  (the predominant form at neutral pH) results in a net uptake of protons which can be followed with pH indicators. The rate of binding

of  $\text{Ca}^{2+}$  to EDTA, is limited by the rate of dissociation of the  $\text{Ca}^{2+}$  from EGTA (eqn 3:3)



eqn 3:3.

A complete solution to this problem would require consideration of all the protonic states involved, however, an apparent rate constant ( $k_{\text{off}}$ ), at a defined pH, is sufficient for practical purposes. The effective rate constants ( $K_{\text{off}}$ ) for  $\text{Ca}^{2+}$  dissociation from EGTA were  $1.0\text{s}^{-1}$  and  $0.31\text{s}^{-1}$  at pH 7.0 and 8.0 respectively. Typical examples of the absorption traces obtained are shown in fig 3-3. Rates obtained, were found to be independent of the starting concentration of  $\text{Ca}^{2+}$  bound to EGTA. The values ( $k_{\text{off}}$ ) are comparable to those calculated from the known association rate constants and equilibrium constants for CaEGTA (Smith et al, 1984).

A value for the equilibrium dissociation constant,  $K_d$ , can be calculated for  $\text{Ca}^{2+}$  and EGTA (eqn.3:4). Values

$$K_d = \frac{k_{\text{off}}}{k_{\text{on}}} \quad \text{eqn. 3:4.}$$

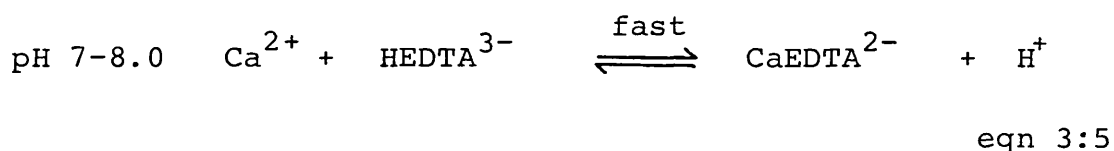
for  $K_d$ , of  $4 \times 10^{-7}\text{M}$  and  $1.6 \times 10^{-8}\text{M}$  were obtained at pH 7.0 and 8.0 respectively, for the dissociation of the CaEGTA complex.

The slow dissociation of  $\text{Ca}^{2+}$  from EGTA may limit the ability of this chelator to control  $\text{Ca}^{2+}$  levels. However, although the net release of  $\text{Ca}^{2+}$  from EGTA occurs on the seconds time-scale, when  $\text{CaEGTA}$  is used as a  $\text{Ca}^{2+}$  buffer at 1 mM, the response to a small ( $\mu\text{M}$ ) change in  $\text{Ca}^{2+}$  levels will occur on the millisecond time-scale. When the total  $[\text{EGTA}]$  is in excess of the total  $[\text{Ca}^{2+}]$ , the rate of re-equilibration after a small change in  $[\text{Ca}^{2+}]$  is given by  $k_{\text{on}}[\text{EGTA}] + k_{\text{off}}$ , where  $k_{\text{on}} = 2.5 \times 10^6 \text{ M}^{-1} \text{ s}^{-1}$  and  $k_{\text{off}} = 1 \text{ s}^{-1}$ , at pH 7.0. In the presence of  $\text{Mg}^{2+}$ , EGTA is often the preferable chelator used to buffer  $\text{Ca}^{2+}$  levels. This is because EGTA has a far higher affinity for  $\text{Ca}^{2+}$  than  $\text{Mg}^{2+}$ , presumably due to the binding cavity which is the right size for  $\text{Ca}^{2+}$ , but cannot constrict to envelope  $\text{Mg}^{2+}$ . Unfortunately, EGTA contains nitrogens which bind protons with pks of 8.96 and 9.58, making the  $\text{Ca}^{2+}$  buffering around pH 7.0, very pH dependent. These groups also greatly slow down the uptake and release of  $\text{Ca}^{2+}$  ions (Tsien, 1980). Tsien discusses these problems and the design of new  $\text{Ca}^{2+}$  buffers and indicators. By replacing the methylene groups of EGTA with benzene rings, as in BAPTA, the pks of the important nitrogen groups are lowered with little effect on the  $\text{Ca}^{2+}$  binding cavity. The result is that BAPTA has three advantages over EGTA; insensitivity of effective  $\text{Ca}^{2+}$  affinity to pH, speed of buffering and the ability to check the  $\text{Ca}^{2+}$  levels of the buffer by ultraviolet spectroscopy. Unfortunately, this third advantage can be a disadvantage, when using BAPTA as a buffering system

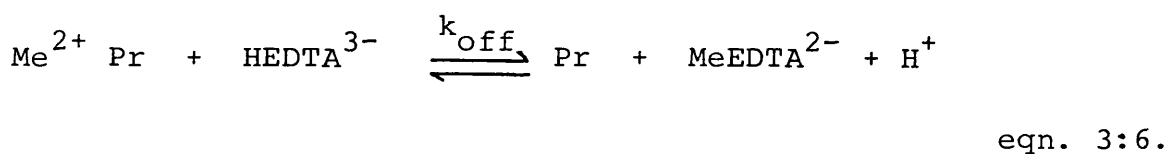
for  $\text{Ca}^{2+}$  in spectroscopic systems. The strong ultraviolet absorption and shift on binding of  $\text{Ca}^{2+}$  to the chelator, may interfere with the signals which are under observation. Hence the uses of this chelator can be severely limited.

Dissociation of  $\text{Ca}^{2+}$  from myosin subfragments

When divalent metal ions bind to the chelator EDTA, protons are released from the chelator in a rapid reaction (eqn. 3:5).

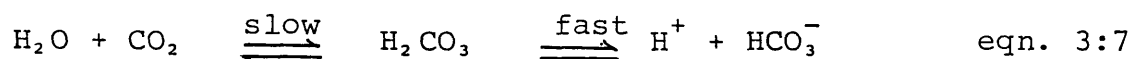


If the metal ions are bound to a protein, provided that there is some difference in the pks of the groups involved, exchange of metal ions ( $\text{Me}^{2+}$ ) between a protein bound state (Pr), and EDTA will be accompanied by a change in pH (eqn. 3:6). This change in pH as divalent metal ions are released from myosin subfragments and bind to EDTA, has been measured using pH indicators.



The results for the dissociation of  $\text{Ca}^{2+}$  from rabbit myosin subfragments, at pH 8.0 and 20°C, are shown in fig 3-4. In fig 3-4 (a) and (c) the rate of dissociation of  $\text{Ca}^{2+}$  ( $k_{\text{off}}$ ), was  $0.70\text{s}^{-1}$  and  $0.77\text{s}^{-1}$  for  $\text{S1}^{+\text{RD}}$  and HMM respectively. No release of  $\text{Ca}^{2+}$  was noted in the

control rabbit chymotryptic S1 (fig 3-4b), which lacks the RLC. Similar traces are shown in fig 3-5 for dissociation of  $\text{Ca}^{2+}$  from scallop myosin subfragments. Values of  $0.64\text{s}^{-1}$  and  $0.44\text{s}^{-1}$  were obtained for  $\text{S1}^{+\text{RD}}$  (fig 3-5a) and HMM (fig 3-5c) respectively.  $\text{S1}^{-\text{RD}}$  (fig 3-5b) showed no release of  $\text{Ca}^{2+}$  over this time-scale. All preparations showed a rapid pH transient,  $t_{\frac{1}{2}} < 20$  ms, assumed to reflect metal ion release from the weak sites (Bagshaw and Reed, 1976). In the work on scallop myosin subfragments 20  $\mu\text{g/ml}$  carbonic anhydrase (Sigma, Poole) was included, because this appeared to reduce "echo" effects due to hydration of dissolved  $\text{CO}_2$ . Any rapid change in pH in the system, will cause a re-equilibration of the ionization of the dissolved  $\text{CO}_2$ . The latter occurs on the seconds time-scale due to the slow hydration step (eqn. 3:7, Gutfreund, 1972).



Attempts to measure the rate of binding of free  $\text{Ca}^{2+}$  to EDTA failed because the reaction was too fast to record.

The rates for dissociation of  $\text{Ca}^{2+}$ , shown by the stopped-flow indicator method agree closely with the previous results of Bagshaw and Reed (1977), using fluorescence stopped-flow. This suggests that the indicator method used, was monitoring  $\text{Ca}^{2+}$  release from the high-affinity, non-specific divalent metal ion binding site. The lack of the slower pH transient in preparations with no RLC

supports this conclusion. There is close agreement between the values obtained for rabbit and scallop subfragments and also between those for the single and double headed subfragments. The presence of the two heads in the HMM molecule, does not appear to affect the dissociation of  $\text{Ca}^{2+}$  from the divalent metal ion binding site of the RLC.

Unfortunately, due to the instability of the system over the longer time periods (>30 seconds) required for  $\text{Mg}^{2+}$  dissociation, results for  $\text{Mg}^{2+}$  could not be obtained by this method. In addition to the problems of stability, RLC are known to dissociate with a rate constant of about  $0.01\text{s}^{-1}$ . This RLC dissociation is likely to complicate the interpretation of any changes in proton concentration observed on this time-scale. Alternative signals were therefore used to measure the rate of  $\text{Mg}^{2+}$  dissociation. Furthermore, pH experiments were limited to the use of soluble myosin subfragments. This is because of the high viscosity of intact myosin, which causes problems with rapid and complete mixing, and also due to the higher buffering capacity of this protein, which would reduce the size of the signal expected.

#### Dissociation of $\text{Mg}^{2+}$ from myosin subfragments

The time-scale of  $\text{Mg}^{2+}$  dissociation from myosin subfragments ( $t_{\frac{1}{2}} = 12\text{s}$ , Bagshaw and Reed, 1977) suggested an alternative strategy for its measurement.  $\text{Mn}^{2+}$  has a very high affinity

for the non-specific, divalent metal ion site of myosin (approximately 50 fold tighter than  $Mg^{2+}$ ). On binding to the protein, the  $Mn^{2+}$  esr spectrum becomes very broad and the amplitude of the first derivative signal is greatly reduced. When the site is initially occupied by  $Mg^{2+}$ , the rate of binding of  $Mn^{2+}$  will be limited by the rate of dissociation of the  $Mg^{2+}$ .

Figure 3-6, shows the rate of dissociation of  $Mg^{2+}$  from scallop  $S1^{+RD}$  (fig 3-6a) and HMM (fig 3-6c), as followed by the decrease in amplitude of the  $Mn(H_2O)_6^{2+}$  signal as  $Mg^{2+}$  is displaced by  $Mn^{2+}$ , at the non-specific binding site. The rate of dissociation of the  $Mg^{2+}$ , was  $0.050s^{-1}$  and  $0.058s^{-1}$  from  $S1^{+RD}$  and HMM respectively. At the end point of the reaction, scans of the esr spectra revealed the characteristic broad spectrum of  $Mn^{2+}$  bound to the RLC site (Bagshaw and Kendrick-Jones, 1979), in combination with a low concentration of free  $Mn(H_2O)_6^{2+}$ . When rabbit  $S1^{+RD}$  (fig 3-6d) was used, comparable results were obtained to those for scallop  $S1^{+RD}$ , the rate of magnesium dissociation was  $0.051s^{-1}$ . In all the experiments on  $Mg^{2+}$  dissociation, EDTA was included to ensure chelation of any contaminant  $Ca^{2+}$ . Formation of MnEDTA did not contribute to the transients observed, as shown by the control experiment using  $S1^{-RD}$  (fig 3-6b).

If the preparations were preloaded with  $Ca^{2+}$ , the amplitude of the observed signal immediately after mixing ( $\sim 1s$ ) was reduced more than 3-fold, when compared to traces in which the proteins were preloaded with  $Mg^{2+}$ . Hence,

Ca<sup>2+</sup> dissociation is mainly complete within the mixing time, which would be expected from the previous pH indicator results. Therefore, Mn<sup>2+</sup> esr displacement techniques were not suitable for measuring dissociation of Ca<sup>2+</sup> from the high-affinity, non-specific sites of myosin.

The results obtained for the rate of dissociation of Mg<sup>2+</sup> from the high-affinity, non-specific metal ion binding site of rabbit S1<sup>+RD</sup>, are again in close agreement with those of Bagshaw and Reed (1977), obtained using the intrinsic protein fluorescence. It is clear that both the rabbit and scallop subfragments, behave in a similar way with respect to dissociation of metal ions from this site. The results for Mg<sup>2+</sup> and Ca<sup>2+</sup> dissociation are shown in table 3-1. The dissociation of Mg<sup>2+</sup> is an order of magnitude slower than for Ca<sup>2+</sup> dissociation.

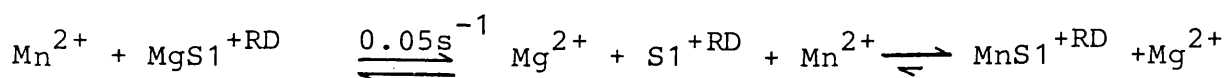
Table 3-1. Dissociation rates of divalent metal ions from myosin subfragments

Protein	Fluorescence (Bagshaw & Reed, 1977)		esr	pH indicator
	Ca <sup>2+</sup> (s <sup>-1</sup> )	Mg <sup>2+</sup> (s <sup>-1</sup> )	Mg <sup>2+</sup> (s <sup>-1</sup> )	Ca <sup>2+</sup> (s <sup>-1</sup> )
Rabbit S1 <sup>+RD</sup>	0.46	0.057	0.051	0.70
Rabbit HMM	N.D	N.D	N.D	0.77
Scallop S1 <sup>+RD</sup>	N.D	N.D	0.050	0.64
Scallop HMM	N.D	N.D	0.058	0.44

ND = not determined

A consequence of this slow dissociation of  $Mg^{2+}$  from the high-affinity, non-specific site, is that this process would limit the rate of  $Ca^{2+}$  binding on muscle activation. Hence, this site, which is common to all myosins (Bagshaw and Kendrick-Jones, 1979) can not be responsible for the triggering of muscle contraction. This conclusion was drawn previously (Bagshaw and Reed, 1977) for rabbit myosin, based on the results of fluorescence studies. It is possible that during a prolonged tetanus this site could bind some  $Ca^{2+}$ . However, it would appear that in molluscan systems this non-specific site plays primarily a structural role, maintaining the RLC in an associated state.

One drawback of the fluorescence method, was that it measured the release of the divalent metal ions indirectly. It is possible that the rate measured was due to a separate protein conformational change, rather than the actual metal ion release step. Double mixing experiments suggested that this was not the case, but the signals obtained were rather small. The use of the  $Mn^{2+}$  esr signal overcomes this problem by directly measuring the  $Mg^{2+}$  release. The close agreement between the results obtained does suggest, however, that the fluorescence signal in rabbit proteins does actually monitor the metal ion release step. It also indicates that the release occurs via a metal free protein state (eqn.3:8), with no existence of a tertiary metal ion complex (ie. 2 divalent metal ions plus the protein,  $[MnMg S1^{+RD}]$ ).



eqn. 3:8

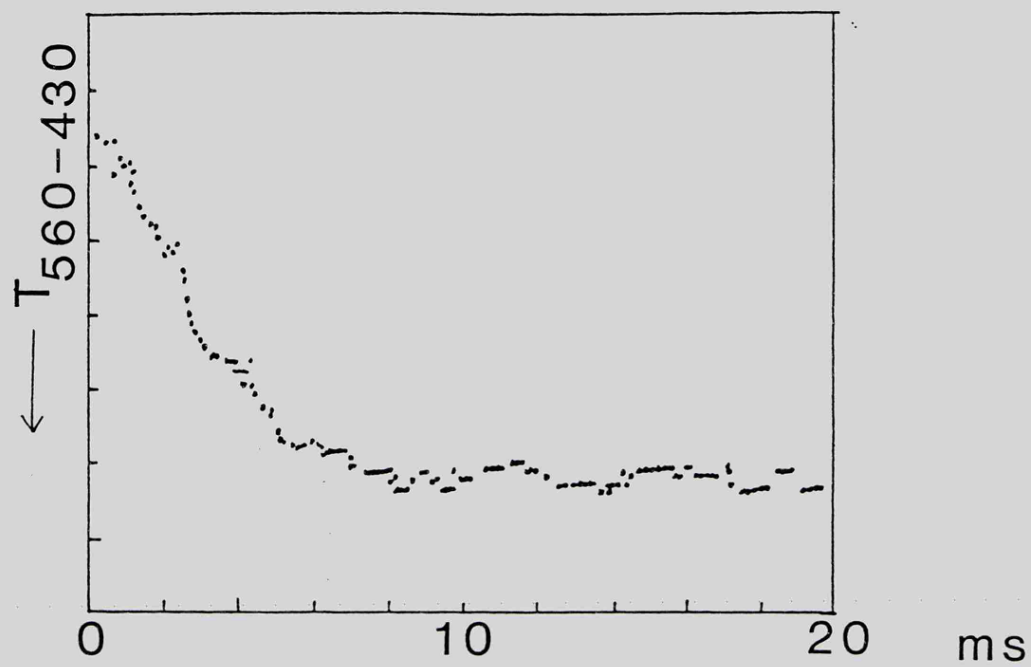
As previously stated, the RLC dissociates on removal of the divalent metal ions from the non-specific binding site of the RLC in scallop myosin, unlike in rabbit myosin. This functional role of the non-specific site in scallop RLC binding, does not appear to be reflected in the kinetics of the divalent metal ion release. However, it is possible the rate of divalent metal ion dissociation from this site, on addition of EDTA, may limit the rate of RLC release, especially when the site is occupied by  $Mg^{2+}$ .

Fig 3-1

The binding of  $\text{Ca}^{2+}$  to EGTA

The binding of  $\text{Ca}^{2+}$  to EGTA was monitored by proton release using a pH indicator. The reaction was followed in a dual wavelength, stopped-flow spectrophotometer set up to record the differential transmission changes at wavelengths appropriate to the indicator. (a)  $5 \mu\text{M}$   $\text{CaCl}_2$  was mixed with  $20 \mu\text{M}$  EGTA (reaction chamber concentrations) in a solvent containing  $40 \text{ mM}$  NaCl,  $100 \mu\text{M}$  EPPS and  $25 \mu\text{M}$  phenol red at pH 8.0 and  $20^\circ\text{C}$ . (b) as in (a) except the buffer was  $100 \mu\text{M}$  MOPS and  $20 \mu\text{M}$  bromothymol blue at pH 7.0. The observed rate constant was measured by a least squares fit to an exponential. These values were plotted against [EGTA] to obtain the second order rate constant  $k_{\text{on}}$  (fig 3-2).

a)



b)

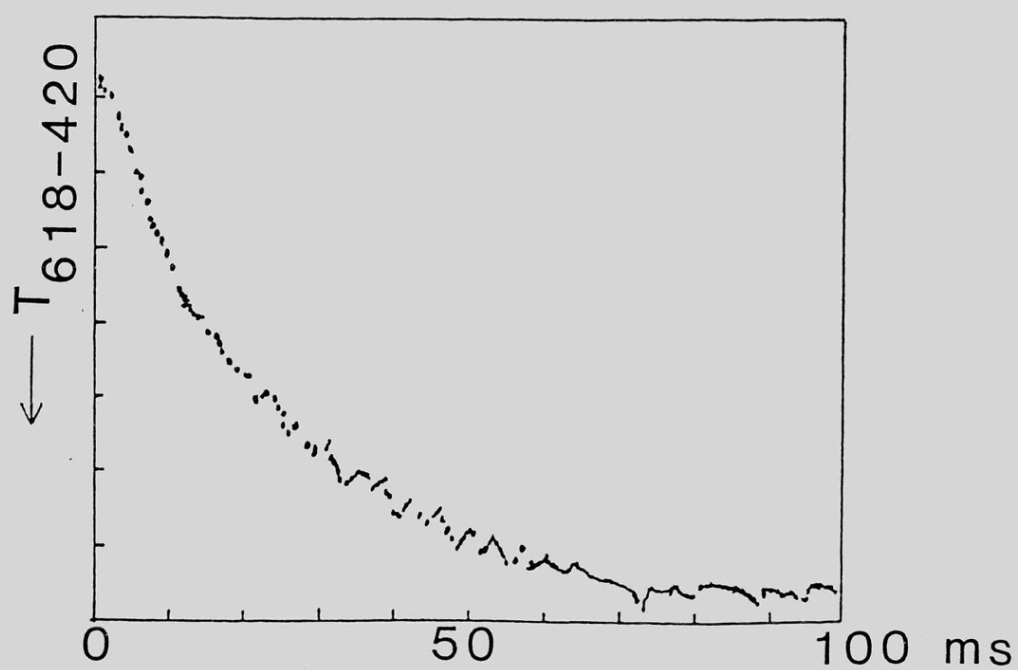
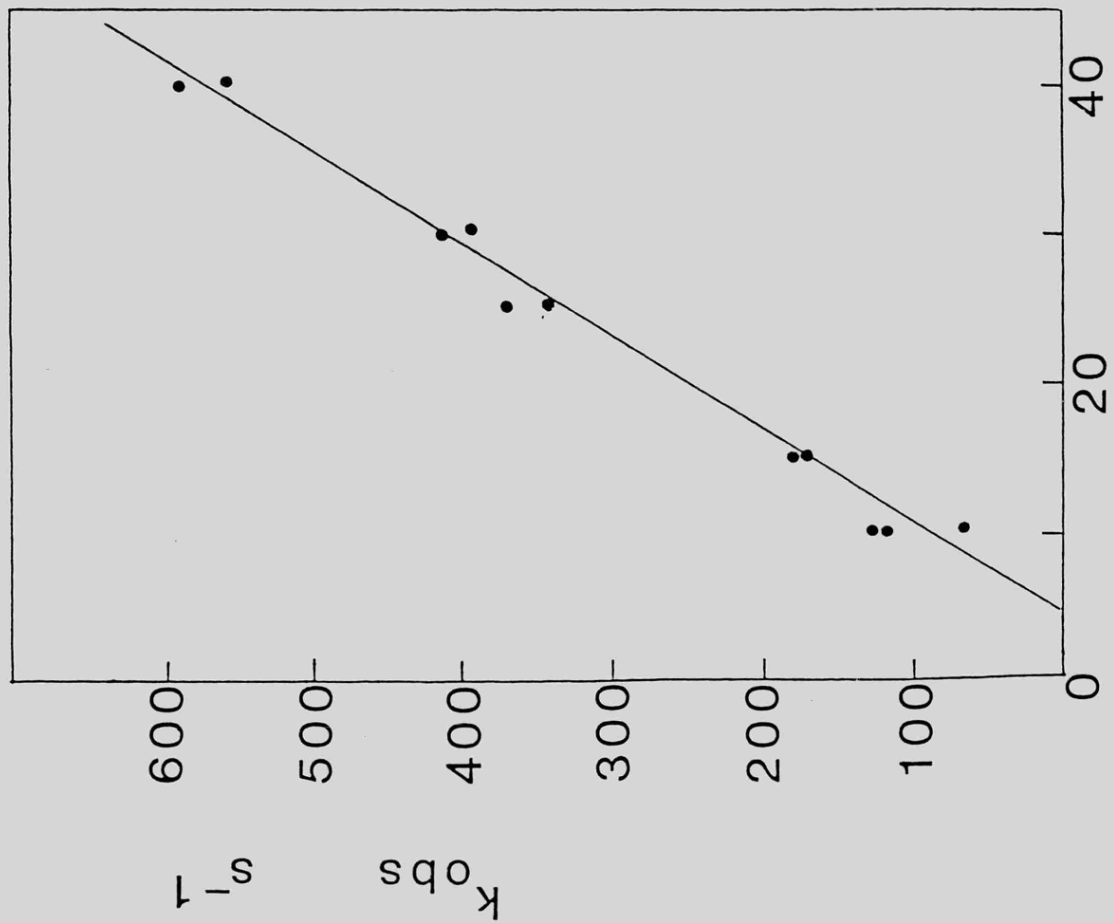


Fig 3-2

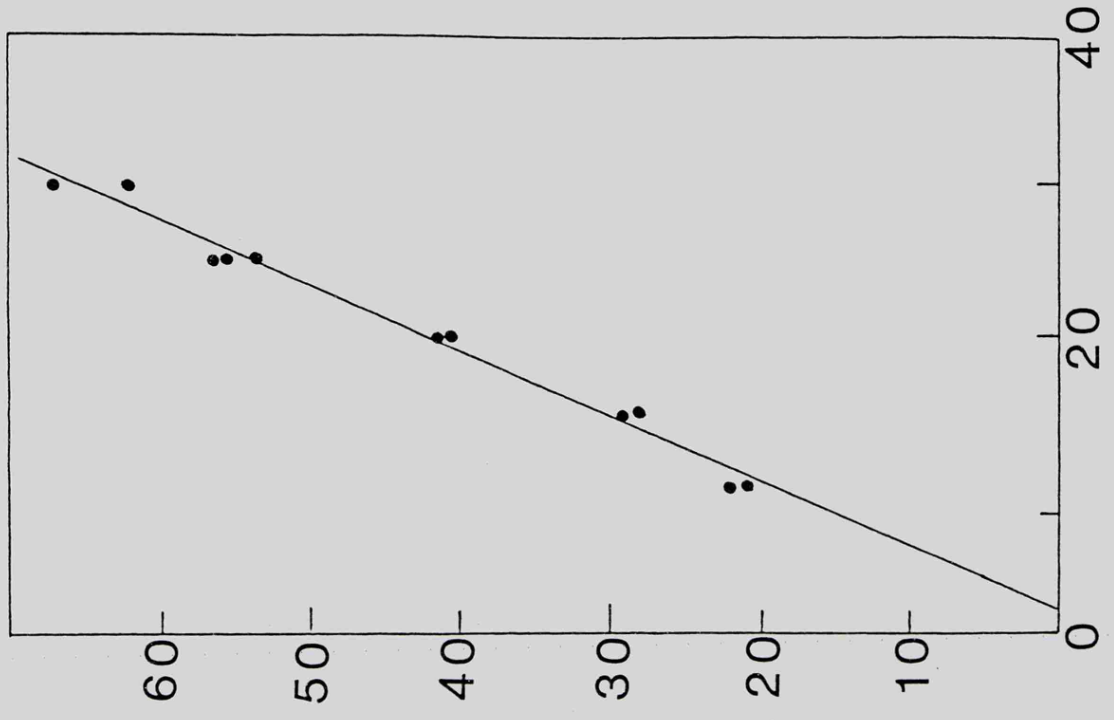
Graphs of  $k_{\text{obs}}$  ( $\text{s}^{-1}$ ) against [EGTA], to obtain a value  
for the second order rate constant ( $k_{\text{on}}$ ) for  $\text{Ca}^{2+}$   
binding to EDTA

The association rate constant ( $k_{\text{on}}$ ) for  $\text{Ca}^{2+}$  binding to EGTA, was obtained by plotting values of  $k_{\text{obs}}$  (fig 3-1) against the [EGTA]. Buffers used were (a) 40 mM NaCl, 100  $\mu\text{M}$  EPPS containing 25  $\mu\text{M}$  phenol red at pH 8.0 and (b) 40 mM NaCl, 100  $\mu\text{M}$  MOPS containing 20  $\mu\text{M}$  bromothymol blue at pH 7.0. The  $[\text{Ca}^{2+}]$  was kept at 5  $\mu\text{M}$  and the [EGTA] varied from 10 to 40  $\mu\text{M}$  (reaction chamber concentrations). Values for  $k_{\text{on}}$  of  $1.9 \times 10^7 \text{ M}^{-1} \text{ s}^{-1}$  at pH 8.0 and  $2.5 \times 10^6 \text{ M}^{-1} \text{ s}^{-1}$  at pH 7.0 were obtained.

a)



b)



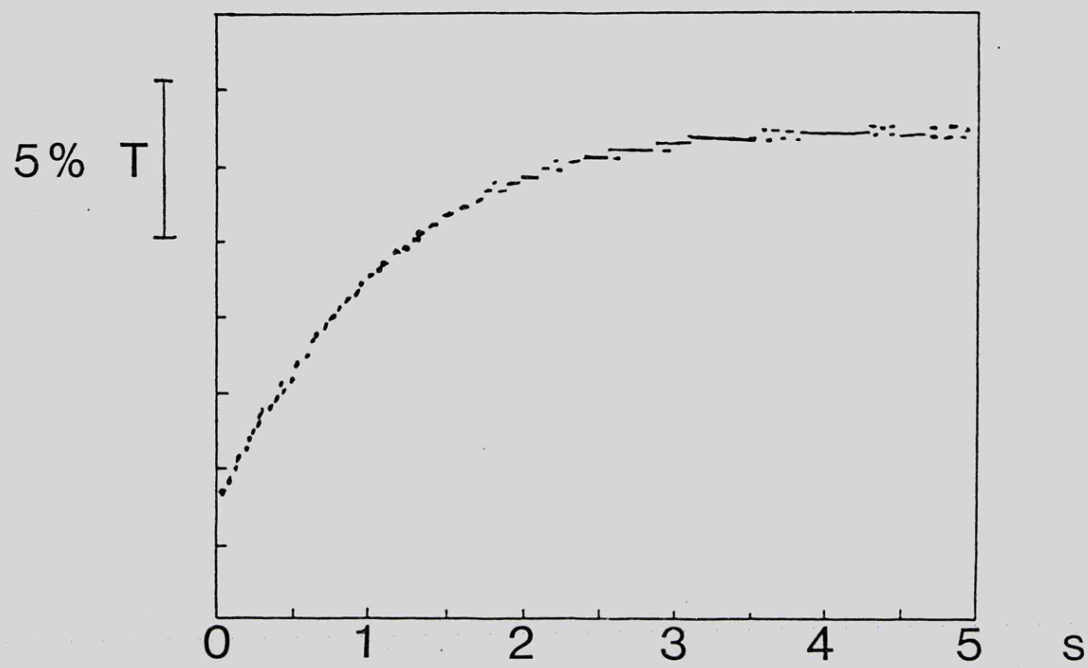
$[EGTA]_{reaction\ chamber}\ \mu M$

Fig 3-3

Dissociation of Ca<sup>2+</sup> from EGTA at (a) pH 7.0 and  
(b) pH 8.0

The dissociation of Ca<sup>2+</sup> from EGTA was monitored by proton uptake, on addition of EDTA using a pH indicator. The reaction was followed in a dual-wavelength, stopped-flow spectrophotometer set up to record differential transmission changes at wavelengths appropriate to the indicators. (a) 5  $\mu\text{M}$  CaCl<sub>2</sub>, 25  $\mu\text{M}$  EGTA was mixed with 50  $\mu\text{M}$  EDTA (reaction chamber concentration) in a solvent containing 40 mM NaCl, 100  $\mu\text{M}$  MOPS and 20  $\mu\text{M}$  bromothymol blue at pH 7.0 and 20°C. The differential transmission at 618 and 420 nm was monitored, and gave an observed first-order rate constant ( $k_{\text{off}}$ ) of  $1.0\text{s}^{-1}$ . (b), as in (a) but the buffer was 40 mM NaCl, 100  $\mu\text{M}$  EPPS, 25  $\mu\text{M}$  phenol red at pH 8.0. The differential transmission at 560 and 430 nm was monitored and gave an observed first-order rate constant of  $0.31\text{s}^{-1}$ . The amplitude of the traces indicates the pH increased by 0.1 during the reaction. In the absence of EGTA, Ca<sup>2+</sup> binding to EDTA was too fast to measure, indicating that the second-order binding constant was  $> 10^7 \text{ M}^{-1} \text{ s}^{-1}$ .

a)



b)

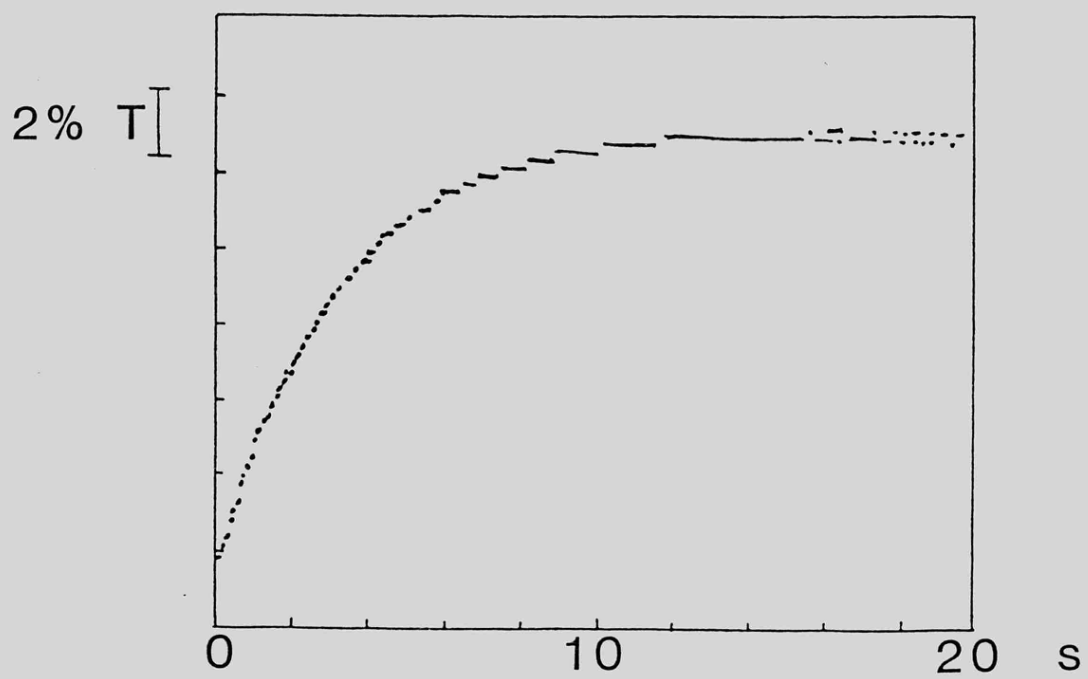


Fig 3-4

Dissociation of  $\text{Ca}^{2+}$  from rabbit myosin subfragments

$\text{Ca}^{2+}$  release was monitored by the decrease in pH on mixing the myosin subfragments with EDTA, using phenol red as an indicator. The differential transmission was monitored at wavelengths of 560 and 430 nm. One syringe of the stopped-flow apparatus contained 10  $\mu\text{M}$   $\text{CaCl}_2$ , 1 mg/ml protein and the other 50  $\mu\text{M}$  EDTA (reaction chamber concentrations). Both syringes contained 40 mM NaCl, 100  $\mu\text{M}$  EPPS, 25  $\mu\text{M}$  phenol red at pH 8.0 and 20°C.

(a) rabbit papain subfragment 1 ( $\text{S1}^{+\text{RD}}$ ), (b) rabbit chymotryptic subfragment 1 (CS1), (c) rabbit chymotryptic HMM. Rabbit  $\text{S1}^{+\text{RD}}$ , prepared by papain digestion in the presence of EDTA, yielded a similar trace to that in (b).

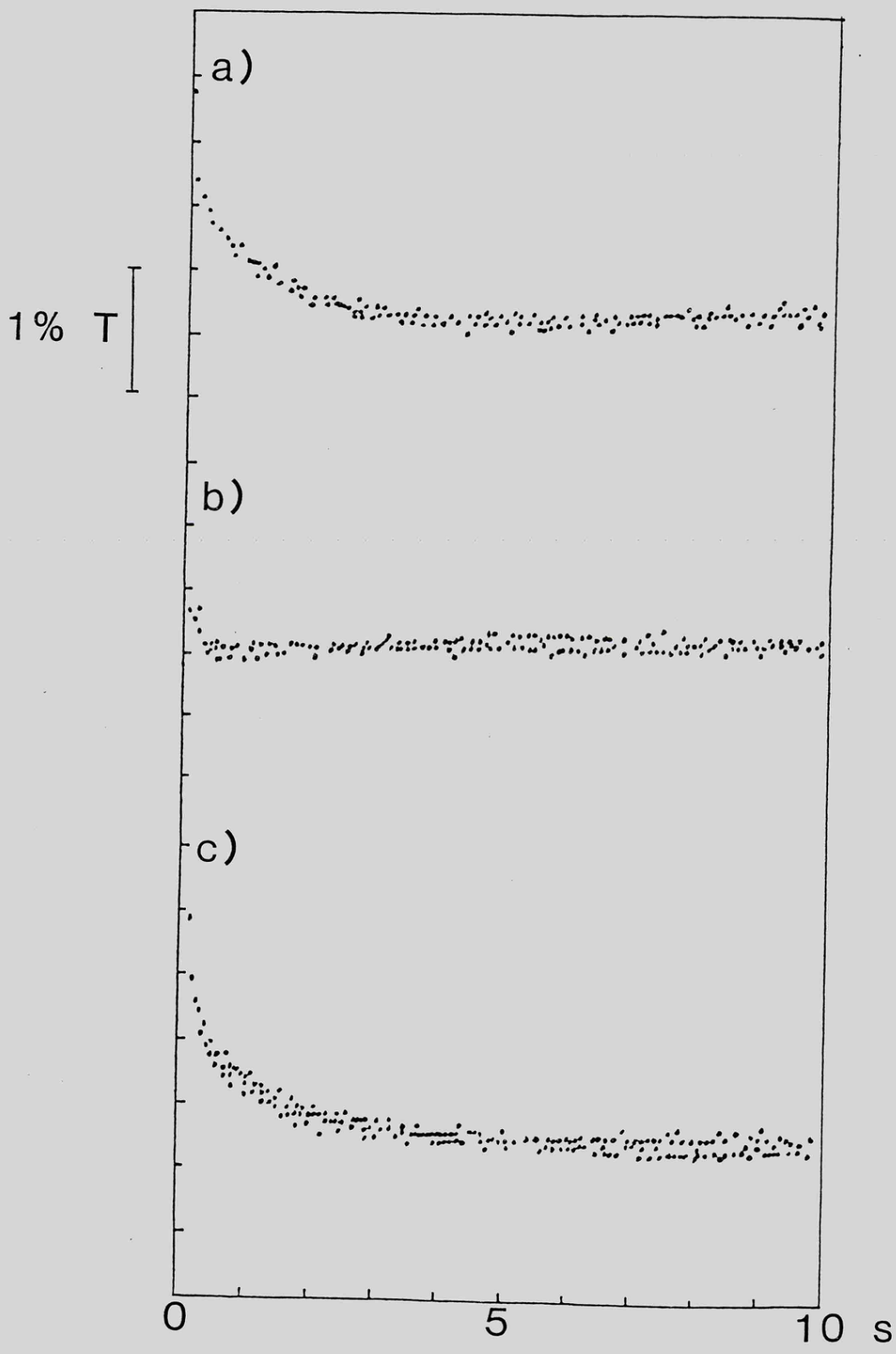


Fig 3-5

Dissociation of Ca<sup>2+</sup> from scallop myosin subfragments

Ca<sup>2+</sup> release was monitored by the decrease in pH on mixing the myosin subfragment with EDTA, using phenol red as an indicator. The differential transmission was monitored at wavelengths of 560 and 430 nm. One syringe of the stopped-flow apparatus contained 10  $\mu$ M CaCl<sub>2</sub>, 1 mg/ml protein and the other 50  $\mu$ M EDTA (reaction chamber concentrations). Both syringes contained 40 mM NaCl, 100  $\mu$ M EPPS, 20  $\mu$ g/ml carbonic anhydrase and 25  $\mu$ M phenol red at pH 8.0 and 20°C. (a) scallop papain S1<sup>+RD</sup>, (b) scallop papain S1<sup>-RD</sup>, (c) scallop tryptic HMM.

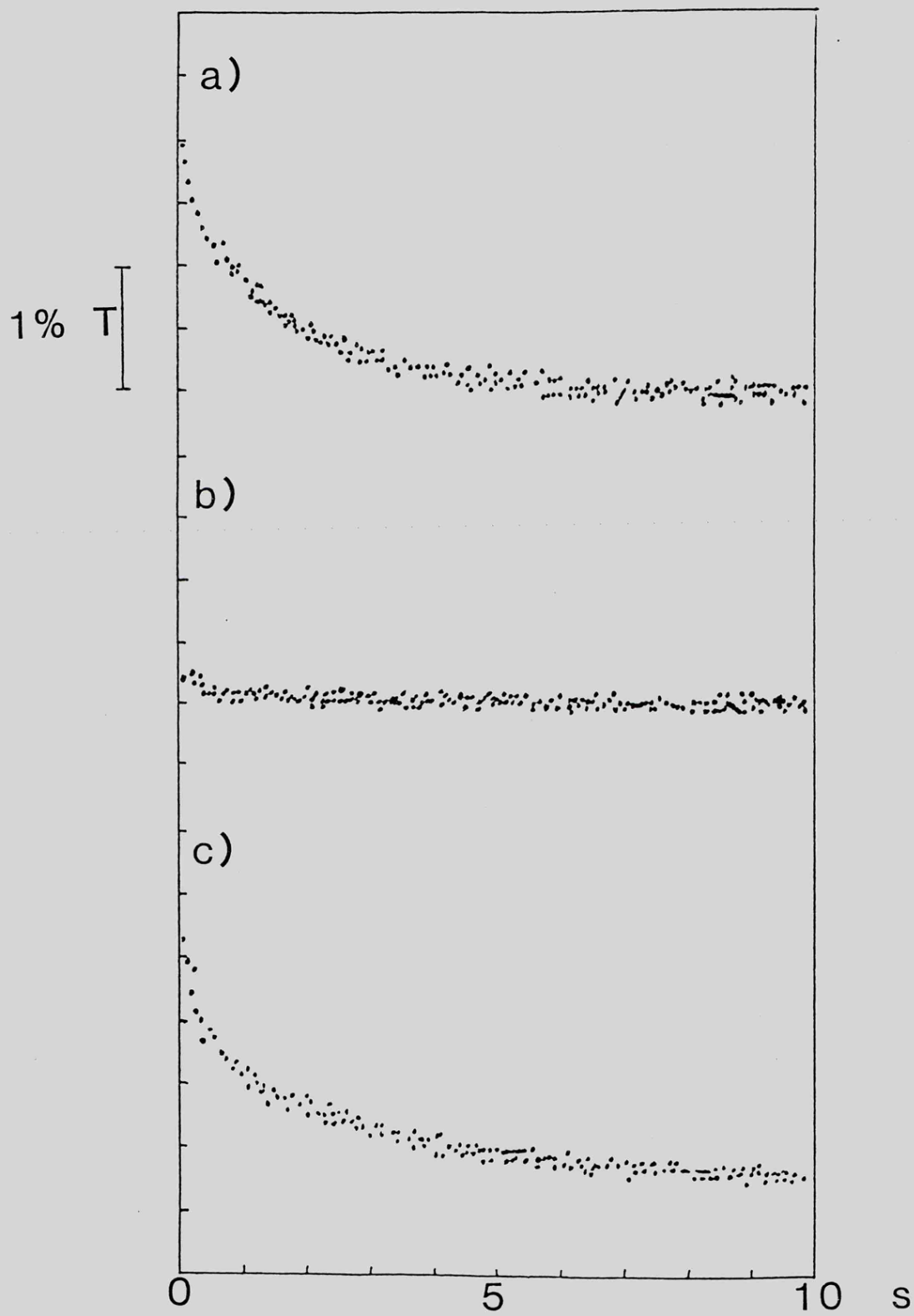


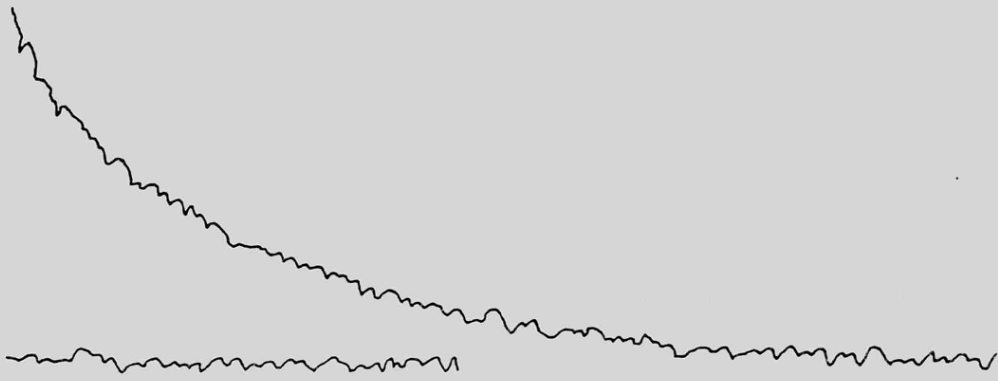
Fig 3-6

Displacement of  $Mg^{2+}$  from scallop and rabbit myosin subfragments

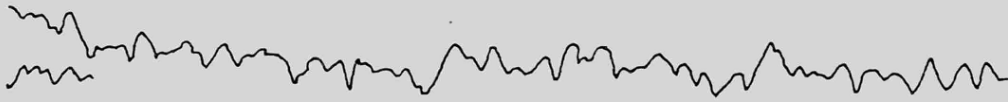
$Mg^{2+}$  was displaced from myosin subfragments with  $Mn^{2+}$ .

The reaction was monitored by the decrease in the characteristic esr signal of the  $Mn(6H_2O)^{2+}$  complex, following the rapid mixing of the  $Mg^{2+}$  loaded protein with  $Mn^{2+}$  as described in the methods. (a) 120  $\mu M$  scallop  $S1^{+RD}$  in 150  $\mu M$   $MgCl_2$ , 100  $\mu M$  EDTA was mixed with 300  $\mu M$   $MnCl_2$ . (b) 83  $\mu M$  scallop  $S1^{-RD}$  in 150  $\mu M$   $MgCl_2$ , 100  $\mu M$  EDTA was mixed with 175  $\mu M$   $MnCl_2$ , (c) 74  $\mu M$  scallop HMM in 150  $\mu M$   $MgCl_2$ , 100  $\mu M$  EDTA was mixed with 150  $\mu M$   $MnCl_2$  (d) 171  $\mu M$  rabbit  $S1^{+RD}$  in 150  $\mu M$   $MgCl_2$ , 100  $\mu M$  EDTA was mixed with 150  $\mu M$   $MnCl_2$ . (all of the above concentrations refer to final concentration after mixing and the HMM concentration refers to the head concentration). Both syringes contained 40 mM NaCl, 20 mM EPPS at pH 8.0 and 20°C. The horizontal traces represent continuation of the records and define the end-point of the reaction.

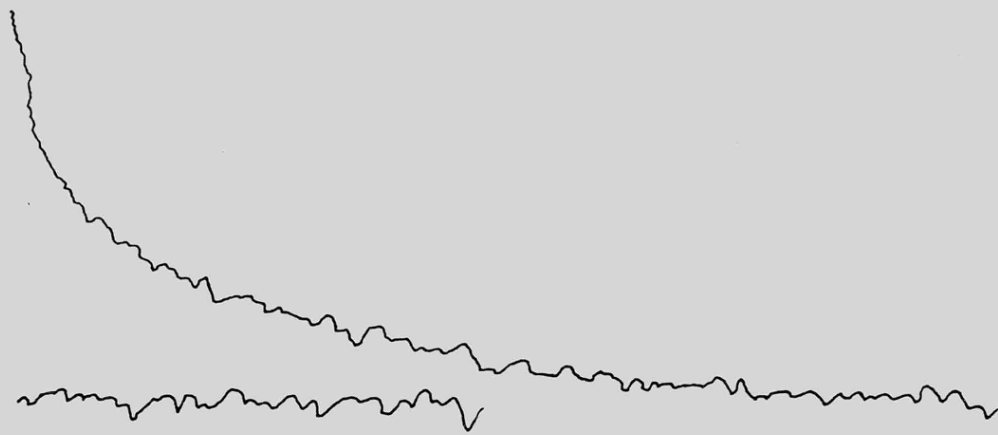
a)



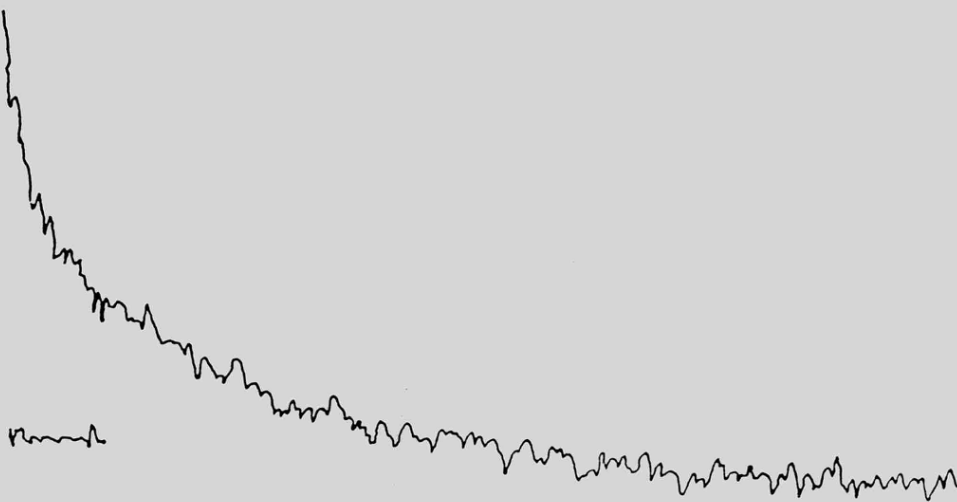
b)



c)



d)



e.s.r. peak height  $\uparrow$

30 sec

CHAPTER 4

8-ANILINO-1-NAPHTHALENE SULPHONATE, A FLUORESCENT PROBE FOR  
THE REGULATORY LIGHT CHAIN BINDING SITE OF SCALLOP MYOSIN

Scallop myosin is unusual in that, on treatment with EDTA to chelate divalent metal ions, the RLC will dissociate from myosin or myosin subfragments. The RLC dissociation mechanism is depicted as a minimal scheme in eqn. 1:1. This is probably an incomplete description of the mechanism, due to a number of factors which may affect the RLC interaction. The RLC are known to have multiple interactions with the heavy chain/essential light chain complex (Bagshaw and Kendrick-Jones, 1980; Hardwicke et al., 1983) and the amount of RLC dissociation depends critically on the myosin subfragment under study (Stafford et al., 1979). Also, the light chain - heavy chain interaction is specifically affected by  $\text{Ca}^{2+}$  which is involved in regulation of the ATPase activity (Szent-Györgyi et al., 1973; Wells and Bagshaw, 1985). The presence of these  $\text{Ca}^{2+}$  specific sites further complicates the evaluation of the RLC dissociation pathway. Hence, further study of the RLC interactions in scallop myosin was required.

In this chapter, the usefulness of ANS as a probe for RLC interactions and the RLC binding site is investigated. Preliminary studies (Bagshaw et al., 1982) had indicated that ANS bound to the denuded heavy chain/ELC complex on removal of the RLC. A study of ANS binding to desensitised myosin was therefore initiated, to test whether the ANS binding reflected the RLC content of the myosin. From these studies several questions arose about the ANS binding to scallop myosin. If the ANS was competing directly for the RLC binding site, what effect does it have on the RLC equilibrium? Where does the ANS bind on the heavy chain/ELC complex and how much information about the kinetics of RLC interaction can be obtained from this ANS binding? In order to answer these questions, the ANS binding to myosin and subfragments was followed.

During the course of this work, ANS was found to be a useful probe for following the desensitisation of preparations. For many spectroscopic techniques, subfragments soluble at low ionic strength are required, mainly because myosin under such conditions is insoluble and in high salt loses the  $\text{Ca}^{2+}$  regulation of its ATPase. (Wells et al., 1985b). Unfortunately, the desensitisation of these subfragments is difficult due to their soluble nature and the problem of separating the RLC from such soluble proteins. A method was therefore developed which allowed a quick desensitisation of HMM to be performed.

ANS BINDING TO SCALLOP MYOSIN

ANS binds to scallop myosin as shown by the emission spectra in fig 4-1. On removal of the RLC, either by prior desensitisation of the myosin (fig 4-1b) or in situ treatment with EDTA (fig 4-1e), the binding of ANS is reflected in the increased fluorescence emission at 460 nm, compared to that in native myosin (fig 4-1a, d). Presumably this is due to the exposure of a hydrophobic site involved in the binding of the RLC. This ANS binding to the preparations can be reversed by addition of  $Mg^{2+}$  to the EDTA treated myosin (fig 4-1f), or by addition of RLC in the presence of  $Mg^{2+}$  to the desensitised myosin preparation (fig 4-1c). The failure of the 460 nm ANS peak of the fluorescence spectrum to revert to exactly that of the native myosin (fig 4-1f cf 4-1d, 4-1c cf 4-1a), is due to non-specific binding of ANS, which is observed in all scallop myosin preparations. This binding appears to be slow and time-dependent, which could reflect denaturation of the protein, or penetration of ANS into the protein core.

The relationship between the amount of ANS bound and the RLC content of the myosin molecule was studied using desensitised myosin. Myosin desensitised at 0°C or 25°C was found by urea-polyacrylamide gel electrophoresis, followed by gel scanning, to contain 0.9 and 0.36 mol RLC/mol myosin respectively. The relative fluorescence at 460 nm was monitored as the preparations were titrated

with exogenous added scallop RLC, in the presence of ANS (fig 4-2). Both preparations showed a similar amount of residual ANS fluorescence, when addition of RLC had no further effect on the fluorescence. This residual ANS fluorescence is that alluded to in the spectra of fig 4-1, due to non-specific ANS binding. Unfortunately, this makes it impossible to rigorously relate RLC content to ANS fluorescence. However, if the data are analysed by a direct least-squares computer fit to a quadratic equation, making the assumption that the final stoichiometry was 2 mol RLC/mol myosin, an approximate value for the apparent RLC binding constant ( $K_4$ , eqn. 1:1) can be obtained. This was calculated to be of the order of 0.1 to 0.3  $\mu\text{M}$ , at 20°C and saturating  $\text{Mg}^{2+}$  concentration. The value obtained for the apparent binding constant of the RLC ( $K_4$ ) is the same order of magnitude as in previous estimates. (Chantler and Szent-Györgyi, 1980).

#### ANS BINDING AND ITS EFFECT ON THE RLC EQUILIBRIUM

The amount of ANS binding to HMM was estimated by the procedure of Hummel and Dreyer (1962). A typical example of the type of trace obtained is shown in fig 4-3. The ANS was found to bind to HMM in both EDTA and  $\text{MgCl}_2$ , however, the binding was reduced in the presence of divalent metal ions. (Table 4-1)

Table 4-1     ANS Binding ratios, measured by the Hummel-  
Dreyer method

[ANS] $\mu\text{M}$	ANS BINDING ( $\mu$ moles)		BINDING RATIO (ANS/HMM)	
	1 mM $\text{Mg}^{2+}$	0.5 mM EDTA	1 mM $\text{Mg}^{2+}$	0.5 mM EDTA
20	$5.9 \times 10^{-4}$	$1.4 \times 10^{-3}$	0.45	1.08
40	$1.3 \times 10^{-3}$	$2.6 \times 10^{-3}$	1.00	2.00
80	$1.9 \times 10^{-3}$	$2.7 \times 10^{-3}$	1.4	2.1

The results indicated that, in EDTA, the ANS/HMM binding ratio reached a maximum of just over 2, even at 80  $\mu\text{M}$  ANS.

This would suggest that ANS is specific for the RLC binding site, as this ratio is equivalent to one ANS to each RLC site. In  $\text{Mg}^{2+}$ , the binding of ANS increased as the concentration of ANS increased, but was always less than the respective binding in EDTA. The binding constant for ANS was estimated to be around 30  $\mu\text{M}$ . Hence, the binding is relatively weak, although the probe at a concentration of 20  $\mu\text{M}$  will have some effect on the RLC binding equilibrium.

The effect of ANS at this concentration, on the RLC binding equilibrium, was studied by following the increase in ANS fluorescence, when the ANS was added to preparations preincubated in EDTA or  $\text{Mg}^{2+}$ . These experiments indicated that 80% of the fluorescence change was complete within the mixing time, the remainder occurring with a time course similar to that for RLC dissociation. Thus, ANS does have an effect on the RLC binding equilibrium, which may

introduce a small systematic error, when this probe is used to determine the rate of RLC binding, or release. However, since all the experiments are performed under the same conditions, this error can be ignored when considering models of RLC interaction.

#### THE LOCATION OF THE ANS BINDING SITE

The binding of ANS to myosin and subfragments was followed as the RLC dissociated and reassociated. These ANS changes occur over a period of several minutes, as shown by the time courses in fig 4-4. On addition of EDTA, the divalent metal ions are chelated, the RLC dissociates from the heavy chain/ELC complex and the ANS binds, with an increase in the fluorescence emission at 460 nm. In order to differentiate between binding of the ANS to the RLC, ELC and the heavy chain, ANS binding to the isolated light chains was studied. Characteristic ANS fluorescence was observed in both RLC and ELC preparations when the ANS was excited directly. When the ANS was excited via tryptophan residues, only the ELC showed ANS fluorescence, because the scallop RLC does not contain tryptophan residues. In all cases the fluorescence was small compared to that observed in the heavy chain/ELC complex (even at a similar protein weight ratio). There is therefore no evidence that ANS binding to the ELC was responsible for the observed changes on addition of EDTA to the subfragments. Hence, the ANS binding site is likely to be located on the heavy chain. It remains possible, however, that the ELC

adopts a new conformation on binding to the heavy chain, which will bind more ANS.

The observed amplitude of the ANS time-courses was dependent on the myosin subfragment being studied. Changes observed with  $S1^{+RD}$  were generally much smaller than those observed with HMM or myosin (fig 4-4c cf. 4-4a,b). This result is expected because the RLC cannot readily dissociate from the  $S1^{+RD}$  molecule (Stafford et al., 1979). With  $S1^{-RD}$ , no fluorescence changes were observed on addition of EDTA, or  $Mg^{2+}$  (fig 4-4d). This preparation does not contain any RLC and is also known to have lost a 4,000 mw peptide from the heavy chain (Wells and Bagshaw, 1983). As the initial ANS binding is not increased in  $S1^{-RD}$  compared to  $S1^{+RD}$ , it is likely that the ANS binding site in the former molecule is no longer competent. Unlike  $S1^{-RD}$ , the regulatory fragment containing both RLC and ELC, binds ANS in the same way as for the larger subfragments (fig 4-4e).

Proteolytic studies (Bennett et al., 1984; Szentkiralyi, 1984) were used to locate the position of the regulatory fragment in  $S1^{+RD}$  and identify the origin of the 4,000 mw heavy chain difference peptide between  $S1^{+RD}$  and  $S1^{-RD}$ , because this was a possible ANS binding site. On the basis of these studies, the regulatory fragment was located at the C terminus of the subfragment 1 molecule. Together with evidence for the lack of an ANS binding site in  $S1^{-RD}$  and the absence of the regulatory fragment in digests of this preparation, the ANS binding site has been tentatively

assigned as on the 4,000 mw difference peptide. This site is thought to be at the extreme C terminus of the S1 heavy chain (fig 4-5). However, the assignment is tentative for the following reasons. (a) the ANS site may be on the ELC fragment lost during S1<sup>-RD</sup> preparation. This is thought to be unlikely because the isolated ELC shows little ANS binding compared to other subfragments, however, it has not been rigorously disproved, (b) the light chains stretch over an extended area and probably protect a large amount of the heavy chain "neck" region. This may occur even if the 12000 mw regulatory fragment is not located directly at the C-terminus, (c) the location of the proposed 24000/20000 precursor of the regulatory fragment (fig 4-5) is based on sequence homology with other myosins and has not been rigorously established, (d) the precursor/product relationship for the larger peptide with the regulatory fragment is difficult to confirm, because of the tendency of the larger peptide to remain associated with N-terminal fragments. Also, labelling of the 24,000 peptide with IAEDANS does not yield a labelled regulatory fragment, (e) the absence of the 12000 mw fragment in S1<sup>-RD</sup> tryptic digests, may be the result of exposure of a trypsin-sensitive site in the S1<sup>-RD</sup>, which is rapidly cleaved in the absence of the RLC. In this case the 4,000 mw peptide lost in S1<sup>-RD</sup> preparation may not come from the regulatory fragment.

DESENSITIZATION OF SCALLOP HMM

Unfortunately, tryptic digestion of RLC denuded myosin does not yield a viable heavy meromyosin preparation (Wells and Bagshaw, 1983) and an alternative method is required to produce a desensitized HMM preparation.

Isolated RLC of scallop myosin are sensitive to cleavage by chymotrypsin, rapidly being degraded to fragments with molecular weights in the 12-14,000 range. The sensitivity of intact myosin to this enzyme, depends on the digestion conditions. In the presence of EGTA, with no added  $Mg^{2+}$ , brief chymotryptic digestion removes the RLC with little or no heavy chain digestion (Kendrick-Jones and Jakes, 1976). Using this enzyme it has proved possible to remove the RLC, with no damage to the heavy chain of HMM, if the digestion is performed in the presence of the chelator EDTA. ANS has proved to be a convenient and rapid method, to probe for the amount of RLC remaining in a preparation and the ability of the remaining heavy chain/ELC complex to rebind RLC.

The rationale behind the method used for checking the extent of digestion is explained in fig 4-6. The normal ANS response on addition of EDTA to HMM, followed by excess  $Mg^{2+}$  is shown in fig 4-6a. However, if chymotrypsin is added instead of  $Mg^{2+}$ , the dissociated RLC is rapidly digested. After stopping the proteolysis with PMSF, addition of  $Mg^{2+}$  has little effect on the ANS fluorescence (as long as all the RLC has been digested). Addition of stoichiometric

RLC from scallop or another species at this point, results in ANS displacement as they bind to the denuded HMM (fig 4-6b). The extent of this binding should be the same as in the control sample if no heavy chain degradation has occurred. Digestion may be performed at higher protein concentrations in the absence of ANS. In this case, if a sample is taken, the ANS response on addition of  $Mg^{2+}$  followed by RLC will then give an indication of the state of the molecule. Polyacrylamide gel electrophoresis (fig 4-7) confirms that under optimum conditions, the RLC (fig 4-7c cf d) can be removed, with little attack on the HMM heavy chain (fig 4-7a cf b).

The Mg-ATPase activity in the absence of actin and the calcium sensitivity of the preparations was checked using a fluorescence method. (Wells et al., 1985). When ATP binds to myosin or myosin subfragments, the intrinsic tryptophan fluorescence increases and remains enhanced until all the ATP has been hydrolysed. The effect of addition of  $Ca^{2+}$  or EGTA, on the rate of hydrolysis, can thus be observed. Native HMM, chymotryptically-desensitized HMM and resensitized HMM were tested for the  $Ca^{2+}$ -sensitivity of their ATPase (fig 4-8). Native HMM hydrolyses ATP typically 2 to 3 times faster in the presence of  $Ca^{2+}$  than in its absence (fig 4-8 b cf a). On chymotryptic desensitization this difference is reduced and the preparation is no longer  $Ca^{2+}$ -sensitive (fig 4-8 d cf c). The  $Ca^{2+}$ -sensitivity is regained after incubation with scallop RLC (fig 4-8 f cf e), typically to about 80% of its initial value.

This confirms that there is little heavy chain damage caused by this procedure, as indicated by the gel electrophoresis. The method has the advantage over gel filtration methods for separating RLC from desensitized preparations of being quick, the RLC can be removed and replaced with another preparation within 30 minutes, if required. One small problem encountered was some variation in the rate of RLC degradation. This is thought to be the result of residual protease inhibitor present from the initial digestion of myosin to produce HMM. However, varying the length of the digestion usually enabled a successful desensitization to be performed. The method should be applicable to all scallop myosin subfragments from which the RLC can be removed by treatment with EDTA.

#### THE KINETICS OF THE RLC INTERACTION

ANS has proved a useful indicator for following RLC association and dissociation as shown by the time-courses in fig 4-4. Similar time-courses were obtained for a turbid myofibrillar suspension, by measuring the ANS fluorescence emission in the front face mode (fig 4-9).

The effect of increasing the NaCl concentration on the time courses was studied, because myosin is insoluble in low NaCl concentrations (less than 0.12M), but loses Ca<sup>2+</sup> regulation in high salt (0.12 to 0.6M). Therefore, it was important to understand the effect of NaCl on the RLC interaction. The rates and amplitudes of the ANS fluorescence changes in HMM were not affected by increasing

the NaCl concentration (fig 4-10a cf b). However, the amplitude of the changes in  $S1^{+RD}$ , were markedly reduced by this action (fig 4-10c cf d). The difference in the response of the two preparations to increased NaCl, was presumably the result of loss of part of the heavy chain from the "neck" region of  $S1^{+RD}$ , or to the presence of the two heads in the HMM molecule. From these results, it would be expected that myosin would behave more like HMM than  $S1^{+RD}$ , with regards to the effect of NaCl. Hence, by studying HMM in low salt (40 mM NaCl), the results for RLC association and dissociation should be generally applicable to the intact myosin.

From the time courses obtained, it was obvious that when  $Mg^{2+}$  was initially bound at the non-specific site, the rate of RLC release, as shown by ANS fluorescence, was partially limited by the rate of  $Mg^{2+}$  dissociation. This was typically reflected in a lag phase in the RLC release, which was unaffected by the EDTA concentration used over the range 0.5 to 5mM. Therefore, the rate of release of the RLC with  $Ca^{2+}$  ions bound at the non-specific site was studied, because the rate of release of these ions is an order of magnitude faster than  $Mg^{2+}$  and should not be rate limiting. (Chapter 3). Unfortunately, manual methods could not be used for this experiment, because of the time required to achieve complete mixing. Stopped-flow methods were thus employed, to follow the rate of RLC dissociation with ANS. Fig 4-11 shows the results for RLC dissociation from HMM by this method. The observed time course for RLC release with  $Mg^{2+}$  was three times slower than that with  $Ca^{2+}$ . However, the  $Ca^{2+}$  trace

is likely to be complicated by other processes involving the  $\text{Ca}^{2+}$  specific site and therefore may not be a true measure of the rate of RLC release. For this reason, all experiments with  $\text{Mg}^{2+}$  also contained EGTA to chelate any contaminant  $\text{Ca}^{2+}$  ions. The profile with  $\text{Mg}^{2+}$ , may be modelled in terms of eqn 1:1, with  $k_{+1} = 0.058\text{s}^{-1}$  and  $k_{+2} = 0.014\text{s}^{-1}$ . This value ( $k_{+2}$ ) in  $\text{Mg}^{2+}$  gives a lower limit to the rate of RLC dissociation from the heavy chain/ELC complex.

The rate of RLC rebinding was found to be  $0.006\text{s}^{-1}$  for both HMM and myosin. Rebinding of the RLC in  $\text{S1}^{\text{RD}}$  was often biphasic and was generally slightly faster ( $k_{\text{obs}} = 0.01\text{s}^{-1}$ ), but this is probably a reflection of the small amplitude of the process (rate of equilibration = sum of forward and reverse rate constants). The concentration dependence of the RLC binding in  $\text{Mg}^{2+}$  was studied using ANS for desensitized myosin and HMM. When the proteins were preincubated with EDTA and up to a ten-fold excess of RLC added with excess  $\text{Mg}^{2+}$ , little effect on the rate of rebinding was observed. (Table 4-2).

Table 4-2

The concentration dependence of RLC rebinding to myosin and HMM

Preparation	molar ratio RLC/myosin	$k_{\text{obs}} \text{ s}^{-1}$
HMM	1:1	0.0055
HMM	2:1	0.0056
HMM	5:1	0.0057
HMM	10:1	0.0061
desensitized myosin	1:1	0.0047
desensitized myosin	2:1	0.0049
desensitized myosin	5:1	0.0049

These results indicate that a first-order step is involved in the association of the RLC with the heavy chain/ELC complex and hence, eqn 1:1 cannot be complete. This first-order step could possibly be explained by a rate-limiting conformational change of one or more of the interacting proteins.

The mechanism of reassociation can also be studied by increasing the RLC concentration, in the absence of divalent metal ions. Addition of up to 16  $\mu\text{M}$  exogenous scallop RLC (5:1 molar excess) to HMM, caused no reversal of the EDTA induced ANS response (fig 4-12a). Therefore, an apparent value for the RLC equilibrium binding constant ( $K_2$ , eqn 1:1), under these conditions, must be at least an order of magnitude greater than this (ie  $> 150 \mu\text{M}$ ). With scallop  $\text{S1}^{+\text{RD}}$ , addition of

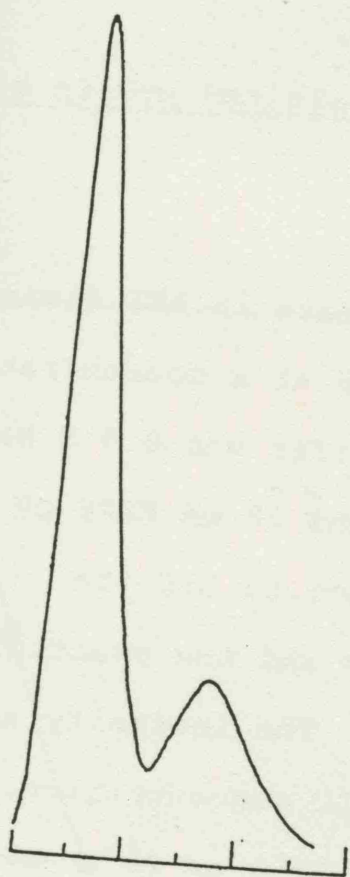
RLC in EDTA caused some release of ANS (fig 4-12b), indicating an apparent value for  $K_2$  of approximately  $10 \mu\text{M}$  for this preparation in EDTA. If the RLC equilibrium binding constants of the double headed preparations in EDTA and  $\text{Mg}^{2+}$  ( $K_2$  cf  $K_4$ , eqn 1:1) are compared, the binding of the RLC is observed to be approximately 3 orders of magnitude weaker ( $> 150 \mu\text{M}$  cf  $0.1-0.3 \mu\text{M}$ ), in the absence of divalent metal ions. This accounts for the ease of dissociation of the RLC from both HMM and myosin on EDTA treatment.

Fig 4-1

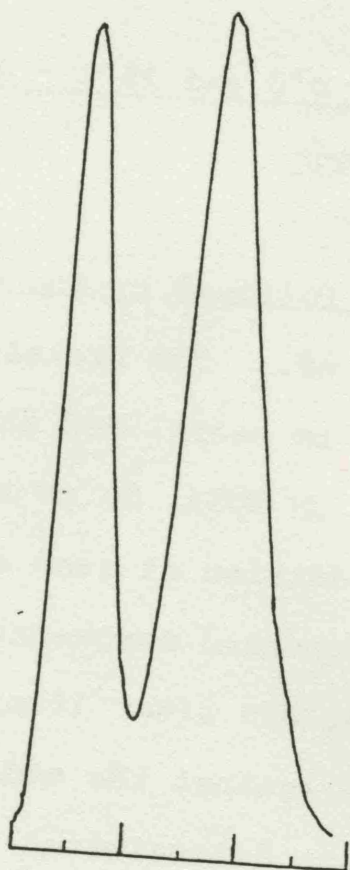
ANS binding to native, desensitized and resensitized scallop myosins

Uncorrected fluorescence emission spectra were recorded by exciting at 295 nm. (a) 0.7 mg/ml myosin (3  $\mu$ M heads) in 0.6M NaCl, 1 mM MgCl<sub>2</sub>, 100  $\mu$ M EGTA and 20 mM EPPS at pH 8.0 and 20°C plus 20  $\mu$ M ANS. (b) 0.7 mg/ml 25°C desensitized myosin in the same solvent. (c) Sample (b), 10 min after addition of 3  $\mu$ M RLC (ie 1:1 with myosin heads). (d) A different preparation of scallop myosin in the same solvent as (a) except [MgCl<sub>2</sub>] was 0.1 mM. (e) Sample (d) 15 min after addition of 0.5 mM EDTA. (f) Sample (e) 15 min after addition of 2 mM MgCl<sub>2</sub>. Although the absorbance of these solutions was about 0.2 cm<sup>-1</sup>, control experiments showed that this parameter, and hence the inner-filter effect, remained constant on addition of effectors.

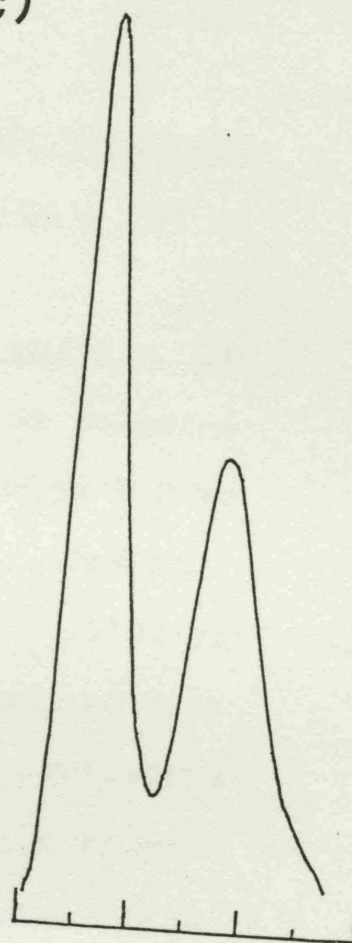
a)



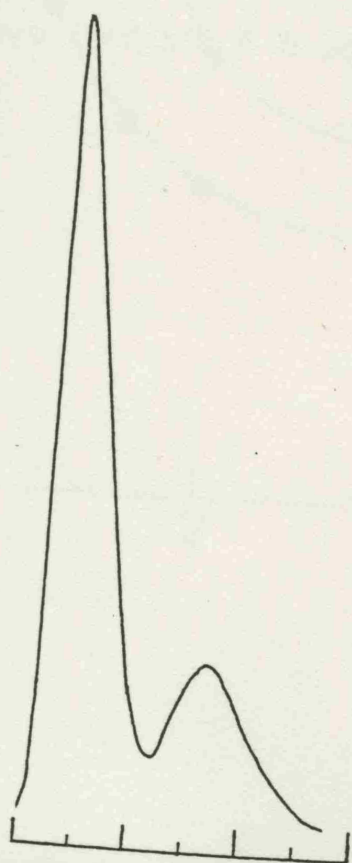
b)



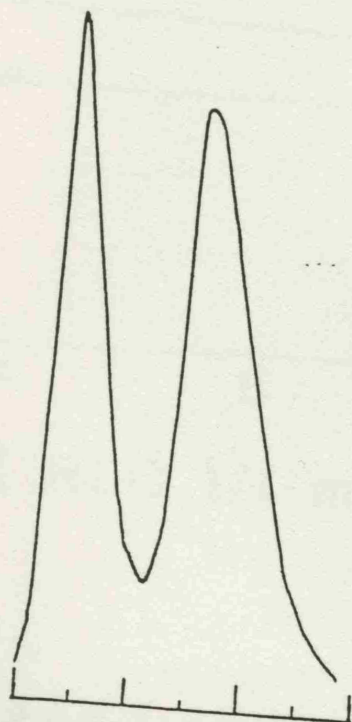
c)



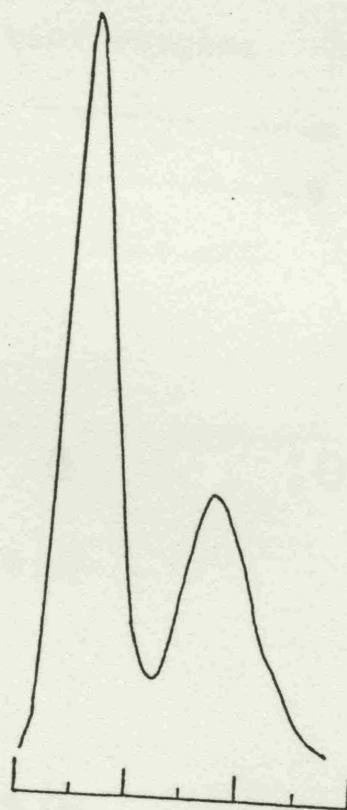
d)



e)



f)



300

500

300

500

300

500

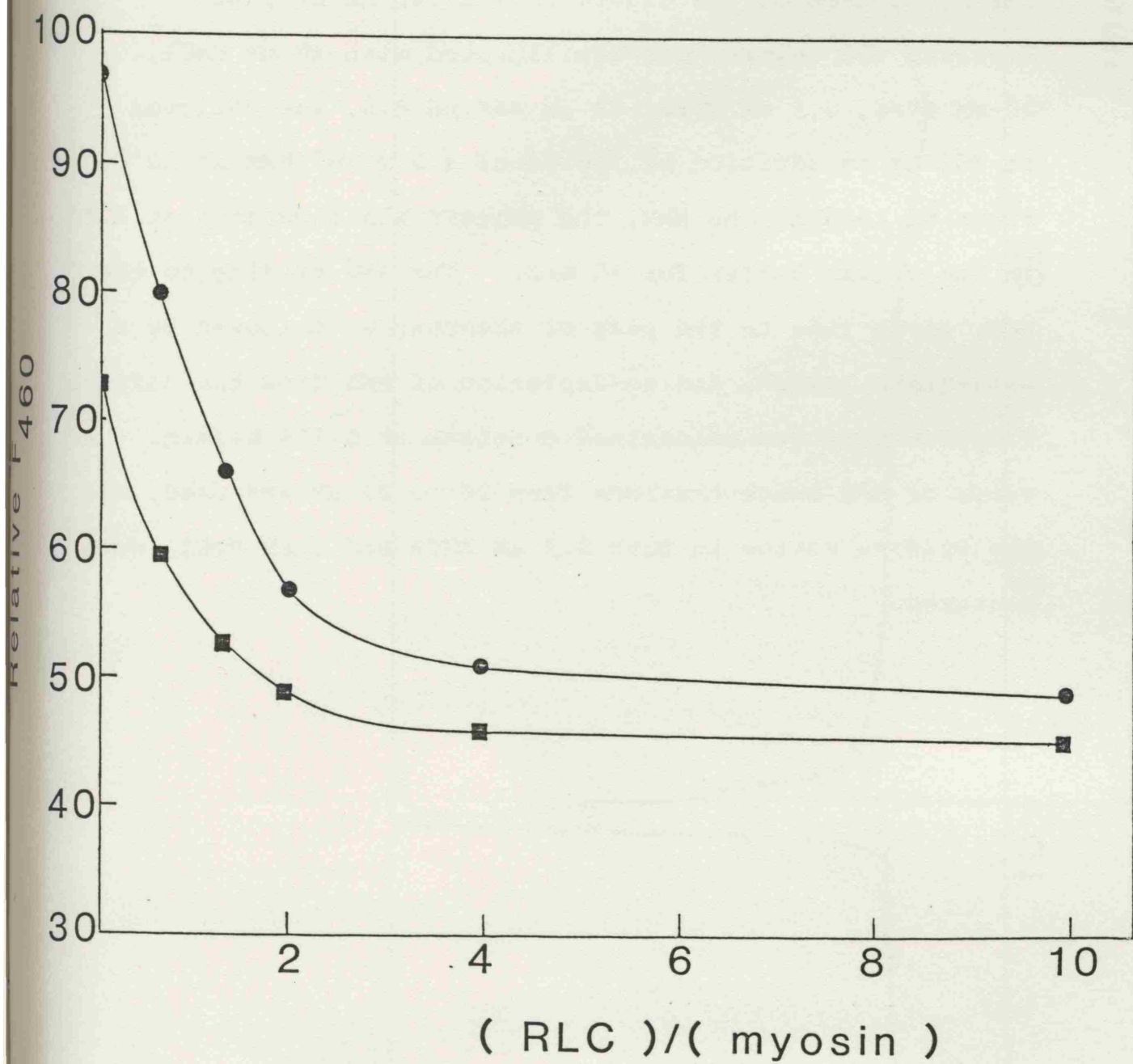
nm

Fig 4-2

Uptake of RLC by 0°C and 25°C - desensitized myosin monitored  
by ANS displacement

RLC binding was followed by the decrease in ANS fluorescence emission at 460 nm. The protein was at a concentration of 0.7 mg/ml (3  $\mu$ m heads) and the buffer was 0.6 M NaCl, 1 mM MgCl<sub>2</sub>, 100  $\mu$ M EDTA, 20  $\mu$ M ANS and 20 mM EPPS pH 8.0 at 20°C. On addition of each aliquot of RLC the fluorescence decreased exponentially and the reaction was effectively complete after 15 min. The intensity at this time is plotted against the added RLC concentration.

● Scallop myosin desensitized with EDTA at 25°C ■ myosin desensitized at 0°C. The initial RLC contents, according to urea gel densitometry, were 0.36 and 0.9 RLC/mol myosin, respectively.



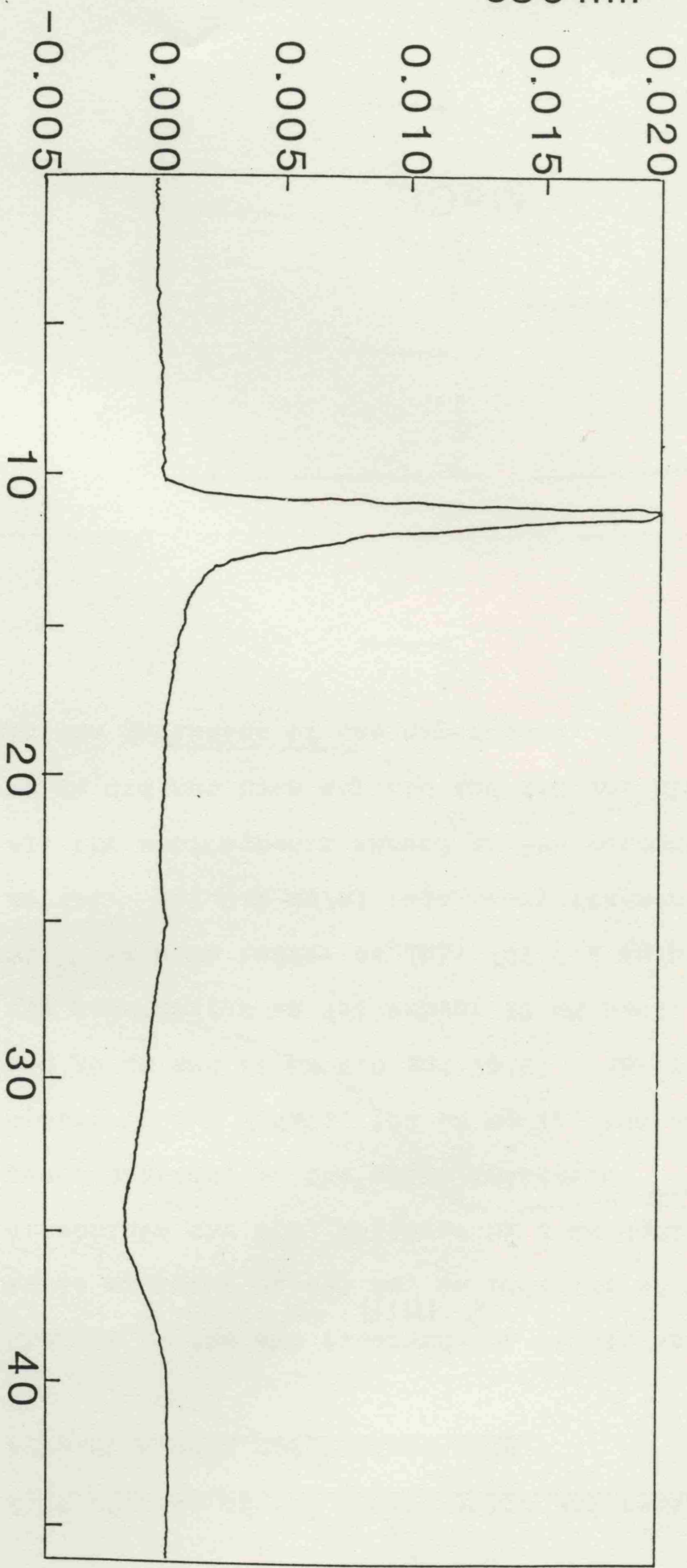
- 25°C desensitized myosin
- 0°C desensitized myosin

Fig 4-3

Typical trace obtained for the estimation of the ANS binding ratio for HMM, using the method of Hummel and Dreyer (1962).

The absorbance of the eluate from a 140 mm by 5 mm Sephadex G50 column, pre-equilibrated with 40 mM NaCl, 20 mM EPPS, 0.5 mM EDTA, 40  $\mu$ M ANS pH 8.0, was followed at 380 nm on addition of 100  $\mu$ l of 4.5 mg/ml HMM at 20°C. Prior to loading the HMM, the protein was incubated at 20°C in the column buffer for 15 min. The ANS binding to the HMM, gives rise to the peak of absorbance, followed by a subsequent trough, due to depletion of ANS from the buffer. The flow rate was maintained constant at 0.175 ml/min. A range of ANS concentrations from 20 to 80  $\mu$ M was used, and the binding ratios in both 0.5 mM EDTA and 1 mM MgCl<sub>2</sub> were measured.

Absorbance<sub>380 nm</sub>



Time min

Fig 4-4

Time courses of RLC dissociation and reassociation in scallop myosin and subfragments

Changes in the ANS fluorescence at 460 nm were followed while exciting at 295 nm, on addition of 0.5 mM EDTA to dissociate the RLC, followed by 2 mM MgCl<sub>2</sub> to cause reassociation, at the times indicated. (a) 0.7 mg/ml myosin in 0.6 M NaCl, 100 μM MgCl<sub>2</sub>, 100 μM EGTA, 20 mM EPPS and 20 μM ANS at pH 8.0 and 20°C. (b) 0.6 mg/ml HMM in the same buffer as (a) except 40 mM NaCl. (c) 0.5 mg/ml S1<sup>+RD</sup> in same buffer as (b), (d) 0.5 mg/ml S1<sup>-RD</sup> in same as (b). (e) 0.2 mg/ml regulatory fragment in same as (b). All the subfragments showed an ANS response except the S1<sup>-RD</sup>, which did not have any RLC and did not bind additional ANS at the beginning of the experiment.

ANS Fluorescence ↑

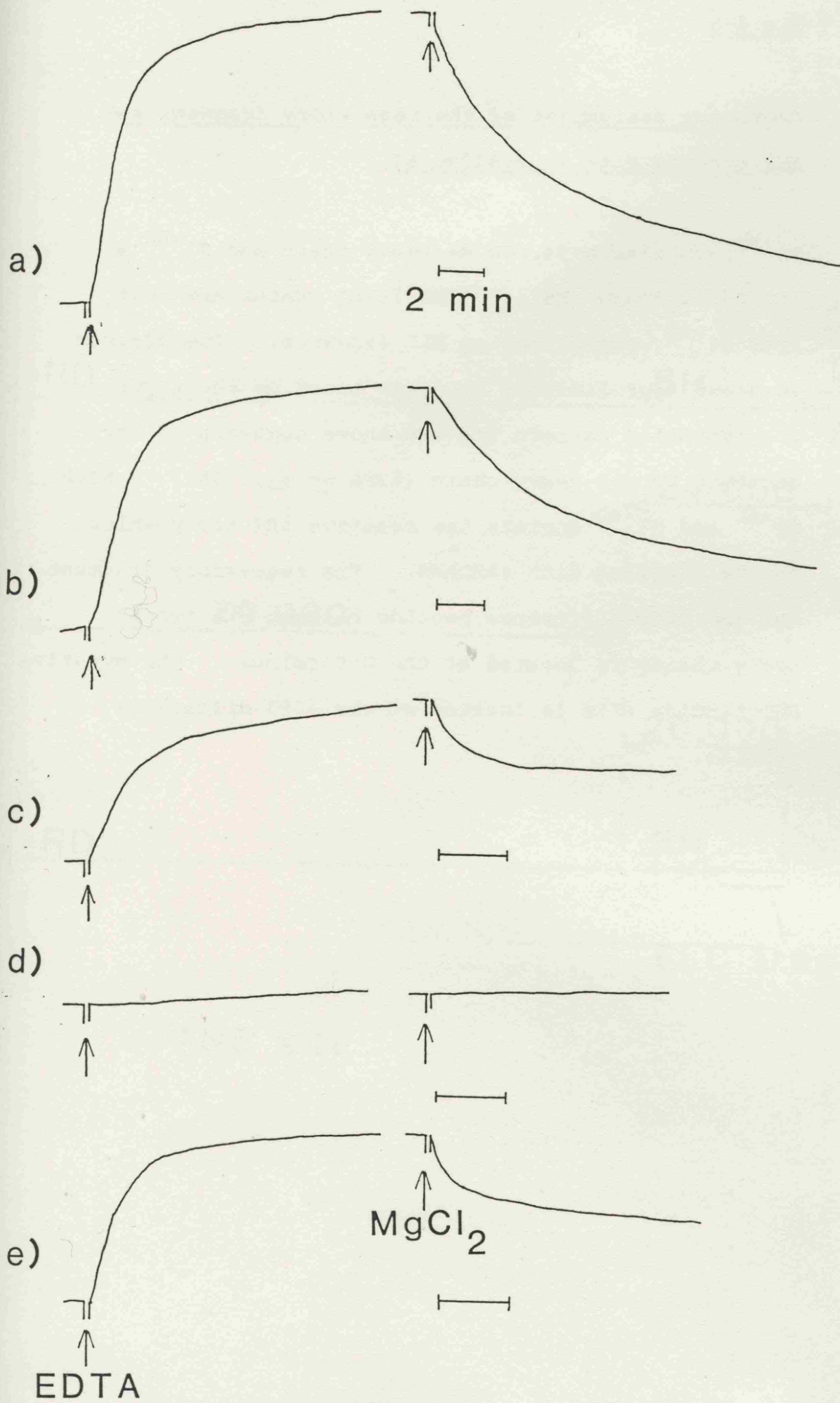
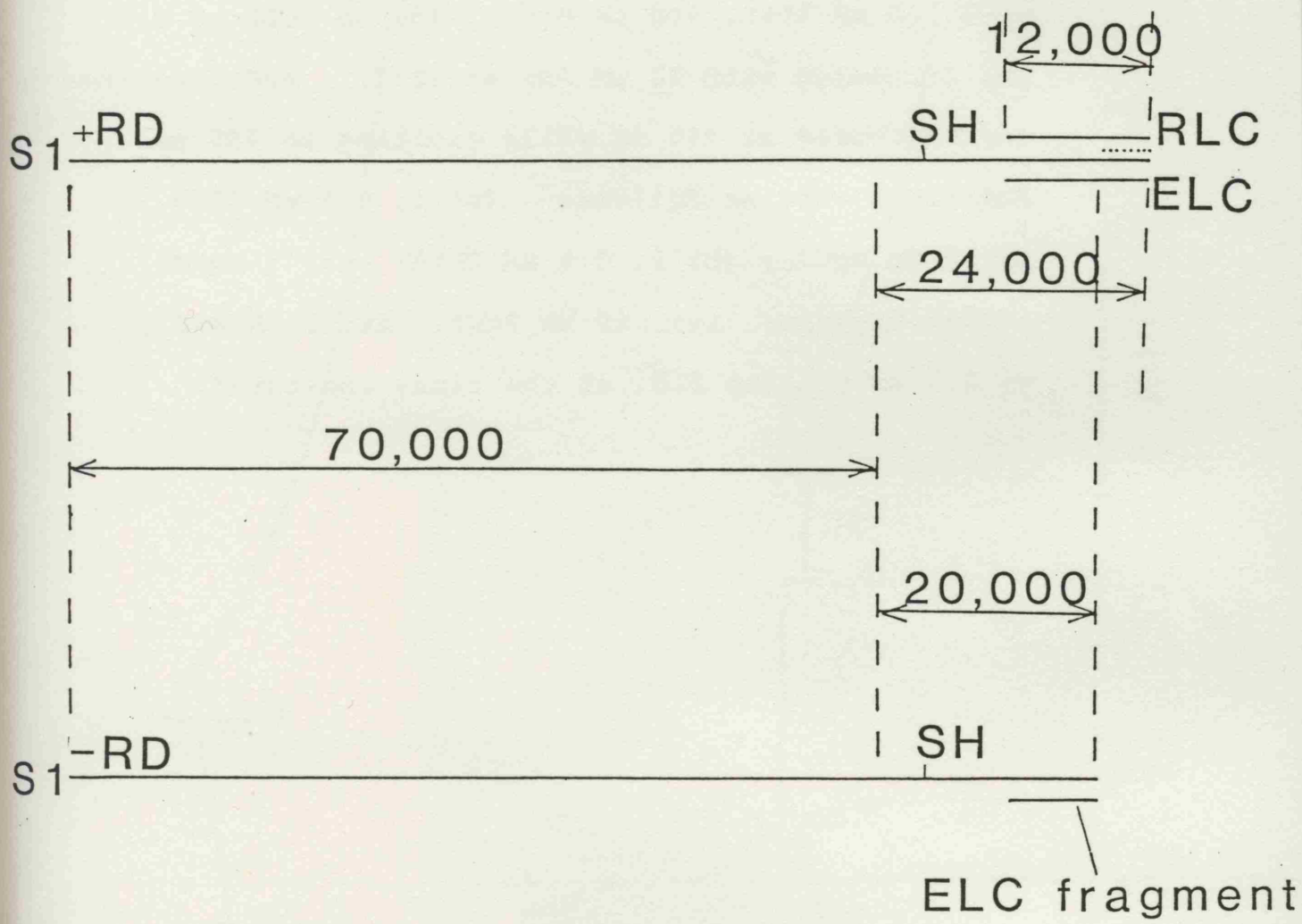


Fig 4-5

Tentative assignment of the regulatory fragment and  
ANS binding site in scallop S1.

S1<sup>+RD</sup> contains a 94,000 mw heavy chain and S1<sup>-RD</sup> a 90,000 mw heavy chain. The light chains are lost from S1<sup>-RD</sup>, except for an ELC fragment. The diagram is drawn approximately to scale based on the tryptic fragmentation pattern and the known sequence of the nematode myosin heavy chain (Karn et al, 1982). Both S1<sup>+RD</sup> and S1<sup>-RD</sup> contain the reactive SH1 group which can be labelled with IAEDANS. The regulatory fragment and the 4000 difference peptide between the two S1 heavy chains is located at the C-terminus. The putative ANS-binding site is located on the 4000 difference peptide.



..... ANS site

Fig 4-6

Removal of RLC from scallop HMM

Scallop (*Pecten maximus*) HMM (3.5  $\mu$ m heads) in 40 mM NaCl, 20 mM EPPS, 100  $\mu$ M MgCl<sub>2</sub>, 100  $\mu$ M EGTA pH 8.0 was incubated with 20  $\mu$ M ANS at 20°C. ANS fluorescence was monitored at 460 nm while exciting at 295 nm. Additions were as follows: (a) i, 0.5 mM EDTA, ii, 2 mM MgCl<sub>2</sub>; (b) i, 0.5 mM EDTA; ii, 1 mg/ml  $\alpha$ -chymotrypsin; iii, 10  $\mu$ M PMSF; iv, 2 mM MgCl<sub>2</sub>; v, 3.5  $\mu$ M scallop RLC, at the times indicated.

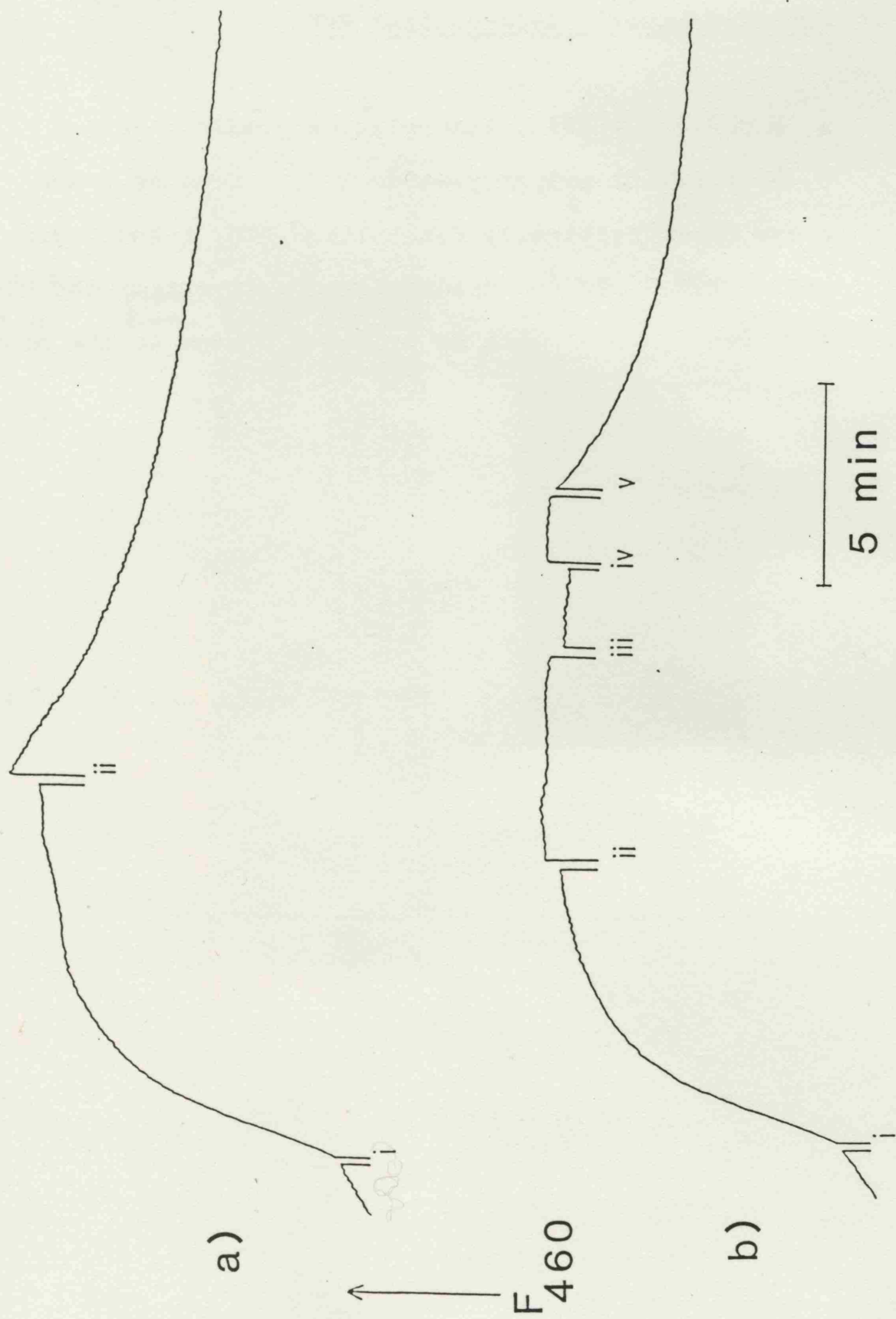


Fig 4-7

Urea and SDS- polyacrylamide gels of HMM and  
chymotryptically desensitized HMM

a, b SDS/7.5 - 20% polyacrylamide gradient gel;  
c, d urea/mini polyacrylamide gel. Samples b and  
c are chymotryptically desensitized HMM, a and d are  
native HMM. In the desensitized preparation the RLC  
have been removed with no apparent damage to the heavy  
chain or ELC.

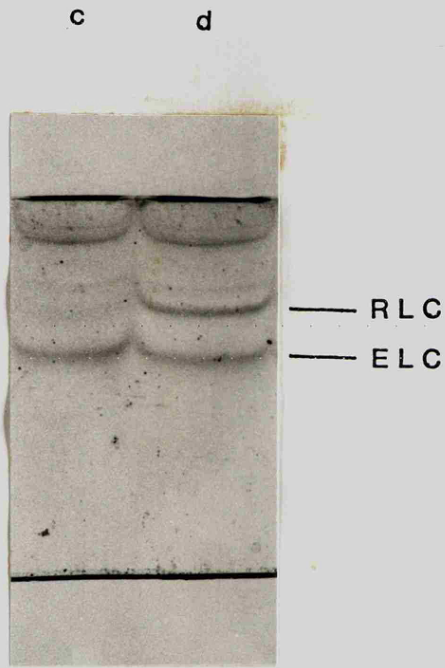
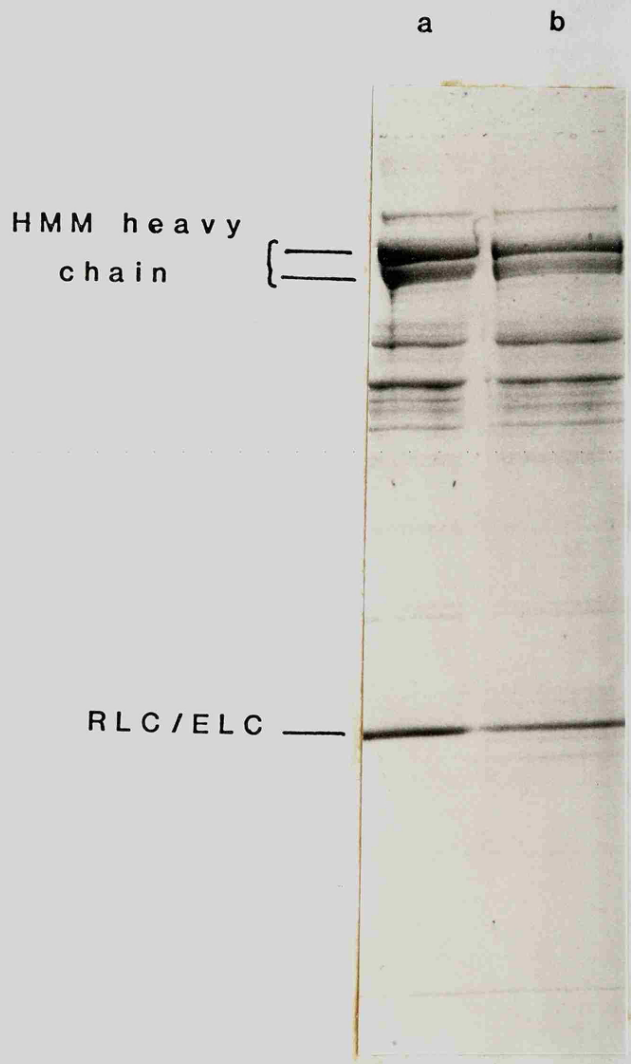
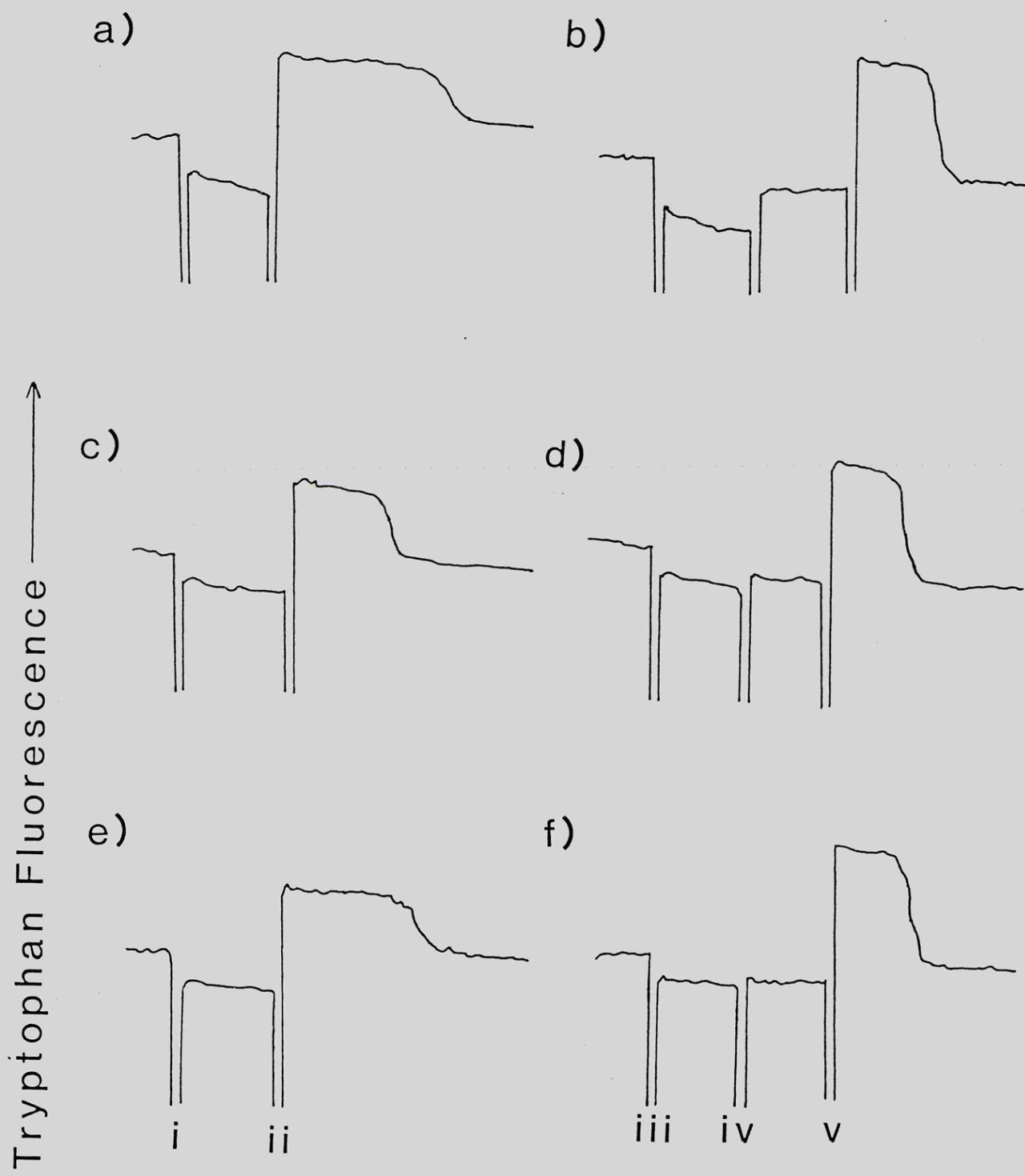


Fig 4-8

Tryptophan fluorescence assays of HMM, desensitized HMM and resensitized HMM to measure Ca<sup>2+</sup>-sensitivity of the Mg-ATPase

The Ca<sup>2+</sup> - sensitivity of the Mg-ATPase of HMM alone was followed by tryptophan fluorescence (340 nm) on addition of ATP. a, b, HMM, c, d, chymotryptically desensitized HMM and e, f, HMM as in c, resensitized by incubation with equimolar scallop RLC. In all cases the buffer was 20 mM NaCl, 10 mM TES, 1 mM MgCl<sub>2</sub>, 10 μM CaCl<sub>2</sub> at pH 7.5 and 20°C. The following additions were made at the times indicated. (i) 100 μM EGTA, (ii) 50 μM ATP, (iii) 100 μM EGTA, (iv) 200 μM CaCl<sub>2</sub>, (v) 50 μM ATP. A 2-3 fold activation of the ATPase of native HMM was observed in Ca<sup>2+</sup> (b cf a). After desensitization the rate of ATPase hydrolysis in the presence of EGTA was the same as in Ca<sup>2+</sup> (c cf d). Readdition of RLC to the desensitized HMM caused inhibition of the ATPase in the absence of Ca<sup>2+</sup>; a two fold activation was observed in its presence.



2 min

Fig 4-9

RLC dissociation and reassociation in scallop myofibrils

The ANS fluorescence at 460 nm was followed while exciting at 295 nm, in the front-face mode. The effect of addition of 1 mM EDTA and 2 mM MgCl<sub>2</sub> at the times indicated was measured, in a 1 mg/ml suspension of myofibrils. The buffer used was 40 mM NaCl, 20 mM EPPS, 0.5 mM MgCl<sub>2</sub>, 100 μM EGTA, 20 μM ANS at pH 8.0 and 20°C.

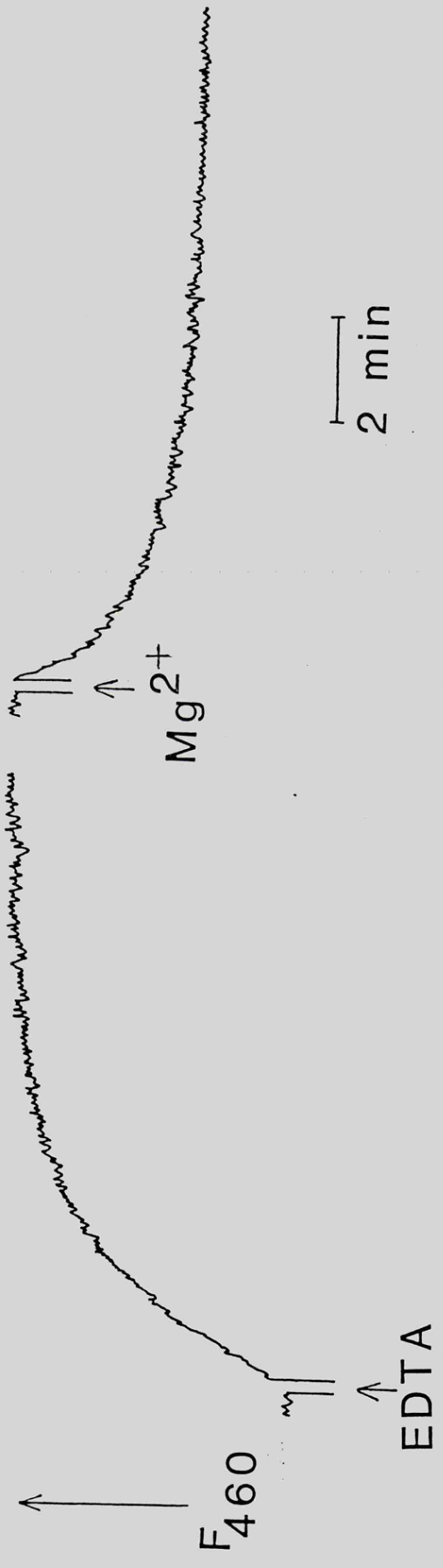


Fig 4-10

The effect of NaCl on RLC dissociation and reassociation

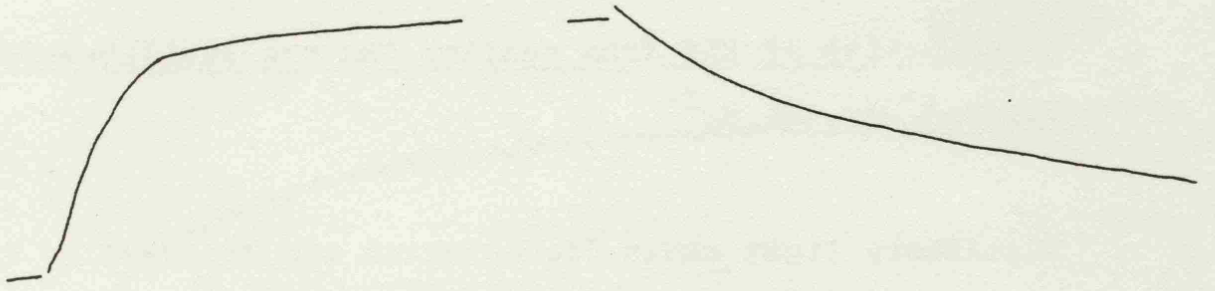
Changes in the fluorescence of ANS at 460 nm were followed while exciting at 295 nm. The buffer used was 20 mM EPPS, 300  $\mu$ M MgCl<sub>2</sub>, 200  $\mu$ M EDTA, 20  $\mu$ M ANS at pH 8.0 and 20°C. NaCl was added as follows:

- (a) 0.6 mg/ml HMM (3.5  $\mu$ M heads) in 40 mM NaCl,
- (b) HMM in 0.6 M NaCl,
- (c) 0.5 mg/ml S1<sup>+RD</sup> (4  $\mu$ M) in 40 mM NaCl,
- (d) S1<sup>+RD</sup> in 0.6 M NaCl.

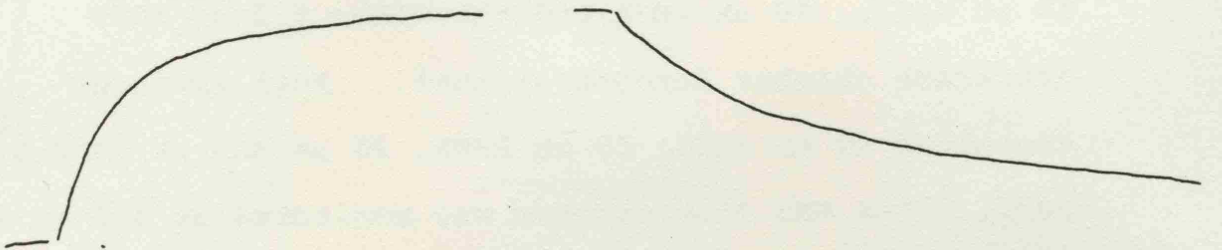
The effect of adding (i) 0.5 mM EDTA and (ii) 2 mM MgCl<sub>2</sub> at the times indicated was monitored. Little effect of increasing the [NaCl] was observed on HMM, however, the response was reduced in S1<sup>+RD</sup>.

F<sub>460</sub> ↑

a)



b)



c)



d)



↑  
EDTA

↑  
Mg<sup>2+</sup>

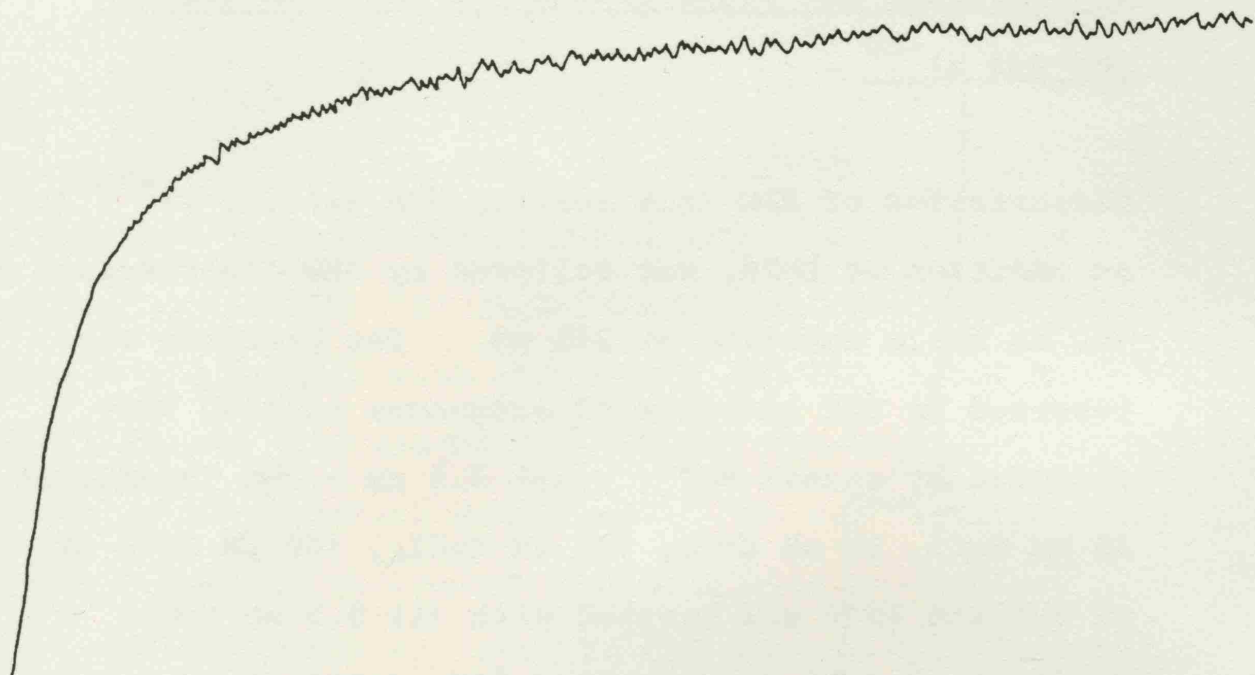
5 min

Fig 4-11

Dissociation of RLC from scallop HMM pre-equilibrated with  
(a)  $\text{Ca}^{2+}$  or (b)  $\text{Mg}^{2+}$

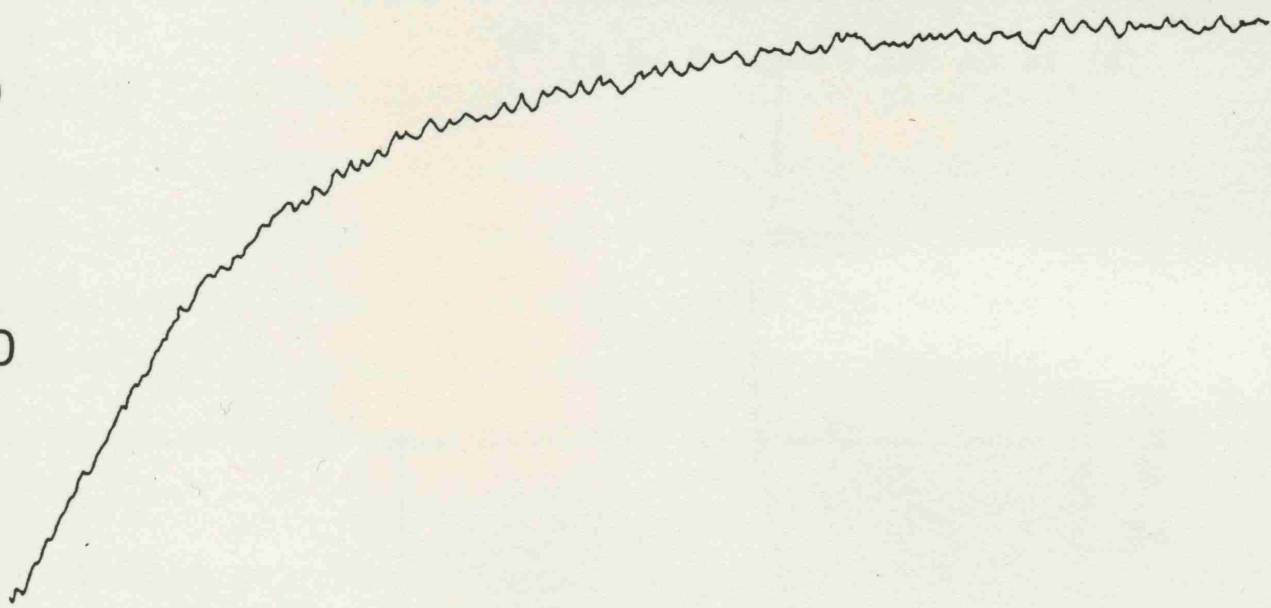
Regulatory light chain dissociation was followed by the increase in ANS fluorescence on mixing scallop HMM with EDTA, using a stopped-flow accessory. One syringe contained 3.5  $\mu\text{M}$  HMM heads and (a) 50  $\mu\text{M}$   $\text{CaCl}_2$ , or (b) 50  $\mu\text{M}$   $\text{MgCl}_2$ , 50  $\mu\text{M}$  EGTA and the other 0.5 mM EDTA (reaction chamber concentrations). Both syringes contained 40 mM NaCl, 20 mM EPPS, 20  $\mu\text{M}$  ANS at pH 8.0 and 20°C. The ANS fluorescence was monitored at 460 nm while exciting via tryptophan residues at 295 nm.

a)



b)

F  
460

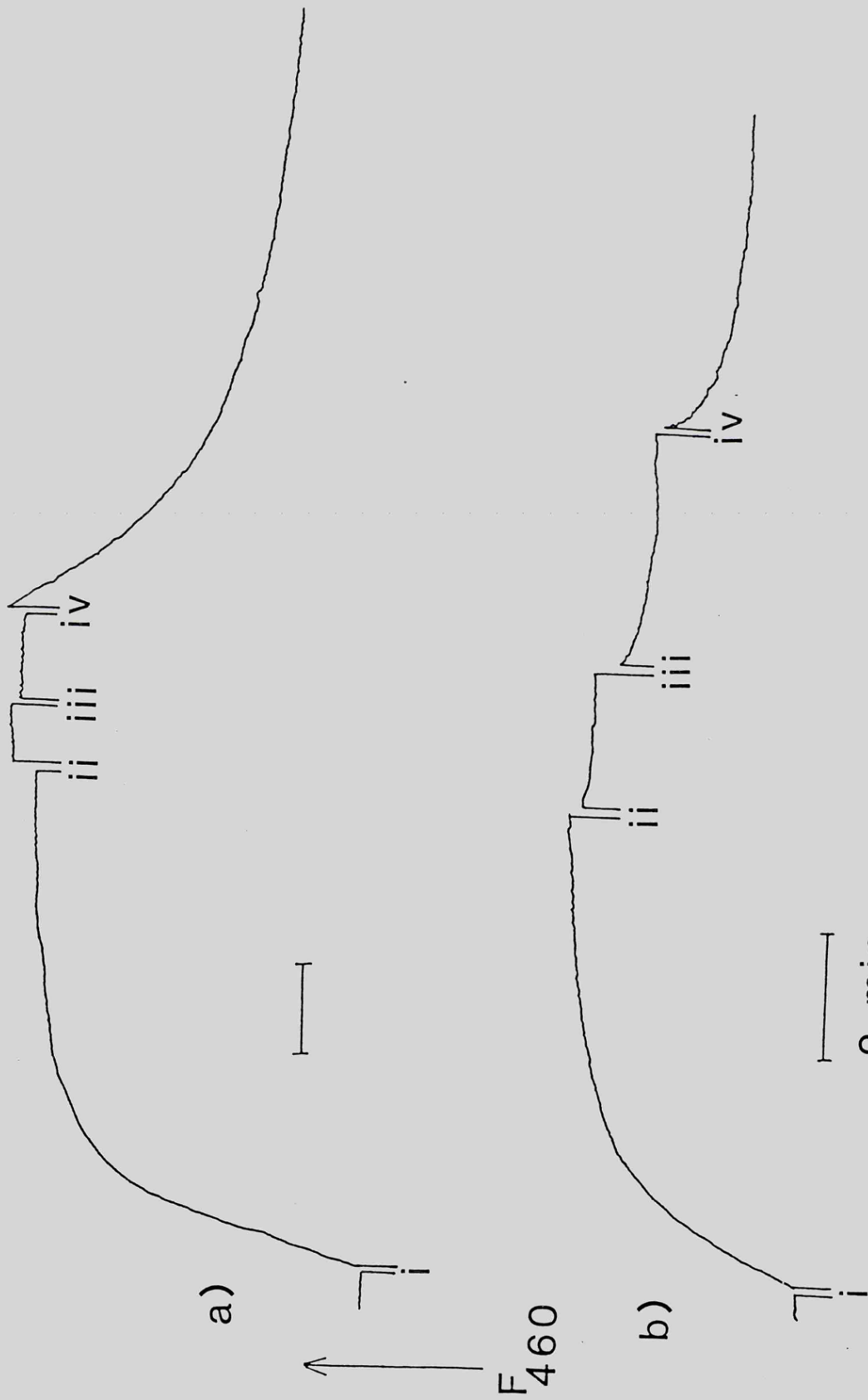


1 min

Fig 4-12

Dissociation and reassociation of RLC from scallop  
HMM and S1<sup>+RD</sup>

Dissociation of RLC from scallop HMM (a) and S1<sup>+RD</sup> (b), on addition of EDTA, was followed by ANS fluorescence at 460 nm while exciting at 295 nm. The reaction was reversed by the addition of exogenous scallop RLC, followed by excess Mg<sup>2+</sup>. (a) 3.5  $\mu$ M - HMM (heads) in 40 mM NaCl, 20 mM EPPS, 100  $\mu$ M MgCl<sub>2</sub>, 100  $\mu$ M EGTA at pH 8.0 and 20°C was treated with (i) 0.5 mM EDTA; followed by (ii) 4  $\mu$ M scallop RLC; (iii) 12  $\mu$ M scallop RLC (ie. total concentration 19.5  $\mu$ M); (iv) 2 mM MgCl<sub>2</sub>. (b) as in (a) except 4  $\mu$ M S1<sup>+RD</sup>.



## CHAPTER 5

### THE BINDING OF *Mercenaria* RLC IN SCALLOP MYOSIN AND SUBFRAGMENTS

The formation of hybrid scallop myosin with foreign RLC has previously been documented (Kendrick-Jones et al, 1976; Sellers et al, 1980). In this chapter the formation of scallop myosin hybrids with *Mercenaria* RLC were studied. The RLC from the pink adductor muscle of *Mercenaria mercenaria* was shown to have unusual properties. It was fortuitously discovered that the *Mercenaria* RLC will bind to scallop myosin with high affinity, even in the absence of divalent metal ions. The binding of this RLC was therefore studied in order to answer the following questions. Are the kinetics of the *Mercenaria* RLC binding affected by the presence or absence of divalent metal ions? How does the binding of *Mercenaria* RLC relate to that of scallop RLC? Does the exchange of RLC follow a simple mechanism with release of scallop RLC prior to binding of the *Mercenaria* RLC or is the exchange more complex?

Two approaches were used to study the interaction. As the *Mercenaria* RLC contains a sulphhydryl group, it was possible to label the light chain specifically. Changes in the environment of IANBD attached to *Mercenaria* RLC were therefore used to follow binding of the light chain, to scallop myosin. The second method involved the use of ANS, which was shown previously (Chapter 4) to be a suitable probe for the RLC binding site.

Binding of *Mercenaria* RLC as followed by ANS displacement

The discovery that *Mercenaria* RLC binds to and displaces ANS from scallop myosin in the absence of divalent metal ions was made during studies on the binding of foreign RLC to HMM and S1<sup>+RD</sup> (fig 5-1 a,b). Binding of the *Mercenaria* RLC, after prior treatment of the HMM preparation with EDTA, was observed to occur at a rate of  $0.0068\text{s}^{-1}$  and was independent of the RLC concentration. With S1<sup>+RD</sup> the profile was slightly faster ( $0.02\text{s}^{-1}$ ) and was preceded by a small burst of ANS release, which was absent in the HMM preparations.

Similar experiments were performed with RLC denuded preparations which allowed the binding of RLC to be studied under varying divalent metal ion conditions, without the complication of competition with the native RLC. Traces for the rebinding of scallop and *Mercenaria* RLC in  $\text{Mg}^{2+}$  and *Mercenaria* RLC in EDTA to desensitized myosin are shown in Fig 5-2. The rates of rebinding for the *Mercenaria* RLC were observed to be the same in both  $\text{Mg}^{2+}$  and EDTA and very similar to that for the scallop RLC. The rates observed were the same as for the initial experiments with HMM ( $0.0068\text{s}^{-1}$ ). Was the binding of the *Mercenaria* RLC in the absence of divalent metal ions occurring in a functional way?

In order to answer the above question, the ability of the *Mercenaria* RLC to restore  $\text{Ca}^{2+}$ -sensitivity to the actin-activated ATPase of desensitized scallop myofibrils was tested. Binding of the *Mercenaria* RLC was performed either in 1 mM  $\text{Mg}^{2+}$ , or in 10 mM EDTA at 20°C, for 20 minutes

and the samples assayed by the pH-stat method. The results are shown in table 5-1.

Table 5-1      Resensitization of desensitized scallop myofibrils  
by *Mercenaria* RLC

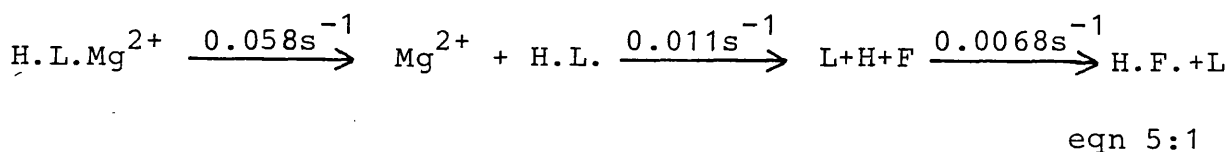
Preparation	Specific activity ( $\mu\text{mol ATP min}^{-1} \text{ mg protein}^{-1}$ )		$\text{Ca}^{2+}$ sensitivity %
	+ $\text{Ca}^{2+}$	- $\text{Ca}^{2+}$	
Native myofibrils	0.330	0.023	93.0
Desensitized myofibrils	0.209	0.128	38.7
Desensitized myofibrils + <i>Mercenaria</i> RLC + $\text{Mg}^{2+}$	0.414	0.053	87.2
Desensitized myofibrils + <i>Mercenaria</i> RLC + EDTA	0.239	0.062	74.1

These results indicate that the *Mercenaria* RLC restores  $\text{Ca}^{2+}$  sensitivity to the scallop myofibrils, both in the presence and absence of divalent metal ions during the resensitization procedure. From the results so far discussed it is apparent that there is a large difference in the affinities of scallop and *Mercenaria* RLC for the scallop heavy chain/ELC complex, in the absence of divalent metal ions. The simplest explanation of these results can be made in terms of conformational differences in the free RLC. It may be assumed that *Mercenaria* RLC exists predominantly in a single conformation regardless of the divalent metal ion content, whereas scallop RLC may have two possible free conformations, one with and one without divalent metal ions. Then, if only the scallop RLC conformation containing  $\text{Mg}^{2+}$  is correct for binding and this

is equivalent to the single free *Mercenaria* RLC conformation, the ability of *Mercenaria* RLC to bind in EDTA and the similarity of the rate of binding of the *Mercenaria* RLC in  $Mg^{2+}$  and EDTA, may be explained.

Since such differences in RLC affinities may arise, competition experiments, such as those performed by Sellers et al. (1980), must be interpreted with this in mind. The conditions under which the experiments are carried out and the order of light chain addition may affect the results. It is possible that, under some conditions, the hybrid myosins produced may be controlled by the kinetics of the RLC binding, rather than by thermodynamic factors.

The results of the initial *Mercenaria* experiments indicated that it should be possible to study RLC exchange using ANS as a probe. The simplest scheme to account for RLC exchange between scallop and *Mercenaria* RLC is given in eqn 5:1, where F is *Mercenaria* RLC, L is the scallop RLC and H the heavy chain/ELC complex.



The scheme comprises three consecutive reactions (i) dissociation of  $Mg^{2+}$ , (ii) release of the scallop RLC and (iii) binding of the *Mercenaria* RLC. The binding of the *Mercenaria* RLC is limited by a first order step, as indicated by the concentration independence of the ANS response and is therefore modelled as such, rather than as a second-

order rate constant. The ANS response observed for HMM (fig 5-1a), on addition of EDTA followed by *Mercenaria* RLC, can be modelled as shown in fig 5-3a. The first phase was fitted to a two step consecutive reaction assuming  $k_{+1} = 0.058s^{-1}$ , from which a value for  $k_{+2} = 0.011s^{-1}$  was obtained. The second phase was modelled as a best fit to a single exponential and yielded a rate constant of  $0.0068s^{-1}$ . If eqn 5:1 was a complete description of the kinetic mechanism of light chain exchange, then, simultaneous addition of EDTA and *Mercenaria* RLC to a scallop HMM preparation pre-equilibrated in  $Mg^{2+}$ , should be accompanied by a transient phase of ANS binding. This phase of ANS binding would be the result of faster formation of the denuded heavy chain/ELC complex (H) than its removal by binding of the *Mercenaria* RLC. The expected ANS fluorescence change in such an experiment is simulated in fig 5-3b using the values obtained for the simulation in fig 5-3a. An amplitude of approximately 50% of the normal EDTA induced ANS response is predicted and hence it should be easily detected.

When this experiment was performed, with EDTA and *Mercenaria* RLC being added simultaneously to an HMM preparation pre-incubated in  $Mg^{2+}$ , the result in fig 5-3c was obtained. No transient phase of ANS binding was observed. Experiments performed using  $S1^{+RD}$  gave the same result, however, with this preparation the expected transient phase would be smaller, due to the reduced ANS response observed on EDTA addition. Thus, it is apparent that eqn 5:1 does not completely explain the RLC exchange. The exchange of the two types of RLC

on the heavy chain/ELC complex does not appear to occur via a simple consecutive reaction.

BINDING OF FLUORESCENTLY LABELLED *MERCENARIA* RLC

*Mercenaria* RLC labelled at their sulphhydryl groups with the fluorescence probe IANBD, have provided an alternative method for following the binding of this RLC to the scallop myosin heavy chain/ELC complex. The binding of the labelled RLC to desensitized myosin has been followed in both EDTA and  $Mg^{2+}$ . As the RLC bound to the heavy chain/ELC complex, the fluorescence was observed to decrease (fig 5-4). The initial rate constants for *Mercenaria* RLC binding by this method was found to be same ( $k_{obs} = 0.017s^{-1}$ ) under both conditions. However, in the presence of  $Mg^{2+}$  the *Mercenaria* RLC binding appeared to be biphasic. This is likely to be the result of competition between the *Mercenaria* RLC and any native scallop RLC remaining in the desensitized myosin preparation, for the RLC binding site. In EDTA this competition does not exist because of the inability of the scallop RLC to bind under these conditions. The values obtained for the RLC binding by this method, were faster than obtained from the previous ANS results. This could be explained if the binding of the RLC was not a simple one step process. If the binding occurred in more than one defined step, then, it would be possible for the two probes (IANBD and ANS) to monitor different steps in the binding pathway.. In such a case it would be possible for the *Mercenaria* RLC to bind initially (as observed by

the fluorescently labelled RLC) prior to causing release of the ANS. Unfortunately, investigations of this binding are limited by the inability to label scallop RLC, due to the absence of a sulphhydryl group and the irreversibility of the *Mercenaria* RLC binding to the scallop myosin heavy chain/ELC complex.

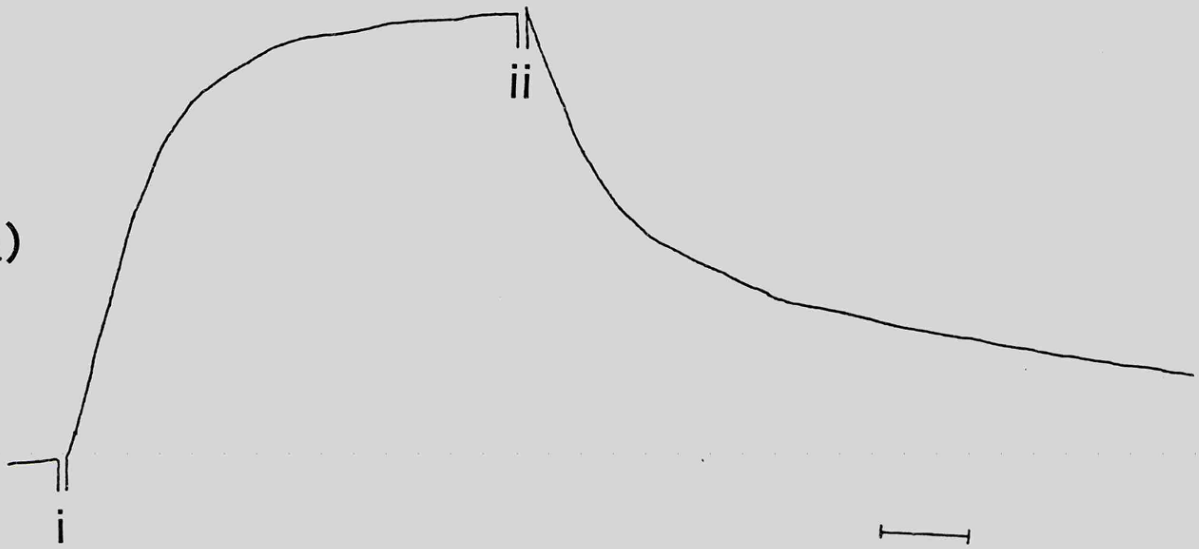
Even with the complications noted above, the labelled *Mercenaria* RLC has proved useful in studying the binding of this RLC during exchange experiments, as performed in the previous section. When myosin was preincubated with EDTA, prior to addition of the labelled *Mercenaria* RLC, binding was observed to occur with a rate constant of  $0.017s^{-1}$ , as for the desensitized myosin (fig 5-5a). However, if the *Mercenaria* RLC and EDTA were added simultaneously to a myosin preparation preincubated with  $Mg^{2+}$ , then the rate constant for binding was  $0.037s^{-1}$  (fig 5-5b). The difference in the rates of *Mercenaria* RLC binding could be explained by there being more than one state of the myosin heavy chain/ELC complex, to which the labelled RLC can bind. This possibility is discussed later (see Chapter 7).

Fig 5-1

Dissociation of scallop RLC and binding of *Mercenaria*  
RLC in scallop HMM and S1<sup>+RD</sup>

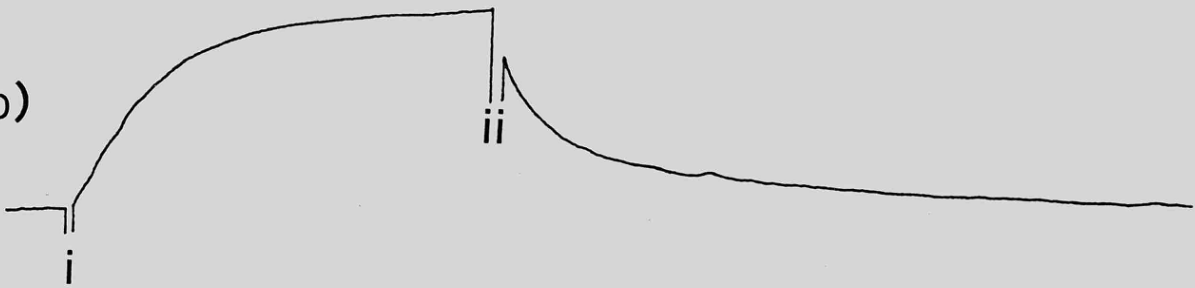
Dissociation of RLC from scallop HMM (a) and S1<sup>+RD</sup> (b) on addition of EDTA, was followed by ANS fluorescence. The probe was excited via tryptophan residues at 295 nm and the fluorescence was monitored at 460 nm. The reaction was reversed by addition of exogenous *Mercenaria* RLC. (a) 3.5  $\mu\text{M}$  - HMM(heads) in 40 mM NaCl, 20 mM EPPS, 100  $\mu\text{M}$  MgCl<sub>2</sub>, 100  $\mu\text{M}$  EGTA, 20  $\mu\text{M}$  ANS at pH 8.0 and 20°C was treated with (i) 0.5 mM EDTA (ii) 3.5  $\mu\text{M}$  *Mercenaria* RLC at the times indicated. (b) as in (a) except 4  $\mu\text{M}$  S1<sup>+RD</sup> and 4  $\mu\text{M}$  *Mercenaria* RLC was added at (ii).

a)



F  
460

b)



2 min

Fig 5-2

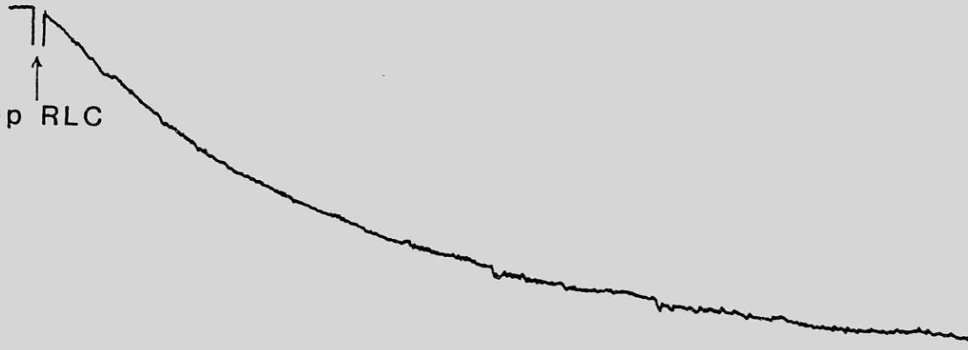
The binding of RLC to desensitized myosin

The binding of scallop and *Mercenaria* RLC to desensitized myosin was followed by ANS fluorescence (460 nm). The ANS was excited via tryptophan residues at 295 nm.

(a) 0.7 mg/ml desensitized HMM in 0.6M NaCl, 20 mM EPPS, 1 mM MgCl<sub>2</sub>, 100 μM EGTA, 20 μM ANS at pH 8.0 and 20°C. At the time indicated stoichiometric scallop RLC was added to reverse the ANS fluorescence. (b) as in (a) except stoichiometric *Mercenaria* RLC was added at the time indicated. (c) as in (a) except the buffer was 0.6 M NaCl, 20 mM EPPS, 0.5 mM EDTA, 20 μM ANS at pH 8.0 and 20°C. At the indicated points stoichiometric *Mercenaria* RLC, followed by 2mM MgCl<sub>2</sub> were added.

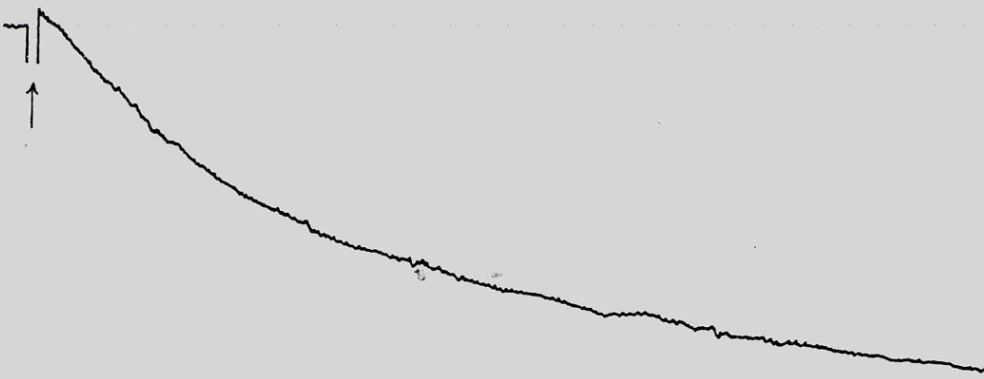
a)

Scallop RLC



b)

F<sub>460</sub>



c)

Mercenaria RLC



Mg<sup>2+</sup>

2 min

Fig 5-3

Simulated and observed rate of *Mercenaria* RLC binding to scallop HMM in the absence of  $Mg^{2+}$

(a) Computer fit of fig 5-1a representing the release of scallop light chains on addition of (i) EDTA followed by (ii), binding of *Mercenaria* RLC. The first phase (i) was fitted to a two-step consecutive reaction assuming  $k_{+1} = 0.058s^{-1}$ , from which a value of  $k_{+2}$  of  $0.011s^{-1}$  was obtained. The second phase (ii) represents the best fit to a single exponential for fig 5-1aii and yielded a rate constant of  $0.0068s^{-1}$ . The incomplete rebinding in fig 5-1a was, at least in part, due to the sloping baseline arising from the slow continuous binding of ANS (Bennett et al., 1984), (b) Computer simulation of the production of H according to eqn 5:1, normalised to the same scale as the first phase of (a). This represents the predicted ANS fluorescence change according to eqn 5:1 when EDTA and *Mercenaria* RLC are added simultaneously (iii) to scallop HMM. (c) Observed ANS fluorescence record when  $3.5 \mu M$  *Mercenaria* RLC and 1 mM EDTA were added simultaneously (iii) to  $3.5 \mu M$  HMM (heads) under identical conditions to those described in fig 5-1.

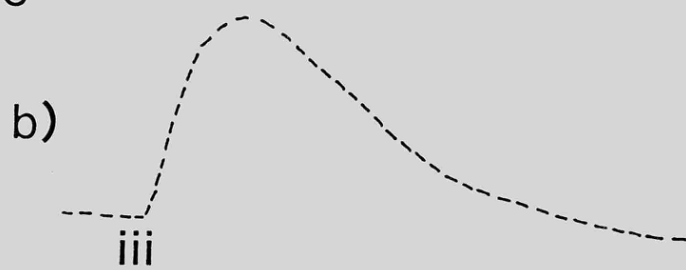
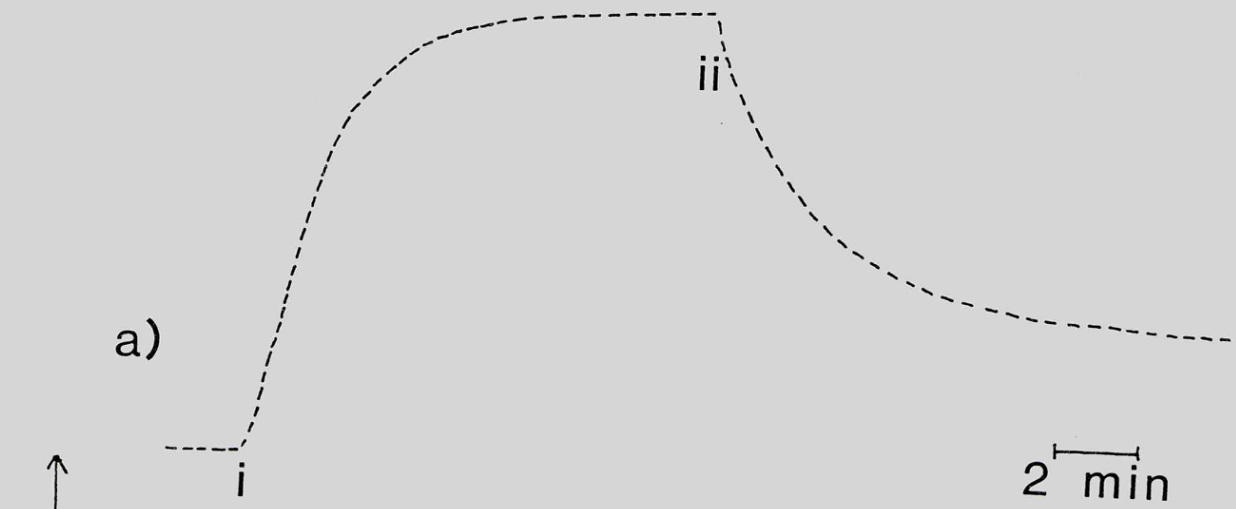
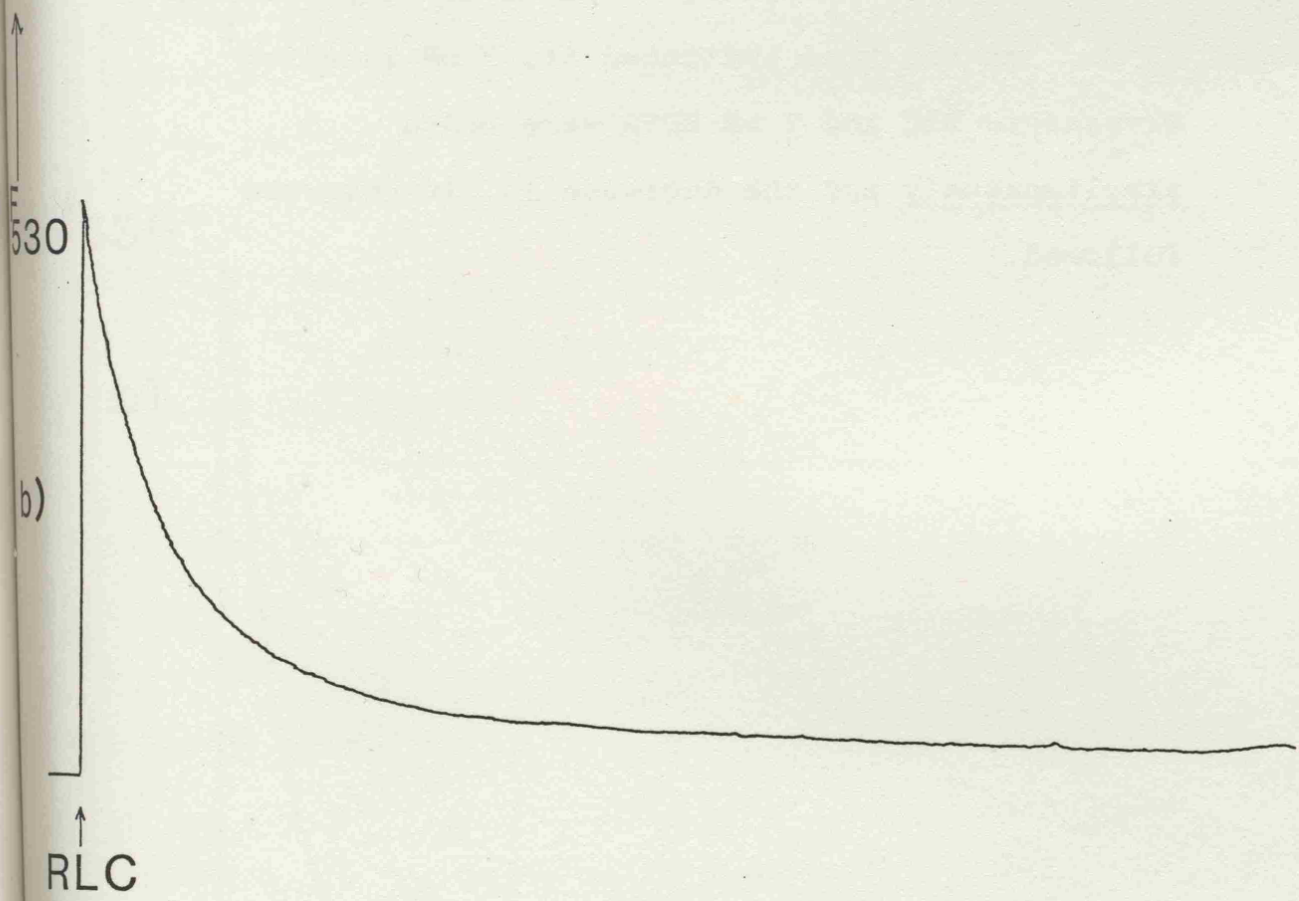
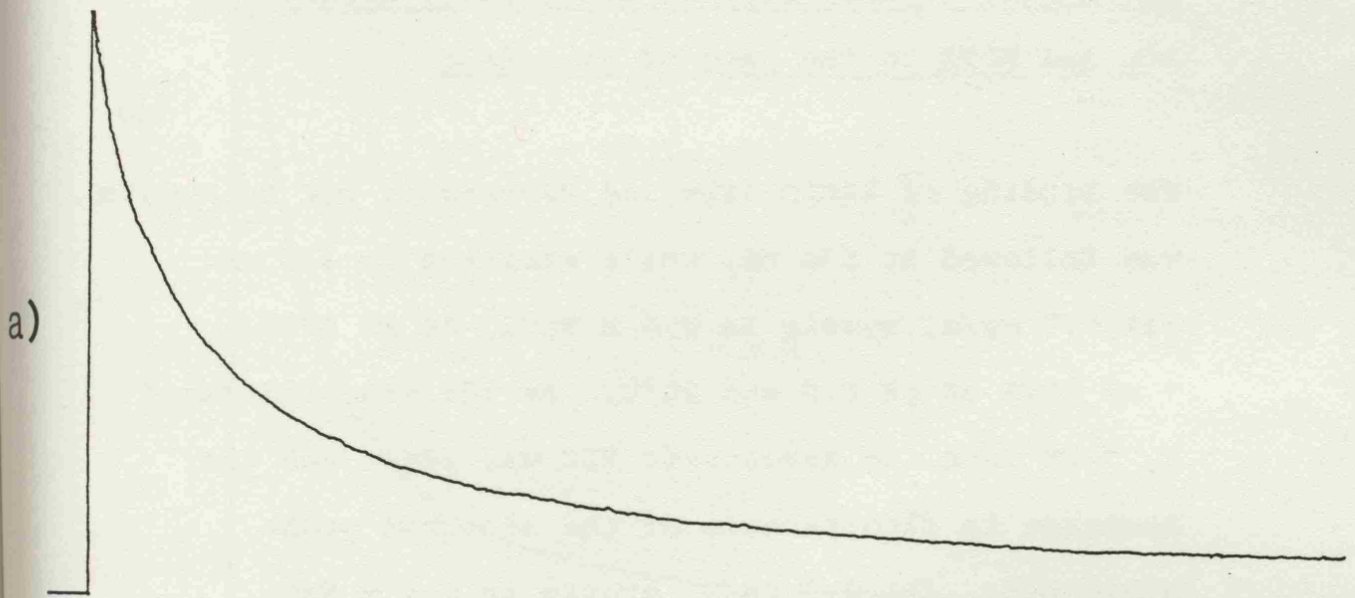


Fig 5-4

Binding of IANBD-labelled *Mercenaria* RLC to  
desensitized myosin in the presence and absence of  
Mg<sup>2+</sup>

The decrease in fluorescence of the IANBD-labelled RLC was followed at 530 nm, as they bound to the desensitized myosin, while exciting at 470 nm. 3  $\mu$ M *Mercenaria* RLC were added at the times indicated, to 0.7 mg/ml desensitized scallop myosin in either (a) 0.6 M NaCl, 20 mM EPPS, 1 mM MgCl<sub>2</sub>, 100  $\mu$ M EGTA at pH 8.0 and 20°C or (b) 0.6 M NaCl, 20 mM EPPS, 0.5 mM EDTA at pH 8.0 and 20°C.



2 min

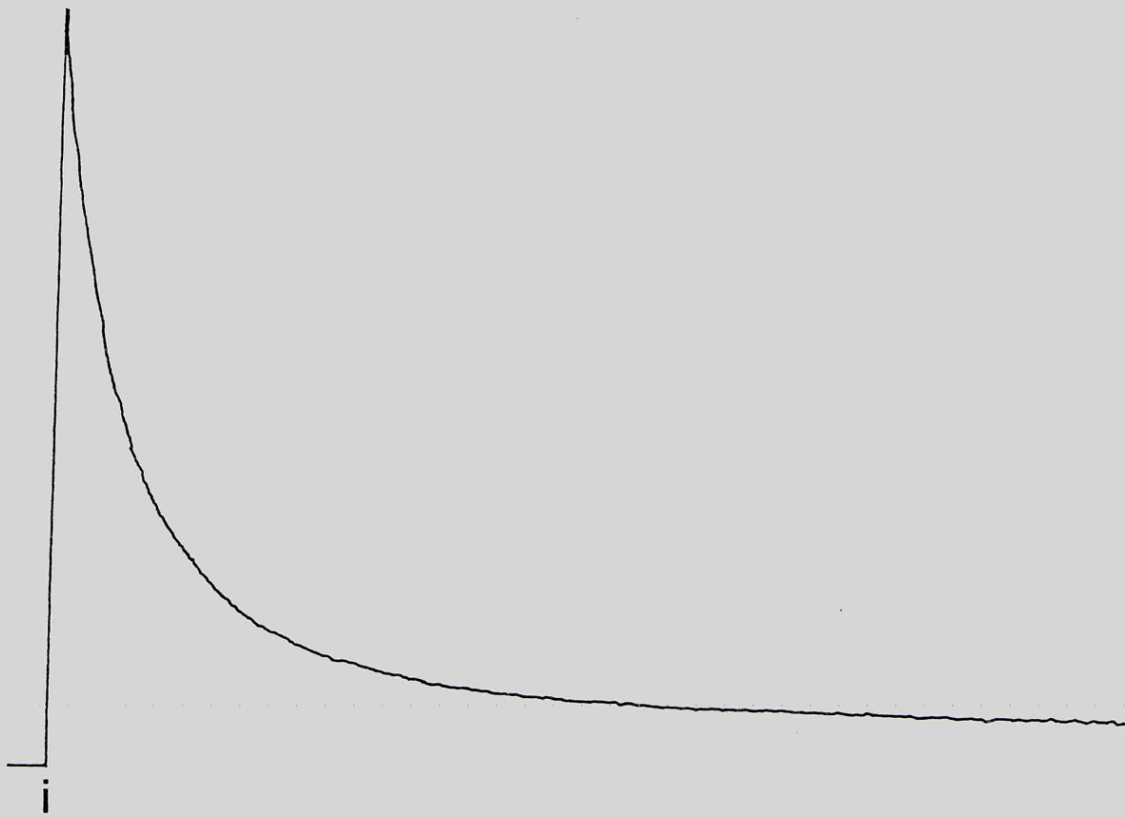
Fig 5-5

The effect of the order of addition of *Mercenaria*  
RLC and EDTA on the rate of rebinding

The binding of IANBD-labelled *Mercenaria* RLC to myosin was followed at 530 nm, while exciting at 470 nm.

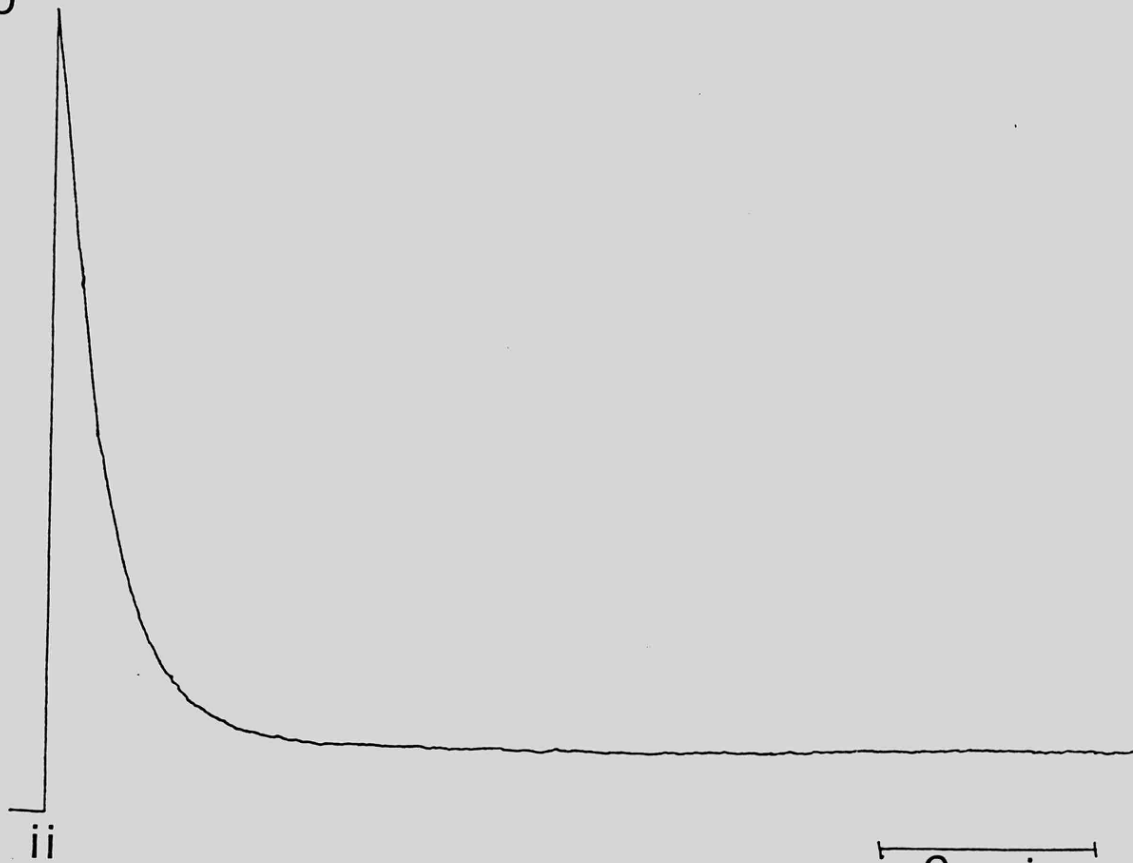
(a) 0.7 mg/ml myosin in 0.6 M NaCl, 20 mM EPPS, 1 mM EDTA at pH 8.0 and 20°C. At the time indicated i, 3  $\mu$ M labelled *Mercenaria* RLC was added and the decrease in fluorescence of the attached probe monitored. (b) 0.7 mg/ml myosin in 0.6 M NaCl, 20 mM EPPS, 0.5 mM MgCl<sub>2</sub>, 100  $\mu$ M EGTA at pH 8.0 and 20°C. At the time indicated ii, 3  $\mu$ M labelled *Mercenaria* RLC and 1 mM EDTA were added simultaneously and the decrease in fluorescence followed.

a)



$F_{530}$

b)



2 min

CHAPTER 6

LIGHT CHAIN INTERACTIONS AND  $Ca^{2+}$  SPECIFIC EFFECTS

The regulatory and essential light chains of myosin are known to lie in close proximity to each other. Regulatory light chains protect the thiol group of the ELC from reaction with iodoacetate, under conditions in which the heavy chain thiols are labelled. If the RLC are removed, then the reactivity of the ELC thiol group is greatly increased, however it cannot be labelled specifically, without labelling the heavy chain (Hardwicke *et al.*, 1983). The discovery by Ashiba and Szent-Györgyi (1984), that the ELC of scallop myosin can be readily exchanged, presented an opportunity to solve this problem. By labelling the ELC prior to exchanging them into the myosin molecule, specific labelling of the ELC thiol group in myosin is effectively achieved. In this chapter, ELC labelled with IANBD have been used to study the exchange of the ELC and interaction of the RLC. What effect does binding or removal of the RLC have on the ELC?

In addition, this chapter considers the effect of  $Ca^{2+}$  binding to the  $Ca^{2+}$ -specific sites of the myosin molecule when  $Mg^{2+}$  occupies the non-specific site. The relative affinity of  $Ca^{2+}$  over  $Mg^{2+}$  for these sites is  $>300$  and  $\sim 10$  for the specific and non-specific site respectively. Therefore, in the presence of  $1 \text{ mM } Mg^{2+}$  and  $10 \text{ } \mu\text{M } Ca^{2+}$ , it is concluded that the non-specific site will be occupied by  $Mg^{2+}$  and the specific site by  $Ca^{2+}$ .

In order to study the effect of micromolar levels of  $\text{Ca}^{2+}$ , Ca-EGTA buffers have to be used. For this work, pH 7.0 was preferred to pH 8.0, because at this pH using sub-stoichiometric  $[\text{Ca}^{2+}]$  to [chelator], it is easier to control the free  $\text{Ca}^{2+}$  levels in the micromolar range. Small variations (10  $\mu\text{M}$ ) in the amount of added  $\text{Ca}^{2+}$  have little effect on the effective free  $\text{Ca}^{2+}$  concentration ( $\sim 0.2 \mu\text{M}$ ), when EGTA is in excess.

The effect of  $\text{Ca}^{2+}$  was studied in native and desensitized preparations, using ANS as an indicator. In desensitized preparations, the non-specific site is absent due to the removal of the RLC. The  $\text{Ca}^{2+}$ -specific site remains with lower affinity, hence, higher  $\text{Ca}^{2+}$  levels are required, but this does not matter due to the absence of the non-specific sites. What effect does  $\text{Ca}^{2+}$  have on the molecule, either in the presence, or absence of the RLC?

#### ESSENTIAL LIGHT CHAIN INTERACTIONS

The rate of exchange of the ELC in desensitized scallop myosin was studied by following changes in the fluorescence of the IANBD-labelled ELC as they were displaced from the molecule by added unlabelled ELC (fig 6-1). Exchange occurred under all the divalent metal ion conditions tested, however, the rates were observed to differ. When the exchange was followed in EDTA or  $\text{Mg}^{2+}$  (fig 6-1a cf 6.1b) the exchange occurred with a rate constant of  $\sim 0.04\text{s}^{-1}$  at  $20^\circ\text{C}$ . This failure of  $\text{Mg}^{2+}$  to have an effect on

the rate of exchange was expected because the preparation lacked RLC and hence the non-specific divalent metal ion binding site.

Addition of  $\text{Ca}^{2+}$  alone (fig 6-1c) or  $\text{Ca}^{2+}$  in the presence of  $\text{Mg}^{2+}$  (fig 6-1d), prior to the unlabelled ELC caused the rate of exchange to be slowed ( $k_{\text{obs}} = 0.015\text{s}^{-1}$ ). This slowing of the rate of ELC exchange suggests that the remaining lower-affinity  $\text{Ca}^{2+}$ -specific binding site still has some function in the desensitized myosin. Presumably the site acts to make the ELC/heavy chain interaction more favourable and hence exchange less favourable. The effect may be mediated by direct binding of the  $\text{Ca}^{2+}$ , the ELC forming part of the specific site, or an indirect effect via the heavy chain which affects the ELC interaction.

Further studies on the effect of  $\text{Ca}^{2+}$  ions, on the fluorescence of the ELC labelled desensitized myosin, were therefore performed. In the presence of 1 mM  $\text{Mg}^{2+}$  ions, addition of  $\text{Ca}^{2+}$  caused a decrease in the fluorescence observed. This change was reversed on addition of EGTA (fig 6-2) to chelate the  $\text{Ca}^{2+}$ . The changes occurred with rate constants of  $0.025\text{s}^{-1}$  and  $0.016\text{s}^{-1}$ , for addition of  $\text{Ca}^{2+}$  and EGTA respectively. The results confirmed the belief that the remaining  $\text{Ca}^{2+}$  site has some effect, even in the absence of the RLC, as indicated by the ELC exchange experiments. Studies on the effect of  $\text{Ca}^{2+}$  in RLC-containing preparations were not performed due to complications presented by the non-specific site of the

RLC and difficulties in defining the absolute metal ion concentrations. This arises because the method of labelling the myosin, involves the use of EDTA to chelate the divalent metal ions and dissociate the RLC to allow ELC exchange to occur.

The effect of RLC on the IANBD-labelled ELC in desensitized myosin was however studied. Addition of scallop RLC caused an enhancement in the fluorescence of the labelled ELC, presumably due to a change in the fluorophore environment (fig 6-3). The rate of the fluorescence change was slower ( $k_{\text{obs}} = 0.003\text{s}^{-1}$ ) than expected from the ANS results for RLC binding. If the RLC binding was reversed, by addition of EDTA to chelate the divalent metal ions, the fluorescence rapidly decreased to its initial level. The rate of this change ( $k_{\text{obs}} = 0.025\text{s}^{-1}$ ) was in this case faster than expected from the ANS results for RLC dissociation. Therefore, it appears that either some rearrangement occurs after RLC association and prior to RLC release, or alternatively that the RLC interaction is not a simple process and has more than one step. In the latter case it is possible that the ANS response and the IANBD labelled ELC changes, are monitoring two different parts of the interaction of the RLC with heavy chain/ELC complex. Regardless of the explanation, it is apparent that the binding of the RLC affects the ELC. This result would be expected from previous work, which indicates the close proximity of the RLC and ELC in the myosin molecule.

CALCIUM SPECIFIC EFFECTS ON ANS FLUORESCENCE

The effect of  $\text{Ca}^{2+}$  was studied using ANS in HMM preparations due to the soluble nature of this myosin subfragment at low ionic strength. Myosin was not used because of the requirement for high NaCl levels to maintain solubility and evidence that the  $\text{Ca}^{2+}$ -specific effects are lost under these conditions (Wells et al., 1985b).

Initially, the effect of adding  $\text{Ca}^{2+}$  to HMM preparations, in the presence of  $\text{Mg}^{2+}$ , was studied at pH 8.0. These experiments indicated that in both native HMM and chymotryptically desensitized HMM, addition of  $\text{Ca}^{2+}$  caused a decrease in the ANS fluorescence. Desensitized HMM gave larger changes than corresponding native HMM (fig 6.4 b cf a), though all the changes were small compared to those for RLC binding and release. The effects were reversible on addition of EGTA to chelate the  $\text{Ca}^{2+}$ . Changes occurred when the ANS was excited directly or indirectly via tryptophan residues, however, when exciting the ANS directly the changes appeared to be smaller.

With desensitized HMM the effects can be attributed to the  $\text{Ca}^{2+}$ -specific site, due to the absence of the RLC. However, with HMM the effects could possibly have been mediated via the non-specific site. For this reason the experiment was repeated at pH 7.0 where the levels of  $\text{Ca}^{2+}$  can be more readily controlled. The effect was still observed to occur (fig 6-4c), even at less than

micromolar levels of free  $\text{Ca}^{2+}$ , indicating the effect must be mediated via the  $\text{Ca}^{2+}$ -specific site.

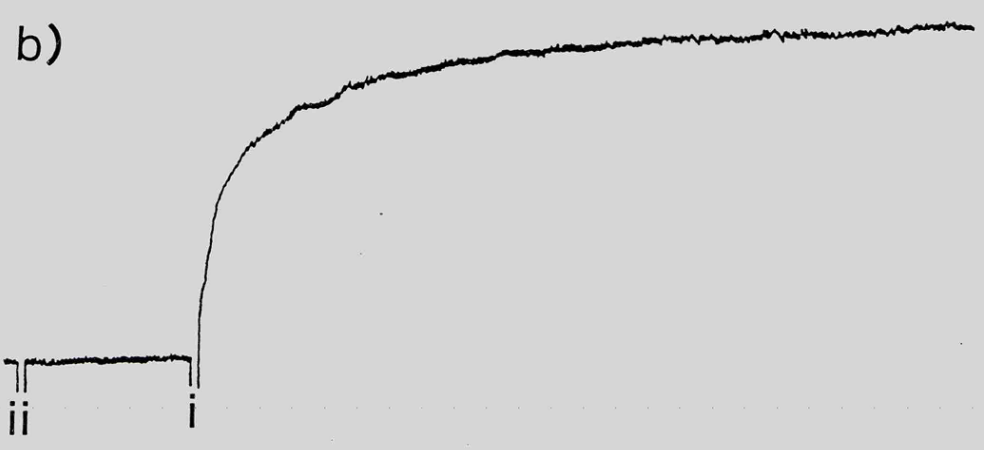
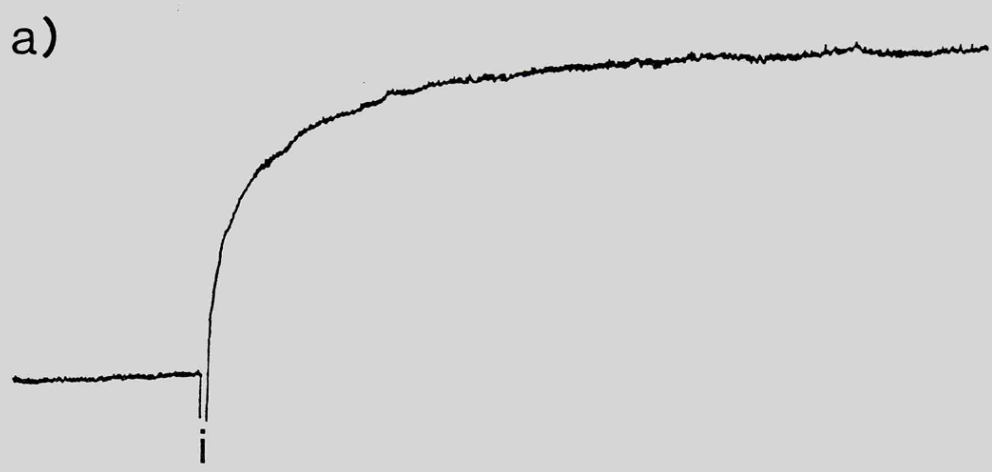
The changes observed in the native HMM could be explained by the  $\text{Ca}^{2+}$ -specific site having an effect on the RLC equilibrium, favouring binding of RLC and thus causing ANS release. However, the results with desensitized HMM suggest this is not the case as no RLC are present in this preparation, unless, the two effects observed are completely different. It is therefore likely to be the result of a conformational change in the molecule which either removes the tryptophan (through which ANS excitation is mediated) away from the ANS site, or causes actual ANS displacement. The fact that the changes occur when the ANS is excited directly, although smaller, would favour ANS displacement. However, it is known that changes do occur in the tryptophan environment on binding  $\text{Ca}^{2+}$ , reflected as a very rapid change in tryptophan fluorescence (Wells *et al.*, 1985b). In this case the larger changes observed with the desensitized preparation could reflect the actual amount of ANS bound to this protein rather than the native protein.

All the changes observed with ANS for  $\text{Ca}^{2+}$  binding or release from the  $\text{Ca}^{2+}$ -specific site were slow, unlike the very rapid changes observed in tryptophan fluorescence ( $>100\text{s}^{-1}$ , C R Bagshaw personal communication) for this site. Hence, these changes cannot be involved in the triggering of muscle contraction by  $\text{Ca}^{2+}$ , although they could possibly have a modulatory effect when there is sustained contraction with the concurrent raised  $\text{Ca}^{2+}$  levels

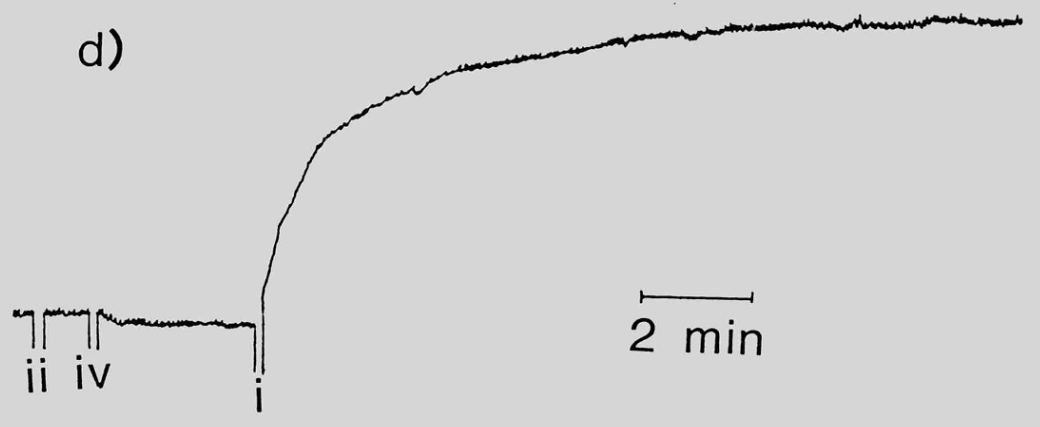
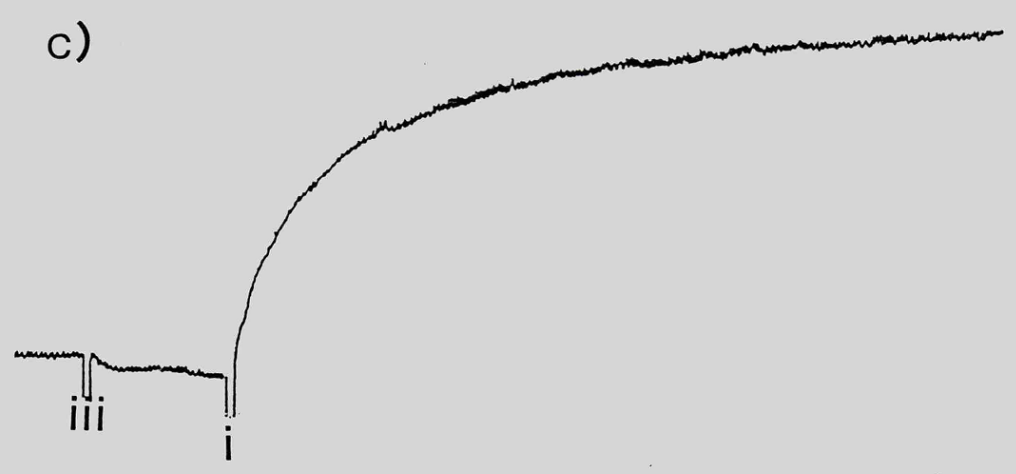
Fig 6-1

The exchange of IANBD-labelled ELC in scallop desensitized myosin

The fluorescence at 530 nm of desensitized myosin into which IANBD-labelled ELC had been previously exchanged (Ashiba and Szent-Györgyi, 1984) was followed, while exciting at 470 nm. In all the experiment 0.7 mg/ml desensitized myosin dissolved in 0.6 M NaCl, 20 mM EPPS, 0.5 mM EDTA at pH 8.0 and 20°C, was used. The following were added as indicated; (i) 6  $\mu$ M unlabelled ELC, (ii) 1 mM MgCl<sub>2</sub>, (iii) 2 mM CaCl<sub>2</sub>, (iv) 700  $\mu$ M CaCl<sub>2</sub>. The exchange was therefore followed in (a) EDTA, (b) MgCl<sub>2</sub>, (c) CaCl<sub>2</sub> and (d) MgCl<sub>2</sub> plus CaCl<sub>2</sub>, on addition of excess unlabelled ELC, which bound as the labelled ELC was released.



$F_{530}$



2 min

Fig 6-2

The effect of Ca<sup>2+</sup> on the fluorescence of IANBD-labelled  
ELC in desensitized scallop myosin

IANBD-labelled ELC were exchanged into desensitized scallop myosin. The fluorescence was monitored at 530 nm on addition of effectors, while exciting at 470 nm. 200  $\mu\text{M}$  CaCl<sub>2</sub> and 300  $\mu\text{M}$  EGTA were added at the times indicated to 0.7 mg/ml desensitized myosin in 0.6 M NaCl, 20 mM EPPS, 1 mM MgCl<sub>2</sub>, 100  $\mu\text{M}$  EGTA at pH 8.0 and 20°C.



F 530

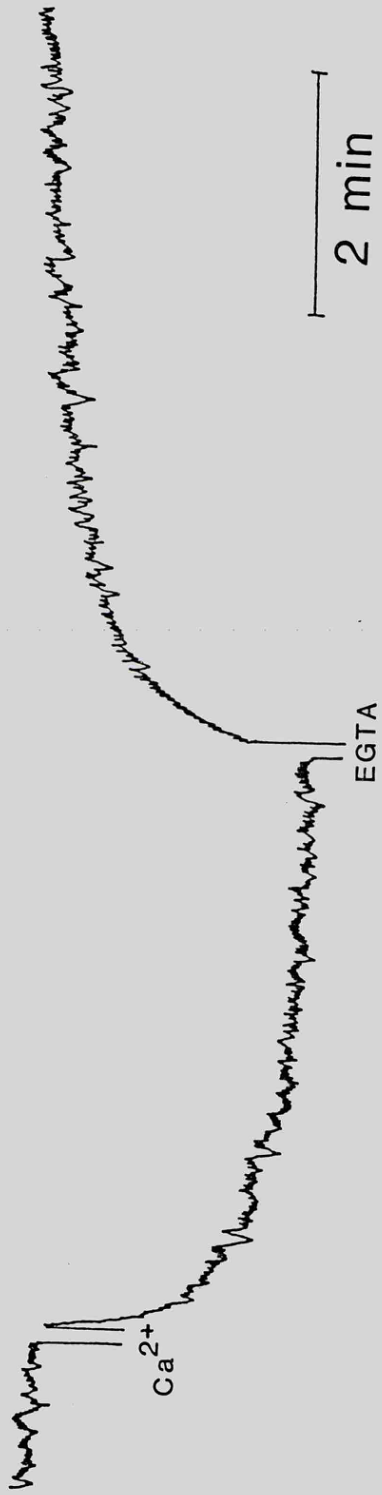


Fig 6-3

The effect of adding scallop RLC on the fluorescence of IANBD-labelled ELC in desensitized scallop myosin

IANBD-labelled ELC were exchanged into desensitized scallop myosin. The fluorescence was monitored at 530 nm on addition of effectors, while exciting at 470 nm. At the times indicated 3  $\mu\text{M}$  scallop RLC followed by 2 mM EDTA were added to 0.7 mg/ml desensitized myosin in 0.6 M NaCl, 20 mM EPPS, 1 mM  $\text{MgCl}_2$ , 100  $\mu\text{M}$  EGTA at pH 8.0 and 20°C.

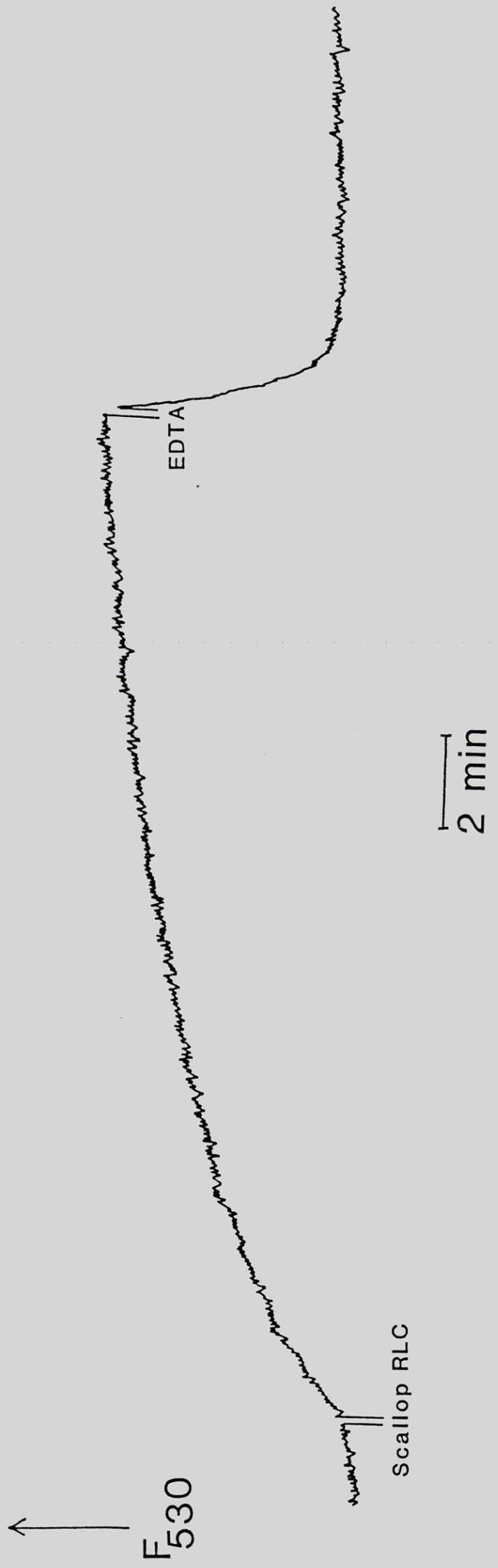


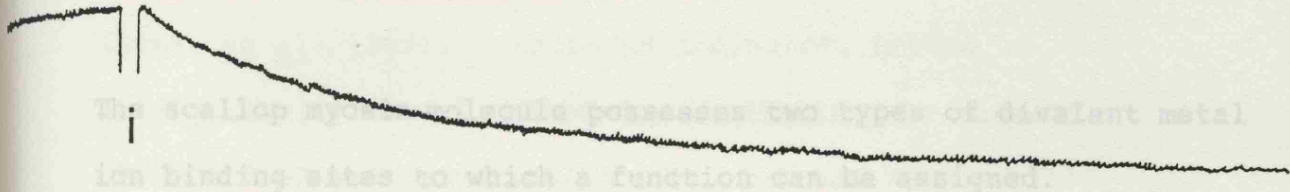
Fig 6-4

The effect of Ca<sup>2+</sup> on HMM as observed by changes in ANS fluorescence

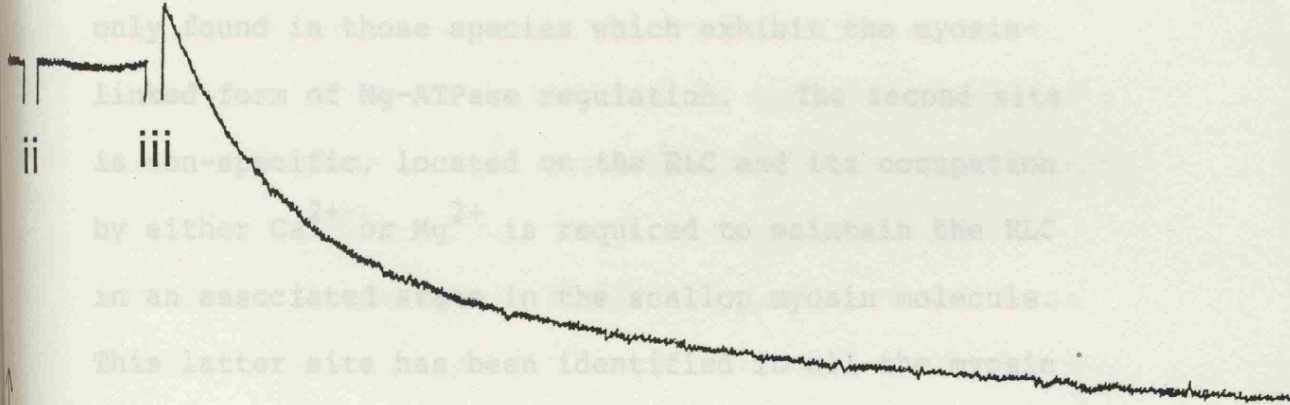
The effect of addition of Ca<sup>2+</sup> to scallop HMM or desensitized HMM, was followed by ANS fluorescence, while exciting at 295 nm. (a) 0.6 mg/ml HMM in 40 mM NaCl, 20 mM EPPS, 2 mM MgCl<sub>2</sub>, 100 μM EGTA at pH 8.0 and 20°C. At the time indicated (i) 150 μM CaCl<sub>2</sub> was added. (b) 0.6 mg/ml chymotryptically desensitised HMM in 40 mM NaCl, 20 mM EPPS, 100 μM EGTA at pH 8.0 and 20°C. At the times indicated (ii) 2 mM MgCl<sub>2</sub> and (iii) 200 μM CaCl<sub>2</sub> were added. (c) 0.6 mg/ml HMM in 40 mM NaCl, 20 mM MOPS, 1 mM MgCl<sub>2</sub>, 100 μM EGTA at pH 7.0 and 20°C. At the indicated time (iv), 50 μM CaCl<sub>2</sub> was added.

a)

The Mechanism of the RLC Interaction

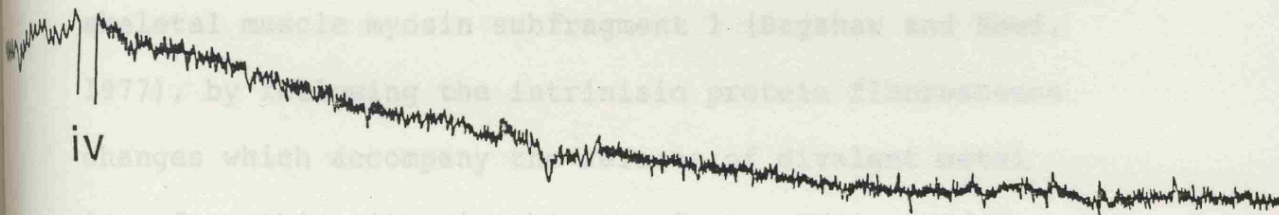


b)



460

c)



2 min

The Mechanism of the RLC Interaction

The scallop myosin molecule possesses two types of divalent metal ion binding sites to which a function can be assigned.

Regulation of the actin-activated Mg-ATPase is mediated via a  $\text{Ca}^{2+}$ -specific site located on the heavy chain/ELC complex, which requires the RLC to give it high affinity and specificity (Chantler and Szent-Györgyi, 1980). This  $\text{Ca}^{2+}$ -specific binding site of the myosin molecule is only found in those species which exhibit the myosin-linked form of Mg-ATPase regulation. The second site is non-specific, located on the RLC and its occupation by either  $\text{Ca}^{2+}$  or  $\text{Mg}^{2+}$  is required to maintain the RLC in an associated state in the scallop myosin molecule. This latter site has been identified in all the myosin RLC studied, however it does not always function to hold the RLC on the heavy chain/ELC complex. In this respect scallop myosins are unusual.

Initially a study was invoked to look at the binding of divalent metal ions at the non-specific site of scallop myosin. Previous work had been performed using rabbit skeletal muscle myosin subfragment 1 (Bagshaw and Reed, 1977), by following the intrinsic protein fluorescence changes which accompany the release of divalent metal ions from this site, in this species. With scallop myosin, this divalent metal ion release from the non-

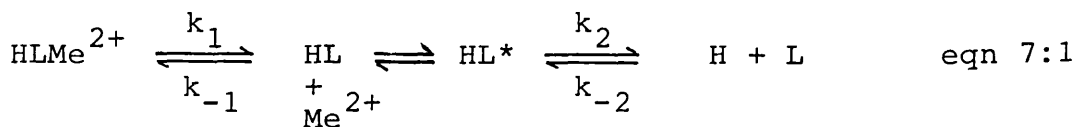
specific site is accompanied by little change in the fluorescence per se, although subsequent dissociation of the regulatory light chains does affect the tryptophan fluorescence (Konno et al., 1983). Using pH indicators proved to be a generally useful method for monitoring the release of  $\text{Ca}^{2+}$  from the non-specific site, but was not suitable for  $\text{Mg}^{2+}$  release. Release of  $\text{Mg}^{2+}$ , from the non-specific site, was therefore studied using  $\text{Mn}^{2+}$  displacement. The results indicate that  $\text{Ca}^{2+}$  release ( $k_{\text{obs}} \sim 0.6 \text{ s}^{-1}$ ) was an order of magnitude faster than  $\text{Mg}^{2+}$  release ( $k_{\text{obs}} \sim 0.04 \text{ s}^{-1}$ ). This means that the non-specific site would not be competent to act as a trigger for  $\text{Ca}^{2+}$  activation of muscle contraction in the scallop, due to the slow release of  $\text{Mg}^{2+}$  which would prevent rapid binding of  $\text{Ca}^{2+}$ .  $\text{Ca}^{2+}$  binding, which is responsible for activation in the myosin-linked regulation of molluscan systems occurs via the  $\text{Ca}^{2+}$ -specific site. Changes in the intrinsic tryptophan fluorescence (Wells et al., 1985a), show binding at this site to be very rapid.

Another consequence of the slow release of the  $\text{Mg}^{2+}$  is that it is likely to limit the rate of RLC dissociation on chelation of this divalent metal ion. This was observed to be the case, the effect often being evident as a lag phase at the start of RLC dissociation traces monitored by ANS. For this reason it might be thought that using  $\text{Ca}^{2+}$  to keep the RLC bound to the myosin molecule initially, in light chain dissociation experiments, would be preferable. This is not the case due to the presence of the  $\text{Ca}^{2+}$ -specific sites, which complicate the interpretation of the results,

because of changes in the molecule related to release from this site. Therefore RLC dissociation experiments were normally performed with  $Mg^{2+}$ , in the presence of EGTA to chelate any contaminant  $Ca^{2+}$ .

The association and dissociation of the RLC from scallop myosin was conveniently followed using the fluorophore 8-anilino-1-naphthalene sulphonate (ANS). Binding of ANS was found to be specific for the RLC site, with the binding site located near the C-terminus of the heavy chain of  $S1^{+RD}$ . The ANS binding was weak, however some effect on the RLC equilibrium was observed. This effect may introduce a small systematic error in any RLC association rates measured, but these can generally be ignored in terms of models of RLC interaction.

The simplest mechanism for the RLC interaction with the heavy chain/ELC complex is given in eqn 1:1. This mechanism is sufficient to explain the mechanism of RLC dissociation, on addition of EDTA to chelate the divalent metal ions, however it cannot account for the kinetics of reassociation. Results for RLC binding using ANS indicate that there is no concentration dependence of reassociation, thus, a first-order step must be involved in the reassociation pathway. A two-step mechanism which could account for this result is given in equation 7:1, where



H = heavy chain/ELC complex and L = RLC and \* denotes a change in the conformation of the HL complex.

In this mechanism the first order step is suggested to be the rearrangement of the myosin molecule after removal of the divalent metal ion. This could either be a conformational change in the heavy chain/ELC complex or the RLC. The mechanism is simplified because the  $LMg^{2+}$  species is ignored; this species is likely to exist on readdition of divalent metal ions to initiate reassociation of RLC in a dissociated preparation.

This mechanism (eqn 7:1), while being possible, was superceded in the light of results from the *Mercenaria* RLC exchange experiments (ch. 5). Addition of EDTA and *Mercenaria* RLC, simultaneously, failed to produce the expected ANS transients (fig 5-5). This led to the conclusion that during the dissociation of the RLC from scallop HMM, the vacated site on the heavy chain/ELC complex briefly exists in a nascent state. This state is proposed to be capable of rapid uptake of *Mercenaria* RLC which would prevent formation of ANS transients. The nascent state is proposed to be distinct from a refractory state of the heavy chain/ELC complex, which predominates on longer exposure to EDTA and which can only bind *Mercenaria* RLC slowly (fig 5-2). A minimal scheme for scallop RLC dissociation and hybrid formation with *Mercenaria* RLC, which would allow for the above observations, is given in eqn 7:2, where F



$k_{+2}$ .  $k_{-2}$  is estimated in conjunction with  $k_{+5}$ , to give plausible values for the apparent equilibrium constant for regulatory light chain dissociation. The value for this dissociation equilibrium constant, must be such that the scallop RLC remains associated in  $Mg^{2+}$ , but dissociates to a significant degree on addition of EDTA. This criterion produces narrow limits for the value.  $k_{-5}$  limits the rate of RLC rebinding to the denuded heavy chain/ELC complex and was measured directly (Chapter 4). The values of  $k_{+6}$  and  $k_{-6}$  must be set so that *Mercenaria* RLC binding to H can compete, both thermodynamically and kinetically, with the transition of the H state to the H\* state, thus preventing a transient in the ANS binding. A value for the apparent equilibrium constant for scallop RLC binding in the presence of EDTA can be calculated by  $(k_{+2}(1+k_{+5}/k_{-5}))/k_{-2}$ . In effect, estimates for the equilibrium binding constants were made directly by observing the effect on ANS fluorescence of RLC addition in the presence of EDTA (fig 4-12). A value of approximately  $1 \times 10^{-5}$  M was obtained for  $S1^{+RD}$  and  $1.5 \times 10^{-4}$  M estimated for HMM. The extent of RLC dissociation from HMM and  $S1^{+RD}$  is different, due to the value of the equilibrium constant  $K_5$ , (which is mainly the result of differences in the value of the rate constant  $k_{+5}$ ). However, the rates of uptake and release, which are controlled by  $k_{-5}$  and  $k_{+2}$  respectively, are similar for the two preparations. By assigning a large value (40) to  $K_5$  for HMM, this ensures that H remains a minor species under all conditions. The existence of this species (H) is obligatory

for the rapid binding of *Mercenaria* RLC observed in the exchange experiments. With  $S1^{+RD}$ ,  $K_5$  is assigned a value close to unity (both H and H\* co-exist in significant amounts) and thus can account for the biphasic re-uptake of the RLC observed in this preparation.  $K_5$  is reduced with increasing ionic strength.

Equation 7:2 is incomplete because the rate of rebinding of scallop RLC, on addition of  $Mg^{2+}$  to an HMM preparation previously treated with EDTA (fig 4-10), occurs faster than calculated from the values assigned to the rate constants for this process. This occurs because at millimolar levels of  $Mg^{2+}$  the sequential binding steps controlled by the rate constants  $k_{-1} [Mg^{2+}]$  and  $k_{-2} [L]$  are not sufficiently rapid, so that the maximum rate of RLC binding ( $k_{-5}$ ) is not achieved. However, the association via a  $LMg^{2+}$  intermediate has been ignored (cf eqn. 1:1) and this is likely to contribute to the rebinding.

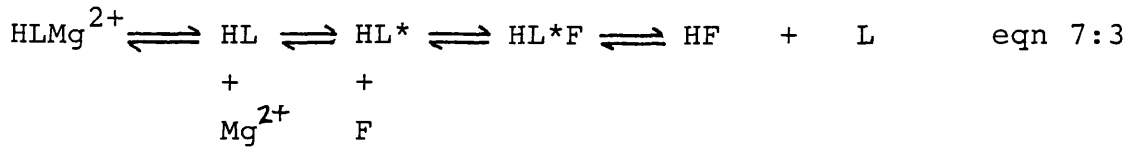
The low value of  $k_{-2}$  for scallop RLC compared with the  $k_{-6}$  for *Mercenaria* RLC (which may approach the diffusion controlled limit) may depend on their respective free conformations. It is likely that the conformation of the former, when isolated, critically depends on the presence of bound divalent metal ions. Therefore, in the absence of these ions only a minute fraction of the scallop RLC exist in a conformation capable of associating with the binding site of H, thus giving rise to the low apparent second-order rate constant,  $k_{-2}$ .

The *Mercenaria* RLC are assumed to exist in a complementary conformation to the binding site H, regardless of divalent metal ion content, and hence the high value for  $k_{-6}$  is obtained. These results indicate that the affinity of the *Mercenaria* RLC for the scallop heavy chain/ELC complex is several thousand fold tighter than that of the scallop RLC for this complex, in the absence of divalent metal ions ( $K_6$  cf  $K_2$ , eqn. 7:2). On addition of divalent metal ions the affinities of the two RLC appear to be similar (Sellers et al., 1980).

If a simulation of the predicted ANS binding is carried out, based on the rate constants given in eqn. 7:2, for the exchange of scallop RLC and *Mercenaria* RLC in HMM, on addition of EDTA and *Mercenaria* RLC simultaneously, the result shown in fig 7-1a is obtained. This is very like the actual result obtained for the ANS response on addition of these effectors to HMM (fig 7-1b).

Equation 7:2, therefore represents the simplest mechanism to account for the changes observed in the ANS profiles with HMM and  $S1^{+RD}$ . The assignments of the values to the rate constants depends on the assumptions that ANS binding to H and  $H^*$  is similar and that the differences between the profiles for HMM and  $S1^{+RD}$  can be accounted for only by differences in the value of  $K_5$ . Lack of complete reversibility of the ANS binding puts limits on the accuracy with which the system may be defined.

The mechanism proposes that the binding of *Mercenaria* RLC to H is faster than to H\*. In practice it should be possible to test this prediction, by labelling the *Mercenaria* RLC with a fluorescence probe and following the rate of binding of this light chain to myosin. Pretreatment of the myosin with EDTA, prior to *Mercenaria* RLC addition would allow isomerisation of H to H\* and allow binding of the RLC to H\* to be followed. Simultaneous addition of EDTA and RLC would allow binding to H, rather than H\*, to be monitored. This experiment was performed using *Mercenaria* RLC labelled with IANBD. Unfortunately, control experiments using desensitized myosin showed the rates of binding of this labelled light chain to be slightly faster than expected from ANS results. It appears, therefore, that more than a one-step binding of the RLC is occurring, with ANS and the IANBD label following different processes in the pathway for RLC interaction. Regardless of this complication, the rates of rebinding of the labelled *Mercenaria* RLC to the H form of the scallop heavy chain/ELC complex were found to be faster than to the H\* form which supports the proposed mechanism (eqn. 7:2). It is possible, that due to the probable existence of more than a one-step RLC binding, the lack of an ANS transient in the exchange experiment is due to a hybrid species. Such a hybrid would transiently contain two RLC per myosin head (cf Asakawa and Asuma, 1983), ie. one of each type, which would allow rapid exchange of the subunits to occur (eqn 7:3).



where L\* is a different RLC conformation to L.

Nevertheless, the significant feature of the mechanism proposed in eqn. 7:2, involving a refractory state of the denuded heavy chain/ELC complex which affects the binding of the RLC, remains.

### Effects of Ca<sup>2+</sup>

As previously indicated, removal of RLC from scallop myosin reduces the affinity of the Ca<sup>2+</sup>-specific site for Ca<sup>2+</sup>. This is observed as a decrease in the equilibrium constant from 10<sup>-7</sup> M to 10<sup>-6</sup> M (Chantler and Szent-Györgyi, 1980). To maintain a thermodynamic balance, it therefore requires that the RLC bind 10-fold tighter to the heavy chain/ELC complex in the presence of Ca<sup>2+</sup>, than in its absence. Hence, low levels of Ca<sup>2+</sup> (micromolar) will be effective in stabilising the H.L.Mg<sup>2+</sup> complex, in the presence of millimolar Mg<sup>2+</sup>. Although the intrinsic affinity of Mg<sup>2+</sup> for the myosin molecule is reasonably high (K<sub>1</sub> = 10<sup>-6</sup> M, eqn 7:2) its apparent value is reduced by the RLC dissociation steps. The effect can be calculated from the following K<sub>app</sub> = K<sub>1</sub>(1+(K<sub>2</sub>(1+K<sub>5</sub>)/[L])). If the HMM concentration was 4 μM (typical for experimental conditions), the values assigned in equation 7:2, indicate that 17% of the regulatory light chains are in a dissociated state, for a [Mg<sup>2+</sup>] = 1 mM. Addition of Ca<sup>2+</sup> to such a preparation at micromolar levels, would

therefore be expected to cause RLC reassociation. The effect would be mediated via  $\text{Ca}^{2+}$  binding to the  $\text{Ca}^{2+}$ -specific site of the  $\text{HLMg}^{2+}$  and the HL complexes, with little binding to the H and H\* complexes. This effect would be sufficient to explain the decrease in ANS fluorescence observed with native HMM preparations (fig 6-4), which were slow and reversible. At higher  $[\text{Ca}^{2+}]$ , binding may also occur at the non-specific site ( $K_1^{\text{Mg}}/K_1^{\text{Ca}} = 10$ , Bagshaw and Kendrick-Jones, 1979). Unfortunately the results of  $\text{Ca}^{2+}$ -binding observed with RLC denuded HMM preparations complicate this explanation. With these preparations, even at the higher  $\text{Ca}^{2+}$  concentrations used, the effect must be mediated via the  $\text{Ca}^{2+}$ -specific site. It is apparent that the binding of  $\text{Ca}^{2+}$  to the  $\text{Ca}^{2+}$ -specific site causes some conformational change in the heavy chain/ELC complex, reflected in the decrease in ANS fluorescence. This occurs in the absence of RLC, so cannot be due to added RLC binding as proposed for the native HMM. From the data available it is not possible to conclude whether the effects observed, in native and RLC denuded preparations, are the result of the same process.

Additional evidence for an effect of the  $\text{Ca}^{2+}$  specific site is presented using ELC labelled with the fluorophore IANBD. The results show that  $\text{Ca}^{2+}$  decreases the rate of ELC exchange in desensitized myosin. Also, addition of  $\text{Ca}^{2+}$  to the ELC-labelled desensitized myosin causes changes in the fluorescence which are reversible. In all cases the effects are too slow to feature in the  $\text{Ca}^{2+}$ -

activation of muscle contraction, although, with sustained increases in  $\text{Ca}^{2+}$  levels a longer term role cannot be ignored.

The possibility that regulatory light chain dissociation may occur even in the presence of millimolar levels of  $\text{Mg}^{2+}$ , has particular relevance to the storage and stability of scallop proteins. The chelator EDTA was traditionally included in myosin storage media, in an attempt to chelate heavy metal ions and reduce  $\text{Ca}^{2+}$ -activated protease activities. For scallop myosin, this procedure was modified by the inclusion of 0.5 - 1 mM excess free  $\text{Mg}^{2+}$  over chelator to maintain the RLC in an associated state (Szent-Györgyi *et al.*, 1973; Stafford *et al.*, 1979). The results presented suggest that inclusion of at least 10  $\mu\text{M}$  free  $\text{Ca}^{2+}$  would also be beneficial in these proteins. This would be particularly useful when dilute protein solutions are stored on a short-term basis at 20°C, as might be required in a stopped-flow assay. It is interesting to note that  $\text{Ca}^{2+}$  has been used for the protection of light chain cleavage during subfragment preparation by proteolysis, even in the presence of high  $\text{Mg}^{2+}$  concentrations (Stafford *et al.*, 1979; Szentkiralyi, 1984).

Wells and Bagshaw (1985) showed that conventional HMM preparations contain 20-30% unregulated molecules using a single-turnover ATPase approach. Some of the unregulated molecules are the result of partial damage by the proteolytic enzyme used. These can be removed by rapid ultracentrifugation

in the presence of actin (C Wells, personal communication). However there remains an upper limit for the population of regulated molecules obtainable, due to the likely spontaneous dissociation of RLC, even in the presence of 1 mM  $Mg^{2+}$ . This dissociation could be minimised by (i) the inclusion of  $Ca^{2+}$  just prior to the experiments, (ii) the addition of extra exogenous RLC to maintain the free RLC (L) in a high concentration and (iii) storage of the stock protein solutions at high concentration and low temperature.

#### The effect of RLC interaction on structure

The large difference in the extent of RLC dissociation from HMM compared to  $S1^{+RD}$  on addition of EDTA, can be explained by a difference in the equilibrium constant  $K_5$  (eqn. 7:2). This dissociation, driven by the transition of the denuded heavy chain/ELC complex from the nascent to the refractory state of the complex, can be explained by a structural model. Previously, Bagshaw (1980) suggested that because light chain denuded preparations aggregated intermolecularly, the two heads might also be capable of interacting in an intramolecular manner. This idea evolved as a modification of those of Kendrick-Jones and Jakes (1976), which were suggested in an attempt to explain the preferential release of one regulatory light chain from myosin at 4°C. Spin labelling studies (Wells and Bagshaw, 1983) provided subsequent evidence in support of this hypothesis. These studies revealed that when the RLC were removed from the molecules, the independent motion of the myosin heads,

around their flexible 'neck' region, was severely restricted. In addition, this loss of motion occurred over the same time scale as RLC dissociation and was not a reflection of aggregation due to ageing of the preparation. Concurrent with the spin-labelling studies, the electron microscopy work of Flicker et al., (1983) showed that the removal of the RLC caused a change in the shape of the myosin head. The heads of intact myosin were typically pear shaped, appearing widest at the end remote from the tail and tapering towards their neck region with a length of  $195 \pm 30 \text{ \AA}$  and a maximum width of  $80 \pm 15 \text{ \AA}$ . Those of desensitized myosin were more rounded, with a long dimension of  $135 \pm 25 \text{ \AA}$  and a maximum width of  $85 \pm 15 \text{ \AA}$ . They noted that the 'neck' region of the myosin tended to 'collapse' on removal of the RLC, but they did not quantitate this effect. If the selected electronmicrographs shown (fig 6, Flicker et al., 1983) are considered, and the distance between the centres of mass of the two heads measured, it is observed to be reduced from an average of approximately 19 nm to 13 nm by the desensitization procedure.

While the interpretations proposed for these observations differ, ie intramolecular aggregation versus neck collapsing (fig 7-2c) cf 7-2d)), they have a common theme. This is that the denuded heavy chain/ELC complex undergoes a major conformational or structural change, subsequent to the RLC dissociation. In addition, both interpretations suggest that the RLC binding site, when vacated, and exposed, is unstable and that it readily interacts with another protein

site, rather than remain exposed to the surrounding solvent. Although the site has been described as a sticky patch (Bagshaw, 1980; Pastra-Landis and Lowey, 1984), it is necessary to stress the dynamic nature of the interaction proposed here. The nascent and refractory states proposed in eqn. 7:2, are envisaged to reflect the two forms of the RLC denuded heavy chain/ELC complex which are in dynamic equilibrium (fig 7-2). It must be appreciated that reversal of the refractory state to the nascent state is rapid ( $t_{1/2} = 100s$ ) compared to the length of time taken in the preparative steps involved in most biochemical and structural investigations. Hence, in processes to visualize the myosin molecule, only the extremes of the states possible on RLC dissociation (ie intact and 'refractory' states) would be observed.

There are two different, but probably related phenomena which must be accounted for with respect to RLC dissociation. With two headed species such as myosin and HMM one RLC is preferentially released from each molecule, which implies some form of interaction between the heads. However, this co-operative release of light chain is only clearly prevalent in myofibrils at low temperatures (Chantler, 1985). When myosin alone is considered the results are found to be more variable (cf Wells and Bagshaw, 1983; Flicker et al., 1983). This suggests that the presence of the actin filament in the myofibrils, is acting to orientate the myosin heads, thus allowing a more homogenous interaction. At the higher temperatures (20°C) at which most experiments were performed, there is little suggestion of co-operativity

(Chantler, 1985). There remains however, a clear cut difference in the behaviour of HMM and  $S1^{+RD}$  at this temperature with respect to regulatory light chain dissociation. It is quite likely that this could reflect a difference in the degree of interaction possible within the neck region of the molecule (fig 7-2) - a consequence of loss of some of this region in  $S1^{+RD}$ . In this respect it would be interesting to investigate the RLC interaction in single headed myosin or HMM. With such preparations it should be possible to determine the 'role' of the neck region and its relevance in the RLC interaction. Single headed myosin can be easily prepared in an impure form (fig 2-8), however for this type of study, a pure preparation free of S1 and double headed myosin is required and this is not easily obtainable.

In this thesis, it has not been attempted to analyse the data obtained for myosin and HMM, with reference to differential binding of the RLC to the two heads. The RLC dissociation step appears to fit a single exponential, after an allowance has been made for the slow  $Mg^{2+}$  release and the resultant lag-phase (fig 5-3a). In any case it would be difficult to distinguish between a biphasic response due to such a differential RLC binding and co-operativity from other causes, such as heterogeneous populations of the molecules (Wells and Bagshaw, 1985). Information from labelled light chain preparations, indicate that the RLC interaction is unlikely to be explained by a single attachment point for the light chain. Any RLC interaction is likely to

involve close interactions with the ELC as well as the heavy chain. The mechanisms proposed will probably therefore have to be modified and additional steps, incorporating further conformationally-significant species, will need to be added.

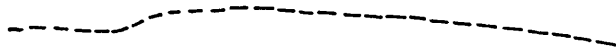
Fig 7-1

Simulated and observed effect of adding *Mercenaria* RLC  
and EDTA simultaneously to scallop HMM

(a) Computer simulation of effect of adding *Mercenaria* RLC and EDTA simultaneously to scallop HMM according to the mechanism given in eqn 7:2, using the values for the rate constants given in the text.

(b) Actual result of following ANS fluorescence at 460 nm exciting at 295 nm, on performing the experiment described in (a). 0.6 mg/ml HMM was preincubated in 40 mM NaCl, 20 mM EPPS, 100  $\mu$ M MgCl<sub>2</sub>, 100  $\mu$ M EGTA, 20  $\mu$ M ANS at pH 8.0 and 20°C. At the time indicated 3.5  $\mu$ M *Mercenaria* RLC and 0.5 mM EDTA were added simultaneously (cf. fig 5:3c).

a)



b)

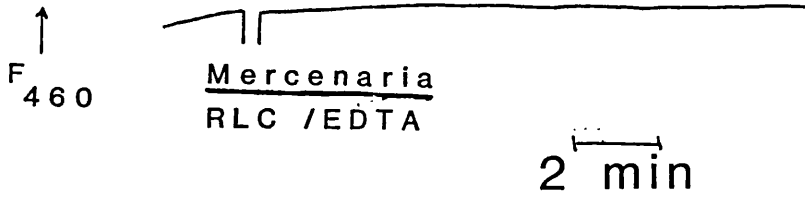
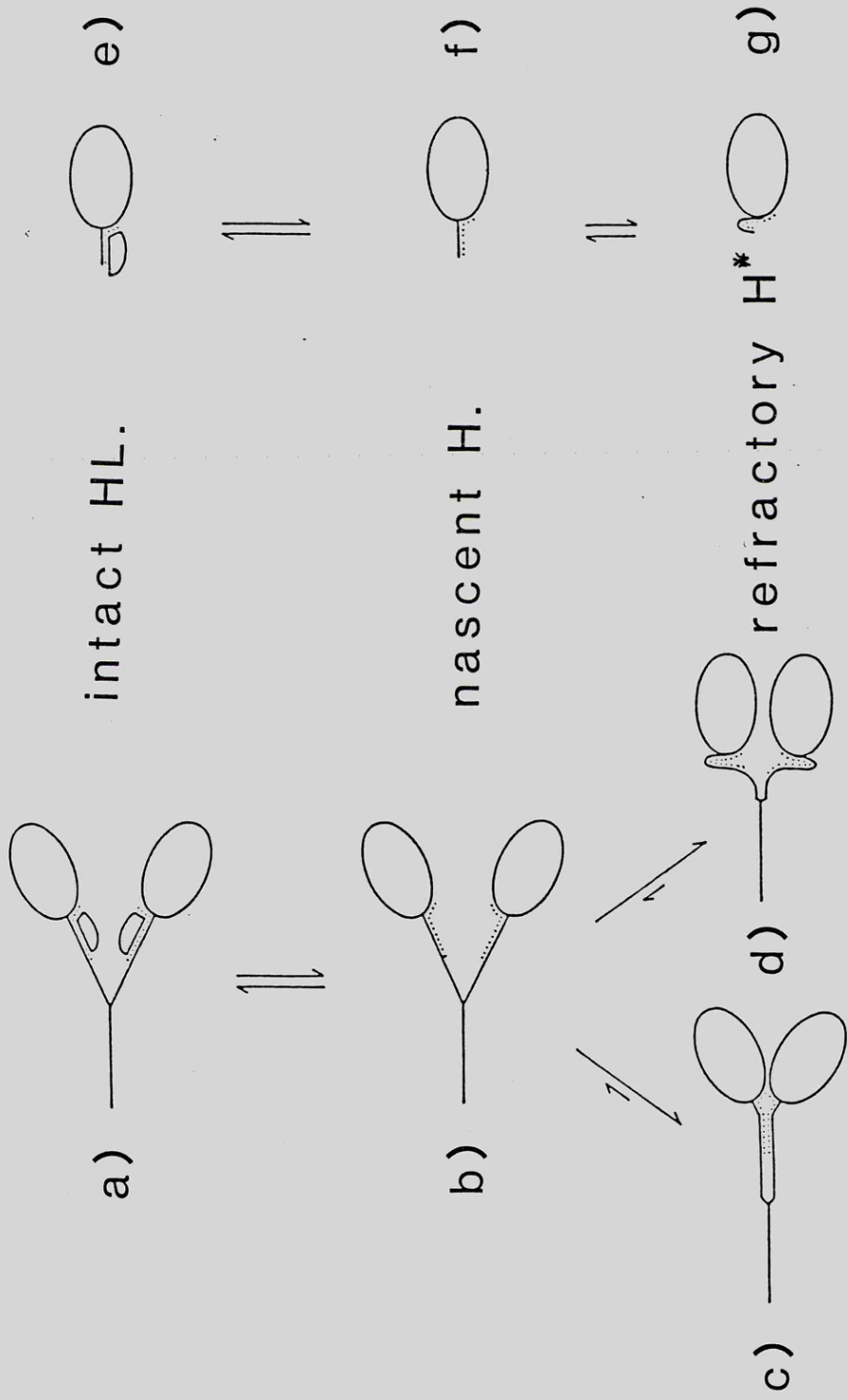


Fig 7-2

Possible structures of the refractory state

On release of the RLC from HMM the neck region might undergo intramolecular association (c) or collapse (d) thereby displacing the equilibrium towards net light chain dissociation. Intramolecular association could give rise to either positive co-operativity, negative co-operativity or random dissociation depending on whether the vacated site on one head tends to bind to the corresponding site on the second head, or another location or shows no preference respectively. Neck collapse might give rise to co-operative effects if one head tends to block the other sterically. Both states (c) and (d) could account for loss of the flexibility of the neck region (Wells and Bagshaw, 1983) and the decrease in the average head-head distance (cf. Flicker et al., 1983). With  $S1^{+RD}$  the less extensive neck region might limit the extent of its collapse (g). Both states (b) and (f) could undergo intermolecular association which would favour light chain dissociation (cf. Pastra-Landis and Lowey, 1984). The ELC has been omitted from these diagrams for clarity but it probably constitutes part of the RLC binding site (Hardwicke et al., 1983). The dependence of the amplitude of the observed ANS profile with  $S1^{+RD}$  on the NaCl concentration (fig 4-10) suggests that the interactions involved at step 5 (eqn 7:2) are, at least in part, ionic in nature.



S1<sup>+</sup>RD

HMM

APPENDIX 1: PUBLICATIONS

BENNETT, A.J., PATEL, N., WELLS, C. and BAGSHAW, C.R.  
(1984) 8-anilino-1-naphthalene sulphonate, a fluorescent  
probe for the regulatory light chain binding site of  
scallop myosin. *J. Musc. Res. Cell. Motil.* 5 165-182.

BENNETT, A.J., and BAGSHAW, C.R. (1985)  
Rapid removal of regulatory light chains from scallop  
heavy meromyosin. *Biochem. Soc. Trans.* 13, 926-927.

WELLS, C., WARRINER, K., BENNETT, A.J. and BAGSHAW, C.R.  
(1985)  
The kinetic mechanism of scallop myosin ATPase activity.  
*Biochem. Soc. Trans.* 13, 925-926.

BENNETT, A.J. and BAGSHAW, C.R. (1986)  
The kinetics of divalent metal ion dissociation from  
myosin subfragments. *Biochem. J.*, 233, 173-177.

BENNETT, A.J., and BAGSHAW, C.R. (1986).  
The mechanism of regulatory light chain dissociation  
from scallop myosin. *Biochem. J.*, 233, 179-186.

## BIBLIOGRAPHY

Adelstein, R.S. and Conti., M.A. (1975) Nature, 256,  
597-598

Ashiba, G., Asada, T. and Watanabe, S. (1980) J. Biochem.  
88, 837-846.

Ashiba, G. and Szent-Györgyi, A.G. (1984) Biophys. J.  
45, 227a

Azakawa, T. and Azuma, N. (1983) J. Biochem. 94, 395-401

Bagshaw, C.R. (1977) Biochemistry, 16, 59-67.

Bagshaw, C.R. (1980) J. Musc. Res. Cell. Motil. 1,  
255-277.

Bagshaw, C.R. and Kendrick-Jones, J. (1979) J. Mol.  
Biol. 130, 317-336.

Bagshaw, C.R. and Kendrick-Jones, J. (1980) J. Mol.  
Biol. 140, 411-433.

Bagshaw, C.R., Patel, N. and Wells, C. (1982) J. Musc.  
Res. Cell. Motil. 3, 463.

Bagshaw, C.R. and Reed, G.H. (1976) J. Biol. Chem. 251,  
1975-1983.

Bagshaw, C.R. and Reed, G.H. (1977) FEBS. Lett. 81, 386-  
390.

Bennett, A.J., Patel, N., Wells, C. and Bagshaw, C.R.  
(1984) J. Musc. Res. Cell. Motil. 5, 165-182

Chantler, P.D. (1985) J. Mol. Biol. 181, 557-560

Chantler, P.D. and Szent-Györgyi, A.G. (1978) Biochemistry  
17, 5440-5448.

Chantler, P.D. and Szent-Györgyi, A.G. (1980) J. Mol.  
Biol. 138, 473-492.

Cheung, H.C. and Morales, M.F. (1969) Biochemistry 8,  
2177-2182.

Dodd, G.H. and Radda, G.K. (1969) Biochem. J. 114, 407-  
417.

Ebashi, S. and Kodama, A. (1966) J. Biochem. 59, 425-  
426.

Eisenberg, E. and Greene, L.E. (1980) Annu. Rev. Physiol.  
42, 293-309.

Elliott, A. and Offer, G. (1978) J. Mol. Biol. 123, 505-509.

Focant, B. and Huriaux, F. (1976) FEBS. Lett. 65, 16-19.

Flicker, P.F., Wallimann, T. and Vibert, P. (1983) J. Mol. Biol. 169, 723-741.

Gordon, A.M., Huxley, A.F. and Julian, F.J. (1966) J. Physiol.(Lond.) 184, 170-192.

Greaser, M.L. and Gergely, J. (1971) J. Biol. Chem. 246, 4226-4233.

Gutfreund, H. (1972) Enzymes: Physical principles, Wiley Interscience, London, New York, Sydney and Toronto.

Hanson, J. and Lowy, J. (1963) J. Mol. Biol. 6, 46-60.

Hanson, J. and Lowy, J. (1964) Proc. R. Soc. Lond. (Biol.), 160, 449-458.

Hardwicke, P.M.D. and Szent-Györgyi, A.G. (1985) J. Mol. Biol. 183, 203-211

Hardwicke, P.M.D., Wallimann, T. and Szent-Györgyi, A.G. (1982) J. Mol. Biol. 156, 141-152.

Hardwicke, P.M.D., Wallimann, T. and Szent-Györgyi, A.G. (1983) Nature 301, 478-482.

Haselgrove, J.C. (1975) *J. Mol. Biol.* 92, 113-143.

Hoh, J.F.Y. (1976) *Biochem. J.* 157, 87-95.

Hummel, J.P. and Dreyer, W.J. (1962) *Biochem. Biophys. Acta.* 63, 530-532.

Huxley, A.F. and Niedergerke, R.M. (1954) *Nature* 173, 971-973.

Huxley, H.E. (1973) *Cold Spring Harbour Symp. Quant. Biol.* 37, 361-376.

Huxley, H.E. and Brown, W. (1967) *J. Mol. Biol.* 30, 383-434.

Huxley, H.E. and Hanson, J. (1954) *Nature* 173, 973-976.

Jakes, R., Northrop, F. and Kendrick-Jones, J. (1976) *FEBS. Lett.* 70, 229-234.

Karn, J., McLachlan, A.D. and Barnett, L. (1982) *Muscle Development; Molecular and cellular control.* 129-142. Cold Spring Harbour, New York.

Kendrick-Jones, J. and Jakes, R. (1976) *Symposium on Myocardial failure (Rieker, G., Weber, A. and Goodwin, J., Eds.)* pp 28-40 Munich : Tergensee

Kendrick-Jones, J., Lehman, W. and Szent-Györgyi, A.G.  
(1970) J. Mol. Biol. 54, 313-326.

Kendrick-Jones, J., Szentkiralyi, E.M. and Szent-Györgyi,  
A.G. (1976) J. Mol. Biol. 104, 747-775.

Konno, K., Arai, K. and Watanabe, S. (1983) J. Biochem.  
94, 1061-1065.

Kretsinger, R.H. (1980) C.R.C. Crit. Rev. Biochem. 8,  
119-174.

Laemmli, U.K. (1970) Nature 227, 680-685.

Lehman, W. (1981) Biochim. Biophys. acta. 668, 349-  
356

Lehman, W., Regenstein, J.M. and Ransom, A.L. (1976)  
Biochim. Biophys. acta. 434, 215-222.

Lehman, W. and Szent-Györgyi, A.G. (1975) J. Gen. Physiol.  
66, 1-30.

Lynn, R.W. and Taylor, E.W. (1970) Biochemistry 9, 2975-  
2983.

Lynn, R.W. and Taylor, E.W. (1971) Biochemistry 10,  
4617-4624.

Margossian, S.S. and Lowey, S. (1973) J. Mol. Biol. 74, 313-330.

Margossian, S.S. and Lowey, S. (1982) Methods in Enzymology 85, 55-72.

Margossian, S.S., Lowey, S. and Barshop, B. (1975) Nature 258, 163-165.

Matsuda, G., Maita, G., Suzuyama, Y., Setoguchi, M. and Umegane, T. (1977) J. Biochem. 81, 809-811.

Maw, M. C. and Rowe, A. J. (1980) Nature 286, 412-414.

Mclachlan, A.D. and Karn, J. (1982) Nature 299, 226-231.

Millar, N.C. (1984) Ph.D thesis, University of Bristol.

Millman, B.M. and Bennett, P.M. (1976) J. Mol. Biol. 103, 439-467.

Pastra-Landis, S.C. and Lowey, S. (1984) Biophys. J. 45, 151a.

Persechini, A. and Rowe, A.J. (1984) J. Mol. Biol. 172, 23-39.

Potter, J.D. (1974) Arch. Biochem. Biophys. 162, 436-441.

Selby, C.C. and Bear, R.S. (1956) J. Biophys. Biochem. Cytol. 2, 71-85.

Sellers, J.R., Chantler, P.D. and Szent-Györgyi, A.G. (1980) J. Mol. Biol. 144, 223-245.

Smith, P.D., Liesegang, G.W., Berger, R.L., Czerlinski, G. and Podolsky, R.J. (1984) Anal. Biochem. 143, 188-195.

Sperling, J.E., Feldman, K., Meyer, H., Jahnke, U. and Heilmeyer, L.M.G. (1979) Eur. J. Biochem. 101, 581-592.

Squire, J.M. (1974) J. Mol. Biol. 90, 153-160.

Stafford, W.F. and Szent-Györgyi, A.G. (1978) Biochemistry 19, 607-614.

Stafford, W.F., Szentkiralyi, E.M. and Szent-Györgyi, A.G. (1979) Biochemistry, 24, 5273-5280.

Stein, L.A., Schwarz, R., Chock, P.B. and Eisenberg, E. (1979) Biochemistry 18, 3895-3909.

Storer, A.C. and Cornish-Bowden, A. (1976) Biochem. J. 159, 1-5

Stryer, L. (1965) J. Mol. Biol. 13, 482-495.

Such, D., Kabasch, W. and Mannherz, H.G. (1981) Proc. Natl. Acad. Sci. 78, 4319-4323.

Suzuki, H., Onishi, H., Takahashi, K. and Watanabe, S. (1978) J. Biochem. 84, 1529-1542.

Szent-Györgyi, A.G., Cohen, C. and Kendrick-Jones, J. (1971) J. Mol. Biol. 56, 239-258.

Szent-Györgyi, A.G., Szentkiralyi, E.M. and Kendrick-Jones, J. (1973) J. Mol. Biol. 74, 179-203.

Szentkiralyi, E.M. (1984) J. Musc. Res. Cell. Motil. 5, 147-164.

Taylor, K.A. and Amos, L.A. (1981) J. Mol. Biol. 147, 297-324.

Trybus, K. M. and Lowey, S. (1984) J. Biol. Chem. 259, 8564-8571.

Tsien, R.Y. (1980) Biochemistry 19, 2396-2404.

Vibert, P. and Craig, R. (1983) J. Mol. Biol. 165, 303-320.

Wagner, P.D. and Giniger, E. (1981) Nature 292, 560-562.

Walliman, T., Hardwicke, P.M.D. and Szent-Györgyi, A.G.  
(1982) J. Mol. Biol. 156, 153-173.

Weeds, A.G. and Taylor, R.S. (1975) Nature 257, 54-56

Wells, C and Bagshaw, C.R. (1983) J. Mol. Biol. 164,  
137-157.

Wells, C. and Bagshaw, C.R. (1984) FEBS. Lett. 168, 260-  
264.

Wells, C and Bagshaw, C.R. (1985) Nature 313, 696-697.

Wells, C., Warriner, K., Bennett, A.J. and Bagshaw, C.R.  
(1985a) Biochem. Soc. Trans. 13, 925-926.

Wells, C., Warriner, K.E. and Bagshaw, C.R. (1985b) Biochem.  
J. 231, 31-38.

Werber, M.M. (1978) Experientia 34, 575-576.

Werber, M.M., Gaffin, S.L. and Oplatka, A. (1972) Mechanochem.  
Cell.Motil. 1, 91-96.

White, H.D. (1982) Methods in Enzymology (academic press)  
85, 698-708.

Winkelmann, D.A., Mekeel, H. and Rayment, I. (1985) J.  
Mol. Biol. 181, 487-501.

Wray, J.S., Vibert, P.J. and Cohen, C. (1975) Nature  
257, 561-564.